Identifying characteristics of thalamo-cortical changes and their relationship with symptoms in schizophrenia

Savić, Aleksandar

Doctoral thesis / Disertacija

2019

UNIVERSITY OF ZAGREB
SCHOOL OF MEDICINE

Aleksandar Savić

Identifying characteristics of thalamo-cortical changes and their relationship with symptoms in schizophrenia

DISSERTATION

Zagreb, 2019.

UNIVERSITY OF ZAGREB
SCHOOL OF MEDICINE

Aleksandar Savić

Identifying characteristics of thalamo-cortical changes and their relationship with symptoms in schizophrenia

DISSERTATION

Zagreb, 2019.

Content:

Abbreviations

Abbreviations

ACC	Anterior Cingulate Cortex
AD	Anterodorsal Nucleus
AM	Anteromedial Nucleus
ANOVA	Analysis of Variance
ANCOVA	Analysis of Covariance
AUD	Auditory Network
AV	Anteroventral Nucleus
BA	Brodmann Area
BACS	Brief Assessment of Cognition in Schizophrenia
BD	Bipolar Affective Disorder
BDp	Bipolar Affective Disorder with Psychosis History
BOLD	Blood-oxygenation-level Dependent
BPRS	Brief Psychiatric Rating Scale
B-SNIP	Bipolar-Schizophrenia Network on Intermediate Phenotypes
Cho	Choline
CIFTI	Connectivity Informatics Technology Initiative
CPZ	Chlorpromazine
Cr	Creatine
CNV	Copy Number Variations
COMT	Catechol-O-methyltransferase
CON	Cingulo-opercular Network
CT	Computed Tomography
DAN	Dorsal Attention Network
DISC1	Disrupted in Schizophrenia 1

DLPFC	Dorsolateral Prefrontal Cortex
DMN	Default Mode Network
DRD2	Dopamine Receptor D2
DSf	Dorsal Superficial Nucleus
DSM	Diagnostic and Statistical Manual of Mental Disorder
DTI	Diffusion Tensor Imaging
DTNBP1	Dysbindin/dystrobrevin-binding Protein 1
DUP	Duration of Untreated Psychosis
EEG	Electroencephalogram
EPI	Echo-planar Imaging
FA	Fractional Anisotropy
FEP	First Episode of Psychosis
FLIRT	FSL linear image registration tool
fMRI	Functional Magnetic Resonance Imaging
FMRIB	Functional Magnetic Resonance Imaging of the Brain
FNIRT	FSL nonlinear image registration tool
FOV	Field-of-view
FPN	Frontoparietal Cognitive Control network
FRS	First-rank Symptoms
FSL	FMRIB Software Library
Fz	Fisher-Z-values
GABA	γ-aminobutyric Acid
GLM	General Linear Model
Glx	Glutamate and Glutamine MRS Peak
GSR	Global Signal Regression
GWAS	Genome-wide Association Studies

HCP	Human Connectome Project
HRF	Hemodynamic Response Function
ICA	Independent Component Analysis
ICD-10	International Statistical Classification of Diseases, Tenth Revision
LGB	Lateral Geniculate Body
MANOVA	Multivariate Analysis of Variance
MANCOVA	Multivariate Analysis of Covariance
MATLAB	Matrix Laboratory
MCMC	Markov Chain Monte Carlo
MD	Mediodorsal Nucleus
MEG	Magnetoencephalograph
MGB	Medial Geniculate Body
MNI	Montreal Neurological Institute
MRI	Magnetic Resonance Imaging
MRS	Magnetic Resonance Spectroscopy
MVPA	Multi-voxel Pattern Analysis
NAA	N-acetyl Aspartate
NIFTI	Neuroimaging Informatics Technology Initiative
NMDA	N-Methyl-D-aspartate
NRG1	Neuregulin 1
OFC	Orbitofrontal Cortex
PALM	Permutation Analysis of Linear Models
PANSS	Positive and Negative Symptoms Scale
PCA	Principal Components Analysis
PCP	Phencyclidine
PET	Positron Emission Tomography

PFC	Prefrontal Cortex
PMM	Posterior Multimodal Network
RDC	Research Diagnostic Criteria
RDoC	Research Domain Criteria
ROI	Region of Interest
RTN	Reticular Thalamic Nucleus
SANS	Scale for the Assessment of Negative Symptoms
SAPS	Scale for the Assessment of Positive Symptoms
SCAD	Schizoaffective Disorder
SCZ	Schizophrenia
SD	Standard Deviation
SMR	Standardized Mortality Ratio
SNP	Single Nucleotide Polymorphism
SOM	Somatomotor Network
SNR	Signal-to-noise Ratio
SNV	Single Nucleotide Variant
SPECT	Single Photon Emission Computerized Tomography
TE	Echo Time
TR	Repetition Time
VA	Ventral Anterior Nucleus
VIS1	Primary Visual Network
VIS2	Secondary Visual Network
VL	Ventrolateral Nucleus
VPL	Ventral Posterolateral Nucleus
VPM	Ventral Posteromedial Nucleus
VPMpc	Parvocellular Extension of VPM

VPS	Superior Ventroposterior Nucleus
WAIS	Weschler Adult Intelligence Scale
WRAT	Wide-Range Achievement Test
YLD	Years of Life Lived With Disability

1. Introduction and background for the proposed research

1.1. Schizophrenia

1.1.1. Defining and diagnosing schizophrenia

Schizophrenia (SCZ) is a severe psychotic mental disorder characterized by changes in perception and thoughts (but also other mental functions like affective responses), leading to impaired testing of reality and reduced functioning that, regardless of different developments and changes of focus in psychiatry, continues to be seen by many as the one paradigmatic mental disorder. Even though there are arguably a number of historical accounts of cases that resemble our current understanding of the clinical entity we call schizophrenia, it was first conceptualized as a separate psychiatric disorder in the 19th century.

Emergence of the definition of this disorder rests on the descriptive work of a number of authors, who, like John Haslam (describing illness in young people characterized by changes in the affect) and Wilhelm Griesinger (describing 'fixed affective madness' presenting among other symptoms with thought disorders and hallucinations, progressing towards dementia), seemed to capture an aspect of what was later to become schizophrenia (1). Bénédict Augustin Morel wrote about deterioration in mental functions in young people following an episode of what we would now most probably call psychosis, and it was Emil Kraepelin who used this concept, along with those of Ewald Hecker (hebephrenia) and Karl Ludwig Kahlbaum (catatonia), to conceptualize '*dementia praecox*' (1, 2). Kraepelin's *dementia praecox* was a separate disorder appearing in the young, characterized by gradual onset, progressive deterioration, and clinically presenting potentially with a different set of dominant symptoms (e.g. paranoid, catatonic). As such, it was the first comprehensive description and conceptualization of a diagnostic entity that we now call schizophrenia. In addition to offering the first comprehensive view of what is to become schizophrenia, and postulating its gradual onset and development, thus even setting the stage for the later research into prodromal phases (3), Kraepelin is to be credited with another important nosological point that steered the future development of psychiatry. Kraepelin introduced a clear delineation between *dementia praecox* and manic-depressive illness, an affective disorder with a course of illness not being characterized by progressive deterioration seen in *dementia praecox* (4). In the absence of objective tests or clear understanding of the underlying pathophysiology, 'Kraepelinian dichotomy' between affective domain characterized by the manic-depressive illness and dementia praecox helped bring a level of nosological order to the field of mental disorders, and still shapes to a greater or lesser extent the accepted classifications systems. Ironically, the same dichotomy could today be an obstacle to disentangling the underlying

pathology, as it forces categories where dimensional approach might describe reality more accurately.

In the early 20th century, building on Kraepelin's work, Eugen Bleuler introduced the term 'schizophrenia' (intended to signify *splitting of the mind*) to describe dementia praecox in a presumably more etiology-oriented manner. He saw schizophrenia as a group of conditions characterized by the loss of coherence between mental functions, and marked the first clearer distinction between groups of symptoms that we would now roughly include into *positive* and *negative* symptom domains. Bleuler notes the existence of *fundamental* symptoms that include changes in affectivity and the way an individual interacts with the outside world (four As: associations, affect, autism, ambivalence), which are present throughout the course of the illness, separating them from *accessory* symptoms (hallucinations, delusions) that might be present only at times and, even though seemingly more disturbing, imply better prognosis (1, 5).

Symptom domains and measuring symptoms

The two already mentioned symptom domains, positive and negative, still represent the basis for understanding the clinical presentation of schizophrenia, but at the same time of other psychotic disorders as well. Positive symptoms could additionally be divided into *core* positive symptoms (delusions and hallucinations) that imply perceptual disturbances and specific thought content, and formal thought disorder seen by some as a separate dimension that affects organization of thoughts and can be evaluated through patients' speech, writing, and behavior. Formal thought disorder (FTD) includes tangentiality, echolalia, verbigeration, thought blocking, poverty of thought content, changes in abstract thinking, idiosyncratic associations, and looseness of association, derailment, and incoherence (word salad being the far end of the incoherence spectrum), and has even been shown to be a predictor of conversion from first-episode psychosis to schizophrenia (6). Negative symptoms include flat affect, anhedonia, amotivation, asociality, and poverty of speech (alogia), and even though they often present prior to hallucinations or delusions and leade to more significant functional impairment, to the patients' surrounding they are usually less noticeable than the positive domain and result in contact with mental health care services less often (7).

In line with the complexity and heterogeneity of the disorder, other symptom domains are included in attempts to outline more accurately all elements of the clinical presentation. Additional symptom domains can include emotions domain, excitement, disorganization domain (sometimes understood to include formal thought disorder), but the one most often mentioned is the cognitive domain. Changes in cognition are a focus of numerous studies, and

it has been observed that they are present even before the onset of frank psychotic symptoms, they persist throughout the course of the illness, and can show changes of up to two standard deviations from the scores seen in healthy population (8-12). Cognitive domain changes have been observed to affect attention/vigilance, working memory, speed of processing, visual learning and memory, verbal learning and memory, verbal comprehension, problem solving and reasoning, and social cognition (13); they affect functioning of patients with schizophrenia, and, due to their presence throughout the course of the disorder, are seen as candidates for a trait marker. Although 27% of schizophrenia patients have been found not to have neuropsychological impairment (14), 98.1% of them perform below expected levels based on specific predictors, like parental education (15). Furthermore, although both cognitive and negative symptom domains show significant impact on functioning and correlation in severity, they are still seen as orthogonal separable entities (16). A relationship between positive symptoms and cognitive variables or improvement in cognition has been reported (17, 18). In general, the relationship between different symptom domains will depend on the model we use to define different symptom domains, and on specific phenomena within those domains that might show differential correlations.

Different computerized and paper-and-pencil tests are used in research and clinical practice to evaluate intelligence and the cognitive domain, like Weschler Adult Intelligence Scale (WAIS) (19), MATRICS Consensus Cognitive Battery (12, 13), and The Brief Assessment of Cognition in Schizophrenia (BACS) (20). Assessment of other symptom domains in schizophrenia (and other psychotic disorders) and of their severity can also be achieved by using a number of validated instruments like The Brief Psychiatric Rating Scale (BPRS) (21), Scale for the Assessment of Negative Symptoms (SANS), and Scale for the Assessment of Positive Symptoms (SAPS) (22, 23). One of the most detailed and most widely used scales for assessment of symptom severity is the Positive and Negative Symptoms Scale (PANSS), grouping items into three subscales (positive, negative, and general psychopathology) (24, 25). In an attempt to reflect more accurately the complex clinical presentation with different symptom clusters, data reduction methods like principal components analysis (PCA) have been performed on available symptom scales to produce multiple-factor solutions representing different symptom clusters. In line with that, in addition to using PANSS to generate the usual positive, negative, and general psychopathology scores, it is possible to apply alternative loadings of items to produce five-factor/cluster solutions (positive symptoms, negative symptoms, disorganization, excitement, and emotional distress/depressed factor) (26, 27). Other factor solutions exist, but almost all of those yielding four or five factors do include the affective component (28-30). It is important to point to the fact that the final factor solution depends on the analysis method used, but also as expected

on the extensiveness of the scale chosen, as more comprehensive scales like PANSS as a rule yield a greater number of symptom dimensions (31). Also, Tibber et al. (31) state that the three-factor model that includes positive symptoms, negative symptoms, and disorganization dimension, ends up being the most robust and useful one, even with the risk of losing fine-grained psychopathology elements that might be of importance at different levels of analysis.

Classification systems

It is clear that diagnosing a heterogeneous disorder like schizophrenia must come with severe obstacles and pitfalls. One of the most important elements in developing clear criteria for diagnosing schizophrenia, however essentially reductionist, was the development of the concept of 'first-rank' symptoms (FRS) by Kurt Schneider. Schneider claimed that in the absence of an organic cause a number of specific symptoms (auditory hallucinations – running commentary, third person; audible thoughts, thought broadcasting, thought insertion, thought withdrawal, delusions of control, delusional perception) can be considered as characteristic for schizophrenia. Although there are clear non-FRS symptom profiles in schizophrenia, while FRS can be seen in other mental disorders, FRS have significantly shaped classification systems, including Research Diagnostic Criteria (RDC), International Statistical Classification of Diseases, Tenth Revision (ICD-10), as well as Diagnostic and Statistical Manual of Mental Disorders, Third and Fourth Edition (DSM-III, DSM-IV) (32-34). The same was corrected in DSM-5 (35). Following the Kraepelinian practice in defining clearly separated diagnostic categories and Schneider's hierarchy of symptoms, current classification systems (ICD-10, DSM V) offer a checklist of category-driven operationalized criteria that lie somewhere between FRS-weighted and polythetic approach (with DSM-5 finally moving away from unbalanced focus on FRS). A person is diagnosed with schizophrenia if they meet a specific number of symptom-related criteria (with specific symptoms playing a more prominent role), as well as additional criteria regarding their duration and functional impairment. In DSM-5 (36), two symptoms from the list including both positive and negative symptoms (delusions, hallucinations, disorganized speech, disorganized or catatonic behavior, negative symptoms) need to be present most of the time during a one-month period. Additionally, at least one of those symptoms needs to be delusions, hallucinations, or disorganized speech, there must be a reduction in premorbid functioning (work, social, interpersonal), and signs of the disturbance must persist for at least six months. General principles of diagnosing schizophrenia from DSM-IV have been carried into DSM-5, with changes that include the above mentioned elimination of the focus on FRS and, the elimination of schizophrenia subtypes of questionable validity, but also a more precise demarcation between schizophrenia and psychotic mood disorders (37).

1.1.2. Epidemiology, burden of illness, and outcomes

Schizophrenia has long been regarded as a low prevalence disorder with small variations in prevalence across different countries, or between sexes, but newer findings on the epidemiology of the disorder are far from consistent. For example, although 1% lifetime prevalence has previously been relatively consistently reported in the literature, there are now differing reports that question that estimate. Based on three systematic reviews, McGrath et al. (38) found that median SCZ incidence is 15.2/100,000 (with central 80% showing variation between 7.7 and 43.0), and the median lifetime morbid risk is 7.2/1,000 persons. Systematic review by Saha et al. (39) found median value for point prevalence at 4.6/1,000 (1.9–10.0/1,000), period prevalence at 3.3/1,000 (1.3–8.2/1,000), and lifetime prevalence at 4.0/1,000 (1.6–12.1/1,000). Charlson (40) found global age-standardized point prevalence to be 2.8/1,000 (with 95% uncertainty interval between 2.4 and 3.1). Prevalence is lower in less developed areas, and higher in migrants than in native-born population (38, 39). There are significant global variations between countries and regions (41). While some reports show no difference in prevalence estimates between male and female SCZ patients (39, 40), they also report incidence rate ratio between male and female patients to be 1.4:1, stating that for every three men that develop SCZ there will be two women with the same disorder (38). Peak incidence is found at an earlier age for males (15-25 years) when compared to females (25-35 years) (42), but females do show a second peak in middle age (41).

Unlike some conflicting findings on incidence, prevalence, variability and sex ratio in schizophrenia, there is a consensus on the burden this disorder presents. A burden of every single disorder depends on the age at onset, nature of impairment, and tendency to develop chronicity. The fact that SCZ appears in late adolescence and early adulthood, a period critical for social, educational and work development, affects a number of mental functions thus compromising functioning at almost all levels, coupled with the fact that it is a chronic disorder, points to the level of expected burden it carries. All-cause mortality was found to be consistently elevated in SCZ patients, with reported standardized mortality ratio (SMR) of 2.6 (1.2, 5.8) and suicide associated with the highest SMR (38). Numerous somatic comorbidities (e.g. cardiovascular disease, cancer, chronic obstructive pulmonary disease, etc.), in addition to accidental deaths and suicide, have contributed to increased mortality in SCZ patients and significant reduction of expected years of life (43-45). Hjorthøj et al. (46) reported the average of 14.5 years of potential life lost (95% CI 11·2-17·8), and, like other authors, they found no sign of reduction in those numbers, with all-cause SMR even increasing over time (38). Given the chronic nature and the impairment it causes, SCZ also produces severe disability with

significant consequent economic burden. The previously mentioned systematic review (40) showed that SCZ contributes to global burden of disease with 13.4 (95% uncertainty interval 9.9-16.7) million years of life lived with disability (YLD). It was listed as the 11th cause of disability in 2013 (47), and the economic burden was estimated to reach 1.65% of gross domestic product with indirect costs reaching up to 85% (48).

With a disorder as heterogeneous as SCZ that potentially carries such a significant burden and functional impairment, trying to elucidate predictors of different outcomes can help in informing the appropriate interventions for those who need it the most. It is difficult to define the outcomes adequately, first because of variations in definitions of remission and recovery, and secondly because patients diagnosed at some point with a schizophrenia-like psychotic episode might end up progressing to another disorder (e.g. bipolar affective disorder – BD). Nonetheless, a favorable outcome was reported for about 20% of individuals with some even achieving complete recovery (36), and there are reports that even a portion of those refusing antipsychotic medications can achieve remission and recovery (41% and 33%, respectively) (49). Using recovery criteria that are based on both clinical and social domains lasting improvement, roughly one in seven individuals diagnosed with SCZ meet the recovery criteria (50). In a study by Wunderink et al. (51), 19.2% of first-episode psychosis patients met criteria for both symptomatic and functional remission. As per Ciompi's study reported by Messias et al. (49), around one-third of SCZ patients are expected to have the course of illness without full and lasting remissions, and therefore with a poor outcome, whereas most of patients seem to show an exchanging pattern of full or partial remissions and recurrences. Since Bleuler's time, positive symptoms have been seen as predictors of better outcome, while a number of studies have recognized specific predictors of poorer outcome and significant reduction in functioning, including male gender, pre-morbid functioning, duration of untreated psychosis (DUP), negative symptoms, lower educational attainment, and symptoms from the cognitive domain (52-55). Although mood symptoms were previously considered to be an indicator of better prognosis, depression in SCZ has been confirmed as a risk factor for completed suicide, functional impairment, relapse, and therefore for poor outcome (56). Negative and cognitive symptoms of schizophrenia have been found to contribute the most to schizophrenia-related disability connected to schizophrenia (57, 58).

Most cognitive domains tested in SCZ patients have shown a clear relationship to functioning at various levels (e.g. social, work), and the score on specific tests can even be used as a predictor of independent functioning in the community and performing daily tasks (59, 60). Apart from being associated with every-day community functioning and performing daily tasks, cognitive domain is associated with educational achievement and work functioning. SCZ patients who are employed full-time show better scores on vigilance, executive

functioning, and working memory than those patients who are unemployed (61), and Evan et al. (62) reported that verbal learning, verbal memory, and cognitive disorganization symptoms could function as predictors of work behavior. Cognitive functioning is also predictive of adherence to psychopharmacological treatment (63, 64), making cognitive impairment an important element in relapse of psychosis. General cognitive ability as measured by intelligence scores, verbal memory, and executive functioning seem to be especially influencing social functioning (65, 66), but all those findings can depend on additional variables, like the stage of the disorder and other symptoms profile. It is important to note, that a number of mediators and moderators may influence the relationships with functional outcome. For example, the processes underlying motivation deficits in SCZ can impair learning during cognitive remediation interventions through aberrant signals for expected value (67).

Absence of clear predictive models of the SCZ outcome or diagnostic indicators, that would help us relieve the burden of SCZ, is a direct consequence of, among other elements, nosological issues, as well as our inability to clearly define the processes underlying the disorder, symptom dimensions, and specific symptoms and their relationships.

1.1.3. Etiology

Complicated etiology hypotheses and pathophysiology models are to be expected in a disorder like schizophrenia, portrayed since the beginning as a heterogeneous disorder (or a group of disorders) with unclear borders with other diagnostic categories. In line with the current bio-psycho-social conceptualization, we can roughly divide its etiology into biological, psychological and social dimensions.

One of the earliest findings was the fact of heritability of the disorder with aggregation of some cases of the disorder in families (4), but even those first studies showed that genetics of schizophrenia does not follow simple monogenic transmission, pointing in the direction of complex genetic underpinnings (68). Apart from being a part of attempts to clarify genetic background of schizophrenia, twin studies allowed us to approximate relative contribution of genetic factors (roughly speaking, of biological aspect) and environmental ones. A large study on twin pairs born in Denmark between 1951 and 2000 (69) found 33% concordance rate in monozygotic twins and overall estimated heritability of 79%, which was comparable to a previous meta-analysis of twin studies (70). Interestingly, comparable heritability was also found for disorders of the schizophrenia spectrum, which will be an important point for a later discussion. Lower concordance rate is seen for dizygotic twins reflecting an expected reduction in risk with reduction of the number of genes shared. Furthermore, genetic risk for an individual with positive heredity risk persists even after adoption into family without history of

schizophrenia (71-73). Presented results, therefore, at the same time reveal a significant genetic risk but, given the monozygotic concordance rate of 33%, also importance of other additional factors (e.g. epigenetic modifications, environment). Epidemiological studies have offered an insight into a number of environmental factors that might interact with genetic risk to bring about the onset of schizophrenia. As already mentioned, schizophrenia was found to be more prevalent in urban and more developed areas, as well as in migrant communities when compared to native populations (2, 38, 39). An association was also found with season of birth, with the perceived risk of prenatal infection (e.g. flu) for those born in the winter (74, 75), and birth complications that include complications of pregnancy (e.g. diabetes, preeclampsia), complications during the delivery, and abnormal development of the fetus (76-78). Recently, there has been a lot of focus on cannabis use as the possible 'second hit' precipitating episodes of psychosis in those with the genetic risk (79-82). Following the above mentioned widely accepted psycho-bio-social model, which includes psychological and social domains as interacting with biological factors, an association was also found between schizophrenia (and wider psychosis spectrum) and lifetime trauma based on the stress-vulnerability model (83, 84).

Chromosomal regions identified as linked with schizophrenia (but also bipolar affective disorder) are 1q, 6q, 13q, 18, and 22q (85-89). With regard to individual genes implicated in schizophrenia, a number of them have appeared often in literature, like disrupted-in-schizophrenia 1 (DISC1), neuregulin 1 (NRG1), catechol-*O*-methyltransferase (COMT), dysbindin/dystrobrevin-binding protein 1 (DTNBP1), and gene for dopamine receptor D2 (DRD2) (68, 85, 90-96). Genes implicated in schizophrenia code for a wide variety of proteins involved in neuronal development (e.g. neuronal migration and maturation), signal transduction, and neuronal plasticity. As presented in the paper by Rees et al. (97), we can divide genetic changes present in schizophrenia into rare, common, and *de novo* risk alleles:

- *De novo* mutations
- Rare copy number variations (CNV)
- Rare single nucleotide variant (SNV)
- Small insertion/deletion mutations and single nucleotide polymorphism (SNP).

Building on previous accumulated knowledge, a significant advance in the field of schizophrenia genetics was introduced by genome-wide association studies (GWAS) that allowed for investigation of common alleles that have a small effect. A large GWAS consisting from combined samples (98) yielded 108 loci with 128 associations. Although a number of loci opened the road for postulation of new theories on etiology of schizophrenia, or strengthening the already existing less accepted ones like links with the immune system, this study also confirmed the leading neurotransmitter theories of dopamine and glutamate.

One of the neurotransmitter theories supported by genetic studies is the most widely accepted and best-known *dopamine theory* of schizophrenia and psychosis. Dopamine theory of schizophrenia rests emerged with the 'lucky' discovery of antipsychotics and realization that these drugs modify dopamine metabolism. This, along with the effectiveness of reserpine in treating psychosis, the realization that drugs that increase synaptic dopamine levels lead to psychotic experiences, and the fact the effectiveness of antipsychotic medications hinges on their affinity for dopamine D2 receptors, has led to postulating the importance of hyperdopaminergic state in schizophrenia (99, 100). Inconsistencies regarding the findings on the level of dopamine metabolites (reduction in dopamine metabolites levels in some patients), and positron emission tomography (PET) studies of D2 receptors showing conflicting results, along with some other findings, have brought about modifications of the initial theory with hyperdopaminergia seen as being located in the mesostriatal pathway and hypodopaminergic state existing in frontal brain regions (101). Frontal hypodopaminergia was thus simplistically seen as the basis for negative symptoms, while striatal hyperdopaminergic state would be expected cause positive symptoms. Present-day conceptualization of the role of dopamine in schizophrenia recognizes multiple roads (environmental, genetic, neurodevelopmental) that lead to the 'final common pathway' of the hyperdopaminergic state in the mesostriatal pathway (dysregulated elevation in presynaptic dopamine level that is released even in the absence of appropriate stimulus) that underpins positive symptoms of psychosis (102). Dopaminergic dysfunction is postulated to give rise to positive symptoms through misattribution of salience (103).

Newer theories on the role of dopamine recognize the fact that heterogeneous clinical presentation of schizophrenia that is much wider than the simple positive dimension (delusions, hallucinations) must involve more than one neurotransmitter system and more than one neural pathway. That is especially the case for negative symptoms and cognitive dysfunction, which can, as previously mentioned precede frank psychosis for significant periods of time and contribute significantly to disability. In line with findings from genetic SCZ studies that identify genes important for glutamatergic neurotransmission, glutamate as the primary excitatory neurotransmitter in the brain has for years been assumed to play an important role in schizophrenia. Those theories are supported by the aberrant glutamate receptor localization in schizophrenia (104), changes in the intracellular effects of the glutamatergic signaling (105), and the fact that N-Methyl-D-aspartate (NMDA) receptor antagonists like ketamine and phencyclidine (PCP) cause schizophrenia-like states with both positive and negative symptoms (106, 107). Integration of dopamine and glutamate theories of schizophrenia has been suggested, with dopaminergic neurotransmission being affected by the glutamatergic projections to the midbrain dopamine neurons (108), either from prefrontal

cortex (PFC) or hippocampus (109). An increasing body of evidence (*post mortem* and neuroimaging) points to the possible preferential dysfunction of NMDA receptors on γ-aminobutyric acid (GABA) interneurons regulating glutamatergic neurotransmission (110-112). Since fast-spiking parvalbumin (PV) GABA interneurons generate synchronous gamma oscillations that are vital for certain cognitive tasks like working memory and associative learning, it is clear that NMDA receptor dysfunction leads to disruption of synchronized activity and can be the basis for emergence of symptoms in schizophrenia (113, 114). Involvement of the widely distributed glutamatergic system in schizophrenia, together with the loss of excitation-inhibition balance with implications for the synchronous oscillations, fits with conceptualizations of schizophrenia as a 'dysconnectivity' syndrome, provoked possibly by the widespread loss of cortical synaptic connectivity (115, 116). Stephen et al. (117) state that the core pathology of SCZ as a dysconnectivity syndrome might rest on plasticity changes caused by aberrant modulation of NMDA receptors by different neurotransmitter systems (dopamine, serotonin, acetylcholine), leading to aberrations in self-monitoring that could underlie FRS. Computational models of disrupted excitation-inhibition cortical balance and its possible effect on behavior have been confirmed in working memory tasks in SCZ patients (118).

Any discussion on connectivity is incomplete without referring to structural changes (gray and white matter changes) in schizophrenia, probably the first aspects of SCZ biology to be investigated. The idea of *dementia praecox* carried within itself the suggestion of inevitable deterioration, in mental functions as well as in presumably brain structure, but the first anatomical and neuropathological studies failed to find anything that would be usable as pathognomonic, with schizophrenia ending up being termed by the neurologist Plum as the 'graveyard of neuropathology' (119). Early pneumoencephalographic research did however show enlarged ventricles in SCZ patients, which might be understood to represent degeneration, that only in some patients exhibited progressive course that was followed by changes in clinical presentation (120, 121). Research on the structure of the brain in SCZ has significantly improved with newer neuroimaging technologies and techniques like computed tomography (CT) and magnetic resonance imaging (MRI), and it showed progression of ventricular enlargement, overall brain volume reduction, reduction in gray matter in prefrontal areas, hippocampus and parahippocampal gyrus, medial temporal and superior temporal regions (122-126). Not all of the findings were found to be progressive in nature, meaning that they might represent a trait feature, and changes in other regions like the amygdala (reduction in volume in early schizophrenia) have also been described (127). The affected regions are important for language processing, emotion regulation, memory, decision making, and a number of other functions that could underlie SCZ symptoms. Described changes were found to generally better chart onto negative and cognitive symptom domains (128, 129), and are

like negative and cognitive symptoms present even before frank psychosis onset (appearance of positive symptoms) or in individuals who are at risk of developing psychosis (130-132). All these findings taken together seem to suggest a strong neurodevelopmental aspect of schizophrenia, but cannot disregard degenerative nature of some of the changes observed after the illness onset. Also, even though antipsychotics are found to contribute to loss of gray matter, they alone cannot explain the entire effect and, furthermore reduction in gyrification in patients has been found to predict response to antipsychotic medications (133).

Cortical gray matter loss was found generally not to be due to loss of neurons but rather due to reduced size of the cell body, dendritic complexity, and spine density, leading to the conclusion that it is the integration and transduction of signals that is primarily affected (134-136). One of the methods that advanced our understanding of connectivity changes is diffusion tensor imaging (DTI) that uses fractional anisotropy (FA) as a measure of myelin integrity. FA anisotropy is based on the constraints forced on the diffusion of water by axon walls (137). Reductions in FA, as the measure of white matter tracts integrity, were found to be present as early as in the first episode of psychosis (FEP) and in those who are at risk of developing psychosis (138-141), and the regions where changes were found include frontal cortex, temporal cortex, parietal cortex, hippocampus, corpus callosum, cingulate bundle, superior and inferior longitudinal fasciculus, and uncinate fasciculus (115, 142). Changes in these connections have the potential to affect cognitive functions like working memory that depend on integration of wide-distributed networks (143). Cognitive impairments were hypothesized to be the result of the disruption in cortico-cerebellar-thalamic circuits leading to 'cognitive dysmetria' (144, 145).

Neuroanatomical changes in SCZ have even been used in pattern classification in attempts to discern possible valid biological predictors of transition into psychosis (146), providing accuracy of 86% and offering a promise of future diagnostic/prognostic tools, while functional connectivity neuroimaging methods, which will be mentioned later, offered new insights into specific changes in SCZ.

1.2. Schizophrenia and psychosis spectrum concept

1.2.1. Overlap of current diagnostic categories

In the previous text, schizophrenia spectrum was already mentioned when discussing a recent twin study (69), and a few outlined elements already hinted at the problem of validity of schizophrenia diagnosis that has important repercussions, not only for the clinical work but also for the research that is supposed to yield possible biomarkers of the disorder. Kraepelinian

dichotomy between non-affective psychosis (*dementia praecox*) and affective disorders (manic-depressive illness) does not come with clear delineation given the absence of pathognomonic signs or symptoms that would not be present in other disorders (147-149), which resulted, as mentioned earlier, in moving away from FRS concept in the newer classification systems (DSM-5) because of its low diagnostic value (150). The fact that different disorders share the same symptoms (e.g. existence of mood symptoms in schizophrenia, and mood incongruent psychosis in BD) leads to lower diagnostic consistency over time, and the possibility of diagnostic category being changed in the course of illness (4, 151). Also, Bleuler's conceptualization of schizophrenia(s) as a group of disorders has not yet resulted in valid subtypes of the disorder, although with as diverse outcomes as we see in schizophrenia (152) one would expect to be able to accurately define and differentiate the subtypes based on specific predictors. Actually, the already existing subtypes were removed from DSM-5 due to lack of their validity (37). The polythetic approach of our current classification systems managed to address problems of diagnostic reliability and reproducibility (153), but given its descriptive nature, so far it almost utterly failed with validity of psychiatric diagnostic categories, if we define validity as pertaining to delineation of categories based on characteristic etiological underpinnings (154).

One of the possible elements that creates an obstacle in pushing forward with explaining the underlying deficits of schizophrenia could be the 'inadequate' patient samples we have used since the first definitions of the disorder. Since the time of Kraepelin and Bleuler our classifications and attempts at elucidation of etiology have depended on examination of individuals requiring care in asylums because of the severe impairment, with patients showing milder impairment not interacting with medical system or exiting care at some point. This concentration of severely ill patients with poor outcomes also creates the room for Berkson's bias, an outcome bias based on research population selection/availability that can lead to spurious correlations (e.g. in co-occurrence of negative and positive symptoms) (155) and consequently even formation of categories based on those correlations (156, 157). In line with that, it was indeed seen that the outcome of schizophrenia worsened with the narrower definitions of the disorder (50, 158). The understanding of categories (diagnostic entities) and psychopathological phenomena of which it consists (syndromes, symptoms) will naturally be hindered by the biases informing the formation of the implicated categories and perceived relationships and the nature of the psychopathology.

One of the ways to address symptom overlaps in psychiatry, other than accepting dimensionality of phenomena and dimensional diagnostic approach, is the use of co-morbid diagnoses or creation of intermediate categories. Understanding the incongruence between Kraepelin's clear delineation of disorders and what was seen in the reality, Jacob Kasanin

described schizoaffective psychosis as a disorder sharing phenotypic expression with both schizophrenia and mood disorders (159). Schizoaffective disorder (SCAD) was difficult to separate from SCZ and BD, as it was seen to appear in both families of those diagnosed with schizophrenia and those diagnosed with bipolar affective disorder (160, 161), and the distinction between those three diagnoses suffers seriously from the lack of reliability (162, 163). There is no clear segregation within families for these disorders (164), and a strong comorbidity index was found between all three disorders (165). Keshavan et al. (166) examined a large sample of SCZ, SCAD, and BD patients using descriptive symptom scale, and found that 45% of cases fell somewhere between prototypical SCZ and BD (significantly exceeding the number of SCAD patients alone). Furthermore, Peralta et al. (167) found no clear distinction point between different adjacent categories of psychotic disorders (including affective and non-affective disorders), and all variables (premorbid functioning, risk factors, clinical presentation, impairment) seemed to be continuously distributed between non-affective psychosis and mood disorders with symptoms of psychosis, supporting the concept of spectra and the continuum model. Premorbid cognition and social functioning seem to differ significantly between SCZ and BD, but these differences diminish after illness onset, as cognitive changes in BD seem to be only qualitatively milder but quantitatively similar to those seen in SCZ (168, 169). Psychotic BD shows, as expected, greater changes in cognition (168), which brings it closer to SCZ. Initially seen as the differentiating factor (with antipsychotics being used to treat schizophrenia and mood stabilizers reserved for BD), psychopharmacological treatment has also moved in the direction of blurring of demarcation lines (170-173), with both classes being used in the treatment of SCZ and BD. The overlap was also confirmed in the studies exploring biological basis of schizophrenia, some of which have already been mentioned.

According to Craddock and Owen (4), the crucial genetic findings leading to the deconstruction of dichotomous view of the relationship between non-affective psychoses and the group of mood disorders include:

- Family studies pointing to co-aggregation between SCZ, SCAD and BD;
- Twin studies proving the existence of some susceptibility genes that defy this nosological dichotomy;
- Linkage studies showing chromosomal regions implicated in both SCZ and BD, in line with the finding of shared susceptibility genes; and
- Identification of genes whose variations mean existence of risk for both SCZ and BD.

A study by Goes et al. (174) reported a shared linkage on chromosomes 13q21-33 and 2p11-q14 between SCZ and BD with mood-incongruent psychotic symptoms, which confers a

risk for familial aggregation and a more severe form of the disorder. Genome-wide linkage scan also revealed linkage at 1q42 and 22q11 (with DISC1 and COMT respectively mapping to those two sites), and the evidence for linkage was contributed across psychosis spectrum by both SCZ and BD (89). The 22q11.2 deletion syndrome, a CNV carrying a high risk for psychosis but also other conditions like autism spectrum disorders (175), shows sensory and executive network disruptions (176). A large BD study found three large CNVs previously associated with SCZ, confirming shared CNVs but also their reduced prevalence in BD (177). A study on dysbindin SNPs showed its importance in a subset of BD patients with psychotic episodes, possibly conferring specific risk for psychotic features across current diagnostic categories (178), and there is plentiful evidence for convergence at the susceptibility locus at G72/G30 (85). Genetic evidence taken together, in line with questionable clinical delineation, supports shared genetic susceptibility risk across SCZ-SCAD-BD spectrum (with extensions into autism spectrum disorders as well). As we would expect from this genetic proof, there is also some evidence for comparable structural changes in SCZ and BD like dendritic spine pathology in pyramidal neurons in dorsolateral prefrontal cortex (DLPFC) (135), and reduction in white matter volume in left frontal and fronto-temporal regions (179). The same study (179), however, also found differing locations of gray matter loss.

With all that was mentioned above, and the fact that almost 50% of BD patients experience psychotic (positive domain) symptoms during their illness (149), it was postulated that psychotic bipolar disorder might present a meaningful subcategory in BD but also of the psychosis spectrum (180).

1.2.2. Conceptualizing psychosis spectrum

Already Bleuler's and other early works on schizophrenia hinted at possible continuum between schizotypy and schizophrenia (5, 181), with term *schizotaxia* introduced by Meehl (182, 183) to signify a not necessarily expressed genetic liability to schizophrenia, and schizotypy describing a number of psychosis-like phenomena related to schizophrenia (184). DSM-5 has formalized the use of schizophrenia spectrum, and recognizes schizophrenia spectrum and other psychotic disorders to include: schizophrenia, schizoaffective disorder, brief psychotic disorder, schizotypal disorder, delusional disorder, schizophreniform disorder, psychosis induced by medications, substance or other medical conditions, other specified or unspecified schizophrenia spectrum and other psychotic disorders (36). It is important to note that psychosis spectrum can be understood as a wider concept than schizophrenia spectrum. Psychosis spectrum itself, however, can be used more narrowly to denote blurry boundaries between psychotic disorders like schizophrenia, schizoaffective disorder, and psychotic mood

disorders (due to previously elaborated lack of valid points of distinctions or clear biological boundaries), or alternatively to portray a wider continuum including psychotic features in numerous other disorders and stretching all the way into psychosis-like experiences in the general population. Schizophrenia then becomes just the 30% of worst outcome cases of the wider psychosis spectrum (156).

Allardyce et al. (157) state that psychosis continuum has been getting more traction due to:

- Distribution of psychotic symptoms in the general population;
- Shared genetic and other risk factors in patients and non-patient populations; and
- The transition to clinically significant psychotic episodes over time.

Psychotic experiences/symptoms were found to be present in the general population with prevalence being reported to range all the way to 17.5% (185). A study by Kendler et al. in the United States (186) showed that 28.4% of the general population endorsed at least one psychosis screening question, and Ohayon (187) reports on 38.7% of the general population sample endorsing hallucinatory experiences, with daytime visual (prevalence 3.2%) and auditory (0.6%) hallucinations carrying the highest risk for actual psychotic pathology. In a large group comparison study reported by Kråkvik et al. (188), 7.3% of those surveyed endorsed lifetime auditory verbal hallucinations, and they also had higher levels of depression and anxiety, as well as more severe life events, and were more likely to be single and unemployed. More than a two times greater prevalence of psychotic phenomena was found in those with depression and anxiety (189). Interestingly, subclinical phenomena from the negative symptoms domain are assumed to be of similar prevalence as positive symptoms, and their co-occurrence predicts later impairment (190). Changes in the cognitive domain are more common in individuals with psychotic phenomena (191, 192), but also in their relatives (193, 194), additionally suggesting an extended continuum. Another element supporting the continuum of psychotic experiences are the socio-environmental risk factors (stressful life events, cannabis use, urbanicity, and childhood trauma) shared across different psychotic disorders as well as subsyndromal psychotic phenomena in general population (195). There is an additive effect for all subthreshold symptom domains, with presence of combinations of subthreshold symptoms raising the risk for future psychopathology and its severity (156). Also, it has generally been accepted that psychosis arises and persists over time in an interplay of susceptibility factors and the environment (195). In addition to explaining the role of trauma or cannabis use on appearance of psychotic experiences, or co-occurrence with other symptoms and their severity, this model could also be used to understand the relationship between different symptom clusters and the environment in a transdiagnostic psychosis spectrum, in

which they impact each other over time and change their connectivity under the influence of cumulative or increasing social and environmental burden (195).

Schizophrenia itself is assumed to represent less than a third of all psychosis spectrum disorders (including schizophrenia spectrum, but also psychotic depression and psychotic BD) whose lifetime prevalence was estimated to be above 3% (196). It was shown that compared to using existing nosological categories, adding dimensional representation of patient symptom dimensions and symptoms also adds to our conceptualization of etiology and outcome, and might prove to be clinically more useful (197). 'Salience syndrome' was used to describe the syndromal nature of schizophrenia and other psychotic disorders with different symptom dimensions (positive symptoms, negative symptoms, disorganization, manic and depressive symptoms) (198), where specific combinations of dimensional psychopathology might warrant categorization. Taken together, these outlined findings, along with research on possible biomarkers (e.g. cognition, neuroimaging) to discriminate the categories failing to find clear boundaries (199), suggest the existence of a psychosis spectrum with largely shared etiology and overlapping symptom dimensions, in which differences arise from an additional genetic burden and the effect of disease modifiers like neurodevelopmental impairments (200). This conceptualization would frame SCZ and BD as being just specific phenotypic expressions on the same spectrum with largely common underlying pathophysiology.

The idea of schizophrenia as a distinct category has additionally seriously been challenged by the Research Domain Criteria (RDoC) initiative (201), with its aim of defining biologically valid diagnoses that do not depend as much on phenomenology, which rests on work of a number of authors suggesting a wider system neuroscience approach including affective and cognitive dimensions in psychosis research (168, 180, 202). The idea of proposed framework is to act agnostically with respect to existing nosological categories, deconstructing them into important clinical phenomena in the hope of linking those with involved brain circuits and the underlying pathology (153). With the hope of defining endophenotypes, measurable biologic traits, instead of diagnosis, it uses domains of dysfunctions (e.g. negative valence system, cognitive system) further subdivided into underlying constructs (e.g. working memory, perception), and links them to lower units of analysis like neural circuits, cells, molecules, and genes (203). While the existing narrow categories of questionable validity (e.g. schizophrenia) might present an obstacle to elucidating the biology of underlying symptoms positioned on a transdiagnostic continuum, approaches like those of RDoC initiative could be used for the future attempts at bottom-up reclassification of disorders (180).

1.3. Thalamus and its role in schizophrenia spectrum disorders

1.3.1. Anatomy of thalamus and its connections to other brain structures/regions

Knowledge on the thalamus in humans rests on the rich history of autopsies, pathological studies, animal studies, but also on recent advances in neuroimaging techniques, including functional connectivity methods. Initially considered as just a simple passive relay station between sensory/motor areas and higher cortical regions, the thalamus has been found to play an active role in regulation and modulation of information transmission to the cortical areas, mediation and modulation of communication between different cortical areas, and even in the control of cortical states (204-208), which makes it relevant for understanding of higher cognitive functions and consciousness (209). Based on the embryonic origin, it can be divided into ventral and dorsal thalamus, with dorsal thalamus representing major aggregation of nuclei we usually refer to when speaking about the thalamus. The ventral part mostly comprises of thalamic reticular nucleus.

The thalamus, a gray-matter structure made up of nuclei with different and wide-distributed projections, is the largest part of the diencephalon. It consists of two symmetrical ovoid structures (hemispheres) whose medial walls represent lateral walls of the third brain ventricle, connected by the intermediate thalamic mass. The anterior part of the thalamus forms the posterior wall of the interventricular foramen of Monro, and the posterior part (pulvinar) lies superior and lateral to superior colliculus. Dorsal (superior) surface of the thalamus is covered by stratum zonale, a thin layer of white matter found in the roof of the third ventricle. Superior part of the thalamus is also in relationship with caudate nucleus, with its head positioned anterior-superior to the thalamus. The internal capsule separates the thalamus from putamen and globus pallidus. The thalamus is continuous with the midbrain tegmentum, and its boundary with the hypothalamus is marked by the hypothalamic sulcus (sulcus of Monro) in the lateral wall of the third ventricle.

Dimensions of the ovoid thalamic structure in humans are around 30 x 20 x 20 millimeters (mm), with estimated around 10 million neurons in each hemisphere (210). Gray matter of the thalamus is roughly divided by Y-shaped white matter internal medullary lamina into anterior, medial, and lateral groups of nuclei, but based on their topographical placement other groups of nuclei can also be conceptualized (intralaminar, periventricular, reticular). In addition to division based on their 'geographical location', thalamic nuclei are also divided according to their general function into:

- Relay thalamic nuclei;

- Association thalamic nuclei; and
- Non-specific thalamic nuclei (intralaminar, periventricular, reticular).

Relay neurons in the thalamus receive excitatory glutamatergic projections from sensory pathways, but also cerebellar and basal ganglia signals, and most nuclei in turn project to one or just few functionally distinct cortical areas (210). Association nuclei receive projections from cerebral cortex and in turn project to association areas of the cerebral cortex, where they exhibit regulatory activity. It also seems that projections from specific thalamic nuclei are not necessarily restricted to one cortical region only, but engage a number of cortical areas, while in turn those cortical areas project onto a number of different thalamic nuclei (211, 212). As indicated by their name, non-specific thalamic nuclei project widely to a number of cortical regions. In addition to projecting to one or more areas of the cortex, thalamic nuclei send collaterals to other brain structures, like amygdala, hippocampus, and striatum (213, 214).

Cortical projections to the thalamus have the property of specifically inhibiting irrelevant information while they strengthen relevant input. Thalamic nuclei also contain a number of inhibitory interneurons that serve as modulators of signal in the thalamus, but the regulatory inhibitory signals are also provided by thalamic reticular nucleus and other neuromodulatory systems (e.g. serotoninergic projections) (215-218). Reticular thalamic nucleus (RTN) is a thin sheet of GABAergic neurons enveloping the thalamus that has a number of afferent and efferent projections with thalamic nuclei, cortical regions, as well as the brainstem. Along with other inhibitory neurons in the thalamus, it plays an important role in the regulation and imposing of synchronous oscillations that underlie a number of important functions like sleep/wake cycle but also higher cognitive functions. Inhibitory interneurons are thought for instance, to be vital players in modulating thalamo-cortical alpha rhythm (8-13 Hz), important for linking sensory input from the retina and visual perception (219).

Since thalamic nuclei receive various afferent projections, as reported by Herrero et al. (210), based on the type of afferent projections received they can be divided into:

- First-order nuclei receiving afferent fibers from ascending pathways, cerebellum, mammillary bodies, as well as cortical projections (from cortical layer 6) that also send collaterals to reticular nucleus;
- Higher-order nuclei primarily receiving input from cortical layer 5 pyramidal neurons (without collaterals to reticular nucleus).

Higher-order nuclei play the role in communication between cortical regions, and therefore in the higher cortical functions (210). Afferent projections to the thalamic nuclei are contralateral, although some of the nuclei receive both contralateral and ipsilateral projections,

while thalamo-cortical connections stay in the same hemisphere except in the case of RTN and midline nuclei (220, 221). As previously mentioned, RTN is reciprocally linked to other thalamic nuclei, which is not the case for other thalamic nuclei and their mutual links thus leaving thalamo-cortical networks mostly well separated.

Although the thalamus represents a relatively well-defined structure, and its nuclei are generally well separated based on different cell size, afferent projections and communication with cortical areas (209), there is still variability between individuals that can be even greater based on age and existence of neurological and psychiatric disorders. It is reported that there is a change (reduction) in the volume of thalamic regions (affecting more anterior portions), as well as changes in the microstructure and integrity of nuclei affecting their projections (222). With over 60 nuclei, there is also a significant discrepancy in terminology describing nuclei and thalamus parcellations in classical studies, which is currently being addressed using neuroimaging and modern computational methods. It has also been suggested to use different level (area, cluster, global) concordance analyses using previously well-established delineations of thalamic nuclei through registration in common space (223), but a detailed report of those attempts would go beyond the scope of this text. The same paper (223), however, also outlines nuclei and regions that carry substantial topographic and functional importance, and that division can be used as a meaningful illustration of parcellation of the thalamus. We can roughly divide thalamus into (223):

- Intralaminar formation with intralaminar nuclei
    - anterior nuclei (central medial, paracentral, central lateral, and the cucullar nuclei)
    - posterior nuclei (centre médian, parafascicular nuclei, and the subparafascicular nucleus)
- Periventricular and midline region (midline nuclei, *substantia grisea centralis thalamica*, subependymal nuclei)
- **Anterodorsal region**
    - anteroventral nucleus (AV)
    - anteromedial nucleus (AM)
    - anterodorsal nucleus (AD)
    - dorsal superficial nucleus (DSf)
- **Medial region** (mediodorsal nucleus MD – medial, central, paralaminar)
- **Lateral region**
    - Motor thalamus
        - ventral anterior nucleus (VA) – medial and lateral
        - ventrolateral nucleus (VL)

- Sensory thalamus
  - ventral posterolateral nucleus (VPL)
  - ventral posteromedial nucleus (VPM)
  - superior ventroposterior nucleus (VPS)
  - parvocellular extension of VPM (VPMpc)
- Geniculate region (lateral and medial geniculate bodies – LGB & MGB)
- **Posterior region** (pulvinar nuclei).

Simplified thalamus divisions reduce the number of groups to three major regions (anterior, medial, and lateral), with pulvinar nuclei being lumped in the lateral region, and geniculate bodies are occasionally completely left out from the thalamus divisions.

Anterodorsal region

Anterior part of the thalamus is positioned between short rostral arms of the Y shaped internal medullary lamina, and it extends to the dorsal surface of the thalamus creating the anterodorsal region. The largest nucleus of the group, AV, also roughly gives shape to the anterior part of the thalamus, and DSf extends posteriorly all the way to the dorsal surface of the pulvinar. Given the difficulty in separating different nuclei in the anterior region, and the fact that they share most of their characteristics, conceptualizations of this region occasionally focus solely on AV. Also, interestingly, interneurons (local circuit neurons) present a significant proportion of neurons of the anterodorsal region, with Dixon and Harper (224) reporting the proportion of 42%. Anterior region of the thalamus is connected to subicular cortex, mammillary bodies (mammillothalamic tract), retrosplenial cortex, but also importantly to the anterior cingulate cortex (ACC), and medial orbitofrontal cortex (OFC), which positions it as a structure important in episodic memory, but also for executive functions and as part of Papez circuit in emotion regulation (225). Reduction of cell numbers in AV was found in individuals with impaired episodic memory due to alcoholism (226). Most projections originate from caudal hippocampal formation either directly by fornix, a major hippocampal output tract, or through mammillary bodies (227). Afferents to this region have also been shown to originate from a number of other neurotransmitter systems, with superior region having the highest innervation density of cholinergic projections to diencephalon, playing a role in the appearance and propagation of theta rhythms (228, 229). Lesions of the anterior region of the thalamus affect memory and cause anomia for proper names and aphasia (210, 230). As reported by Mai and Forutan (231), it is supposed that different nuclei of this region play a role in one of three major functions:

- Cognition – extensive reciprocal connections of AM with a number of rostral cortical areas, including anterior cingulate cortex, thought to contribute to cognitive flexibility and executive functions;
- Synaptic plasticity – extensive connections of AV to retroplenial cortex and hippocampal formation, while playing the role of theta rhythm pacemaker with majority of its cells showing specific rhythmic activity;
- Encoding head orientation and mental navigation – with almost no connections to frontal cortex and projections to postsubiculum and retrosplenial cortex, AD is thought to play a role in manipulation of visual mnemonic processes (227).

Medial region

The medial thalamic region extends from the interthalamic adhesion to the level of posterior commissure, and roughly covers about 2/3 of the thalamus. MD represents the majority of the medial region, but it is not a homogenous nucleus, and is usually divided into medial, central, and paralaminar parts, although other divisions based on cell size and cytoarchitectonic features are also used (solutions for those definitions are not unambiguously supported by findings in humans) (223). This region receives projections from rhinal and dorsolateral prefrontal cortex (DLPFC), but also from amygdala, ventral globus pallidus, and substantia nigra (232-234). Medial portion of this region is thought to be the part defined by afferent projections from the amygdala (235). It sends efferent projections to orbital, medial, and dorsal prefrontal cortex, and the afferents from innervated areas in turn end up in the same general MD area (210, 236). It is exactly this reciprocal innervation between MD and prefrontal cortex that was used earlier for the demarcation of prefrontal cortex. Additionally, different areas of MD reach different specific prefrontal subregions creating separate circuits (medial MD – lateral OFC, caudodorsal MD – medial frontal/cingulate cortex, lateral MD – lateral PFC) (237). We can also use divisions based on the cell features, magnocellular (medial third) and parvocellular (larger lateral portion) MD, to define connectivity, with magnocellular MD receiving projections from ventromedial PFC and medial temporal lobe, and sending projections to OFC and ventromedial PFC, and parvocellular MD reciprocally connected to DLPFC (220, 238, 239). When outlining importance of MD-PFC connections, it is vital to mention that MD nonetheless does not represent the only thalamic nucleus connecting to PFC. Other nuclei like AV, AL, pulvinar, RTN, and intralaminar nuclei also have connections to PFC (221).

In addition to PFC, efferent projections from MD are directed towards cingulate, insular, premotor and parietal cortex (231). The medial region of the thalamus is an important location on the road of important stimuli to the amygdala, and is not expected to play just a passive role

in that process. As stated by Yaniv et al. (240), thalamic input entering through external and extreme capsule, along with the one from sensory cortex areas, allow amygdala to focus attention to stimuli that might present a danger to the individual (231). Activity of MD seems to also prime PFC and makes it more responsive to the input coming from other different brain regions. Communication of MD with the mentioned cortical and subcortical areas implies its role in the circadian cycle and some vegetative functions, integration of somatic and visceral activity, but importantly also in higher functions like different cognitive processes and functioning, as well as emotional processing and integration of other functions with emotions (210). As an example, role of the medial thalamic region and its connection to limbic regions in pain processing involves motivational and affective aspects of pain, unlike the more sensory-centered role of the lateral region (241). Lesions of the medial and anterodorsal regions of the thalamus result in memory and other cognition impairments (although differential contribution of specific areas is difficult to discern), and bilateral infarction that affects medial regions results in a syndrome involving apathy and amotivation (242). Although the thalamus is usually mentioned in the context of most sensory inputs except for olfaction, olfactory information reaches MD as well indirectly through OFC or piriform cortex, while functional neuroimaging studies show activation of MD in olfactory task conditions, and lesions of this route seem to affect olfactory attention (243).

Lateral region

The lateral region is relatively a well defined region, bordered medially by internal medullary lamina, posteriorly by the pulvinar, and laterally by external medullary lamina, reticular nucleus, and internal capsule. Nuclei of the lateral region of the thalamus relay and process sensory and motor information, and can be divided accordingly into sensory and motor parts, with motor parts being positioned in front of the sensory area. Motor portion of the lateral thalamic region can additionally be divided into anterior region (VA) that receives projections from basal ganglia (*substantia nigra* and internal pallidum), and posterior region (VL) that receives projections from the cerebellum (231). VA is additionally divided into medial and lateral parts, with medial VA receiving additional afferents from amygdala and limbic cortex, and VL receiving additional connections from the vestibular system (223). Efferents from the motor lateral region project to premotor, motor, somatosensory, and supplementary cortex, but also to cingulate and prefrontal cortex linked to motor planning, while those areas then project to spinal cord and cerebellum influencing motor activity as well as complex behavior (221, 223). Net activity in VA, as part of the circuit linking cortical areas, basal ganglia and the thalamus, can activate or inhibit internally generated motor activity patterns (244), and cerebellar projections to VL play the role in synergy of multiple muscles, balance, and fine

motor skills (231). Canavan et al. (245) reported how lesions to the region roughly corresponding VA and VL severely disrupt or block relearning of motor tasks. Cerebellar communication with the thalamus plays an important role in movement disorders (e.g. Parkinson's disorder), and lesions to the region corresponding to the area of cerebellar afferents are associated with abnormal movements.

Sensory thalamus is the main relay for somatosensory and viscerosensory inputs, and represents one of the most investigated and well known parts of the thalamus. Somatosensory part consists of VPL, VPM, and VPS, while VPMpc is considered to be a part of the viscerosensory-input sensory thalamus. VPL and VPM are the nuclei that receive mainly contralateral surface and deep sensory inputs, with VPM receiving trigeminal tract, and VPL spinal and lemniscal tracts (231). VPL and VPM project in a topical manner with segregation of modalities to primary somatosensory cortex, postcentral somatosensory areas (246). VPS receives proprioceptive information, and VPMpc receives gustatory information and visceral afferents (cardiovascular, gastrointestinal) and projects to lateral postcentral gyrus, insula (gustatory areas), amygdala, and auditory cortex (231).

Geniculate region (MGB, LGB) is the relay area for auditory and visual information, and their position within the thalamus subdivision has been questioned. They are termed 'bodies' since in addition to nuclei, they contain derivatives of other parts of the thalamus (223). LGB has six layers and receives retinal input (layers 1, 4, and 6 from contralateral retina, and 2, 3, and 5 from ipsilateral retina) and projects via optical radiation to the occipital lobe's primary visual cortex in a topographical manner. MGB receives tonotopically organized auditory information from inferior colliculus with some fibers directly from lateral lemniscus, and projects via auditory radiation to primary auditory cortex on the superior temporal gyrus. Lesions in MGB and auditory radiation can cause auditory illusions, sound agnosia, and extinction of contralateral ear input, while lesions in LGB cause homonymous quadrantanopia and homonymous hemianopia (210).

Posterior region

The posterior region of the thalamus contains pulvinar nuclei that are usually referred to as simply the pulvinar, given there is no clear distinction between different areas and no consensus on the division or nomenclature. The pulvinar represents around 25% of the total mass of the thalamus (247). Pulvinar nuclei show wide distributed reciprocal connections almost exclusively with the neocortex, but with the limbic system as well (amygdala). Medial and lateral regions connect with different cortical and subcortical areas (frontal, cingular, orbital, temporal, parietal), and inferior and lateral regions with primary visual (striate) and

extrastriate cortex (247). As a general rule, as outlined by Mai (231) and based on work by Gutierrez et al. (248), different parts of the pulvinar are reciprocally connected using separate pathways to specific different cortical regions linked to different modalities. LGB and the pulvinar are a good example of the already mentioned first-order and higher-order nuclei respectively, where LGB represents a relay for sensory retinal information and projects to primary visual cortex, while the pulvinar connects to extrastriate cortical regions and receives the majority of its information from the cortex (249). In addition to acting as sensory relay and sending efferents to specific cortical areas, first-order nuclei like LGB also receive projections from cortical layer 6, while higher-order nuclei receive projections from layers 5 and 6, and send projections back to the cortex forming cortico-thalamo-cortical loops. The pulvinar is assumed to play a role in visual attention filtering when exposed to distractors in the surrounding, and it was stated that different aspects of attentional processes depend on the network involving PFC, the pulvinar, and posterior cortical neurons (222).

Other thalamic nuclei

Paraventricular region nuclei are important for wakefulness, but also represent a relay station connecting brainstem and hypothalamus internal states information with higher limbic cortical regions that provide 'emotional context', and it was reported that the features these nuclei 'ascribe' to stimuli include aversiveness, reward, novelty, and surprise (250). Van der Werf et al. (251) suggest that midline and intralaminar thalamic nuclei are important for different aspects of awareness, and outline following groups based on topographical position and assumed activity:

- ventral group – multimodal sensory processing (reuniens nucleus, rhomboid nucleus, and posterior part of the central medial nucleus);
- dorsal group – viscero-limbic processing (paraventricular, parataenial and intermediodorsal nuclei);
- lateral group – cognitive functions (central lateral nucleus, paracentral nuclei, and the anterior part of the central medial nucleus);
- posterior group – limbic motor functions (centre médian and parafascicular nuclei).

Intralaminar and midline nuclei form numerous connections with cortical regions, which led Saalmann (252) to state that along with MD that projects mainly to PFC, intralaminar nuclei connecting with fronto-parietal cortex, and midline nuclei connecting with medial temporal lobe and medial PFC, underlie a number of cognitive functions like attention and memory, as well as reward-based behavior. It was postulated that this is done through modulatory activity on

synchronization between different groups of cortical neurons and their oscillatory patterns (208, 252). Intralaminar and midline nuclei also receive inputs from reticular nucleus. Thalamic reticular nucleus is a non-specific nucleus consisting of GABAergic neurons forming a thin sheet between internal capsule and external medullary lamina of the thalamus. Most neurons linking the thalamus and different cortical areas in either direction send collaterals to reticular nucleus neurons, which then in turn send inhibitory projections to thalamic relay neurons, giving rise to conceptualization of reticular nucleus as involved in changes in activity during sleep-wake cycles, attention and information flow regulation (253). However, despite layer stratification and differential connections of those layers with thalamic nuclei, it was reported that a number of neurons in reticular nucleus receive projections from more thalamic nuclei, which probably enables them to integrate various subcortical and cortical inputs and provide differential inhibition in order to filter specific information flow through the thalamus (253, 254).

Non-invasive neuroimaging methods confirmed the wide-spread connectivity of the thalamus with the cortex, and classification of gray matter based on connectivity patterns with cortex yielded areas corresponding to previous histological findings (255, 256). In summary, it is clear from the previous general overview that the thalamus can indeed be understood as a motor and sensory relay station, receiving glutamatergic sensory input from the periphery and projecting onto specific cortical areas, making it important for wakefulness-sleep cycle, arousal, and primary sensory processing (257). However, the same is not done passively, as it also serves as a sort of the 'thalamic gate' that with the help of local and outside GABAergic inhibitory inputs gates the information flow to the cortex, as well as a site for modulation of the transmitted information. Thalamic inputs can be divided into drivers and modulators, but the separation is not made on the basis of separation of glutamatergic and non-glutamatergic inputs because a number of glutamatergic inputs to the thalamus can also be characterized as modulatory. In the case of glutamatergic connections, drivers are characterized by activating ionotropic receptors and producing larger initial excitatory postsynaptic potential showing paired-pulse depression, and modulators by activating also metabotropic receptors and producing smaller initial excitatory postsynaptic potential with paired-pulse facilitation (257). In the case of first-order relay cells in the thalamus, we can conceptualize glutamatergic sensory driver input from the periphery and the projection being sent to the appropriate cortical area, predominantly to layer 4. However, reciprocal feedback cortico-thalamic communication originating from the cortical layer 6 will have a modulatory effect. In the case of higher-order thalamic nuclei like MD or the pulvinar, projections from the cortical layer 5, however, represent the driver input for those nuclei making them a part of the feedforward cortico-thalamo-cortical loop and the transthalamic route for cortical communication (258). The indirect transthalamic route for communication between cortical areas hints at the role in modulation and 'enriching'

of the information being transmitted between cortical areas, and therefore at the role the thalamus plays in more complex cognitive processes.

Based on the expanded understanding of the role of the thalamus in integration of sensory and motor information with inputs from the limbic system and different cortical areas, as well as in indirect cortico-cortical communication, Wolff and Vann (259) offered a revised model of the 'cognitive thalamus' that plays an important part in cognitive processes like learning and memory, and in shaping cognitive maps/mental representations. The role of the thalamus in these functions seems to be a complex one, as for example MD lesions impair spatial memory tasks but as it seems because of compromised strategic aspects, motivation, reward-related functions, impulsivity, and interference sensitivity (259, 260). In communication with cortical areas, the thalamus contributes to maintaining, monitoring and updating mental representations that are crucial for the successful interaction with the surrounding (259, 261, 262). In addition to corticothalamic and thalamo-cortical connections, links between the thalamus and subcortical structures and the role of integration of subcortical information have also been reported as important for cognitive functions. Cholinergic inputs to the anterior thalamic region are vital for learning and memory, as is its connectivity with hippocampal formation (227, 263, 264). Thalamic projections to basal ganglia (rostral intralaminar, midline nuclei, and centro-médian/parafascicular complex) play a role in behavioral flexibility and have been associated with goal-directed behavior (265-267). Motor thalamic lateral region nuclei are major recipients of projections from basal ganglia, and have been shown to play a role in performance monitoring, value updating, and adaptive behavior (268), while interaction with another recipient of basal ganglia inputs, MD, mediates cognitive components of outcome-specific Pavlovian-instrumental transfer (269). Connectivity of the thalamus and basal ganglia plays a part in language as well, with the thalamus monitoring language-specific cortical activities, while supported by basal ganglia in both perceptual and productive aspects (270). All mentioned facets of thalamic interactions and activity have given rise to more complex models of interacting cortico-striato-thalamo-cortical loops that underlie the complex cognitive functions and behavior, with the thalamus being postulated as one of the possible key areas for information integration (271).

1.3.2.   Previous research on the role of thalamus in schizophrenia

If we take into account that schizophrenia and psychosis spectrum disorders are characterized by perceptual disturbances, affect, motivational impairment, and changes in cognition, and that the thalamus plays a significant role in integration of motor/sensory information and communication with/between cortical areas, it is easy to imagine a role for

thalamic changes and disturbances in thalamic connectivity in schizophrenia (272). The thalamus has been proposed as an important nexus in parallel cortico-thalamic-striatal-cortical loops (273), and, accordingly, changes in thalamo-cortical loops have been proposed as the basis for different symptoms in SCZ (144, 274). Our knowledge of the thalamic changes in schizophrenia rests today on extensive research ranging from *post mortem* studies to structural and functional neuroimaging of different modalities. Furthermore, a possible role of the thalamus in SCZ was also conceptualized early through examination of behavioral syndromes caused by lesions to different thalamic regions. Strokes affecting anterior thalamic region cause apathy, poverty of speech, executive dysfunction, and intrusion of unrelated ideas, and those affecting MD in the medial thalamic region cause behavioral disinhibition, distractibility, apathy, amotivation, and confusion, whereas strokes affecting the pulvinar were reported to less often cause behavioral syndromes that resemble mental disorders (275, 276). Nonetheless, vascular lesion affecting posterior thalamus has been reported to present with paranoid schizophrenia-like syndrome (277). Lesions involving anterior and medial thalamic regions, which in addition to MD and anterior nuclei usually affect also intralaminar and midline nuclei, cause impairment in semantic and working memory, episodic memory, attention, and error monitoring (221).

Lesions of the brainstem and subcortical structures can impair subcortical inputs that modulate and control flow of information, leading to deficits in integration of sensory information and higher cognitive processes and resulting in hallucinations (peduncular hallucinosis) sometimes followed by other behavioral disturbances (278, 279). Analysis of five patients in a paper by Benke (280), as reported by Cronenwett and Csernansky (279), showed a combination of hallucinations and impaired reality monitoring can appear even in lesions affecting the thalamus only.

Structural changes and changes in neurochemistry

The thalamus of SCZ subjects compared to that of healthy controls seems to be smaller, with, although not consistent, volume reduction of around 10% (281). Konick and Friedman (282), in their meta-analysis on either imaging (magnetic resonance imaging) or postmortem studies found small to medium effect sizes, –0.41 for absolute volume, and -0.30 for volume relative to the whole brain. Neuroimaging studies performed on patient population *in vivo* show bilateral volume reduction, particularly in medial region that includes MD, while changes in first-episode psychosis (even antipsychotic naïve), although not consistent, were seen in some studies to be more pronounced or showing larger effect size than in chronic SCZ (283, 284). Some studies that did not find thalamic volume reduction did, however, report

changes in the shape affecting primarily areas that outline association nuclei with connections to different association cortical areas and the limbic system (anterior nuclei, MD, the pulvinar), which was even confirmed in some structural magnetic resonance imaging (MRI) studies reporting specific thalamus regions volume change (279). Regional specific changes hint at the differential contribution of different thalamic subnuclei. Even with conflicting findings, evidence from voxel-based morphometry studies overall suggests reduction in thalamic gray matter in SCZ (221, 285), and Wagner et al. (286) reported reductions in white matter volume as well.

Research into thalamic changes in FEP patients seems overall to support the idea of thalamic changes (reduced volume) independent of the disease stage (283, 287, 288), although possible progressive nature might be masked by different variables like small effect of the change, technical limitations, or sample size (279). Research has yielded conflicting results on the longitudinal thalamic changes in schizophrenia, and Csernansky et al. (289) found no correlation between illness duration and changes in the shape or volume. Furthermore, thalamic volume was found to be reduced in those at an increased risk for developing schizophrenia (first/second-degree relatives of SCZ patients) (290), but thalamus volume in that population was not found to be predictive of transfer to schizophrenia (291). Changes seen in SCZ patients' family members center on areas that connect to frontotemporal regions (anterior and posterior regions) and, like in SCZ patients, it might explain that regional changes can be present even with overall volume generally the same (279). There is still no consensus on the relative contribution of genetic and environmental factors.

Postmortem studies of thalamic pathology in SCZ largely found, unlike in cortical gray matter volume loss, reduction in the number of neurons and glia in MD, although some conflicting results were also reported with no changes in thalamic or MD volume or cell numbers (292). Pakkenberg (293) found 40% reduction in the number of MD neurons in SCZ, which seemed not to be related to medication status (294). A postmortem study on eight SCZ patients using stereologic procedure to count neurons in MD and AV/AM thalamic nuclei, found neuron numbers reduced by 35% and 16% respectively, with MD volume reduced by 24% (281). The role of changes in MD and AV/AM in SCZ patients might additionally be supported by changes observed in the projection areas of those nuclei (DLPFC, OFC, and insular cortex for MD, and cingulate cortex for AV/AM). No reduction in the number of cells was observed in the mentioned projection areas, but there is reduced cortical neuropil, decreased spine density for certain pyramidal neurons, and in cingulate cortex changes in GABA receptors in lamina II and II (281, 295, 296). Reduction in excitatory MD neurons that drive prefrontal cortex was also proposed as the main factor underlying metabolic hypofrontality observed in schizophrenia (281). Structural MRI analyses confirmed reduced volume in medial region that

includes MD but also midline nuclei, even in FEP patients not receiving antipsychotics (297-299). MRI analyses in general revealed volume reduction findings in MD region (but also anterior regions and the pulvinar) consistent with postmortem research (300), with meta-analysis of voxel-based morphometry showing reduced gray matter estimates for the MD region (301). Neuroimaging research on anterior region nuclei is less consistent and, as stated by Pregola et al. (221), implies more morphometric changes than volumetric anomalies.

The pulvinar, another higher-order association nuclei group that connects with a significant number of different cortical association areas and the limbic system (PFC, multimodal sensory association areas in parietal and temporal lobes, visual cortical areas, insula, cingulate, amygdala) has mostly consistently shown to have reduced volume and cell numbers in SCZ (279, 302). Previous studies have found a 19-22% volume reduction of the pulvinar in SCZ subjects (303). Neuroimaging morphometric studies showed changes in the posterior medial thalamus in SCZ, and smaller volume or density of gray matter was shown in both FEP and SCZ patients (221, 299, 304). As reported by Dorph-Petersen & Lewis (303), postmortem studies on the role of the thalamus in SCZ are generally consistent on structural changes in the pulvinar (reduced number of cells and volume), while other changes, including those in MD and findings on lower number of neurons, seem to be less consistent. However, *in vivo* brain mapping study by Cobia et al. (305) reported changes in SCZ group including MD and anterior nuclei, as well as longitudinal changes for MD and the pulvinar. The same study found cortical correlations for the pulvinar in frontal, temporal and parietal areas, and for MD in frontal areas (305). Changes in regions other than MD, anterior, and pulvinar were reported, although significantly less consistently. Byne et al. (302) showed changes in intralaminar nuclei in their postmortem study. The role of thalamic reticular nucleus was also postulated based on changes in sleep spindles seen in SCZ and the importance of inhibitory/modulatory function of reticular nucleus in the circuit including MD and PFC (306). Several proton magnetic resonance spectroscopy (MRS) studies reported reduced thalamic levels of N-acetyl aspartate (NAA), a putative marker of neuronal viability, and function (307). This finding converges on postmortem and neuroimaging studies of neuronal loss and possible dysfunction in the thalamus in SCZ.

Changes in glutamatergic neurotransmission in the thalamus have been postulated due to glutamate's proposed place in SCZ etiology and the role glutamatergic projections play in communication between the thalamus and other areas. NMDA receptor antagonists are used to approximate the underlying impairments and behavioral changes in schizophrenia, and ketamine model has been arguably the most used pharmacological model of SCZ (308). The role of the thalamus in mediation of glutamatergic cortical effects was shown by Sharp et al. (309) through injection of non-competitive NMDA receptor antagonist (MK801) directly into the anterior thalamus. This procedure caused the same cortical changes as systemic injection of

the antagonist, hinting at the possible thalamic role in the glutamatergic changes underlying psychosis. Review of the literature suggests that glutamate receptor abnormalities and changes in other molecules involved in glutamatergic neurotransmission are present in the thalamus of SCZ patients (310). Pratt et al. (311) suggested that thalamo-cortical loops dependent on glutamatergic neurotransmission, and playing an important role in creating synchronous oscillations vital for cognitive functions, might present a window into the origins of SCZ. In addition to glutamate system changes, elevated dopamine was found in MD and the anterior region of the thalamus, a finding that seems to be independent of the medications, although these findings have been questioned (307). Yasuno et al. (312) used PET to define MD and the pulvinar as regions with low D2 binding, and theorized about the role of dopaminergic changes in these thalamic regions for positive symptoms of schizophrenia. Dandash et al. (313) postulated the role of dopamine system dysfunctions in the fronto-striato-thalamic network in psychosis.

Thalamic connectivity changes in SCZ

Connectivity can be divided into structural and functional connectivity, assessed by different methods. As thalamic functional connectivity (primarily in the context of fMRI) will be discussed later on, this brief overview will focus just on the changes in structural connectivity between the thalamus and other brain regions. Thalamic dysconnectivity is postulated as a theoretical model explaining SCZ symptoms and, as expected, its structural changes aspect is supported by experimental findings. Morphometric correlational studies using cortical thickness, showing patterns similar to DTI data, were used to assess disruption of thalamo-cortical connections, and found reduced connectivity in bilateral inferior frontal gyrus, left superior temporal gyrus, and right parieto-occipital region in SCZ patients (314). Volumetric white matter studies found reduced volume of the anterior limb of the internal capsule, a structure that connects the thalamus with DLPFC and anterior cingulate cortex (315).

DTI, a MRI modality used to determine FA of water diffusion approximating white matter tracts continuity, is most commonly used to investigate structural connectivity. Wagner et al. (316) detected lower FA in the right anterior limb of the internal capsule, right thalamus, and the right corpus callosum of SCZ patients. Meta-analysis by Bora et al. (301), looking at volumetric and diffusion-weighted images, found decreased FA in anterior thalamic radiations (but also other white matter tracts like fornix and cingulum) in SCZ. In line with changes seen in anterior thalamic radiation, which connects the thalamus to frontal cortical areas, Clark et al. (317) showed increased mean diffusivity in anterior thalamic radiation of SCZ patients. DTI and probabilistic tractography study by Marenco et al. (318) showed reduced connectivity with

lateral PFC, and Kubota et al. (319) reported lower FA in the right thalamo-orbitofrontal pathway in SCZ patients. Dysconnection with OFC, as evidenced by reduced FA in right thalamo-OFC, correlated with thickness of the right frontal polar and lateral orbitofrontal cortices (319). A multimodal study by Wagner et al. (320) showed disrupted white matter connectivity in MD and fronto-cingulo-thalamic network, indicating that this might present the underlying cause of the fronto-cingulo-thalamic dysconnecitivty. These findings are in line with the previous works that have identified thalamic connectivity changes primarily in networks with frontal regions (221, 321). With regard to connectivity of specific thalamic regions, Mitelman et al. (322) reported that correlation between right putamen volume and OFC and occipital cortex, as well as centromedian nucleus and DLPFC, differed between SCZ patients and healthy controls.

Even brain region that were not in focus, like cerebellum, have been recently more widely investigated, with thalamic-cerebellar connectivity changes in schizophrenia being confirmed across different modalities (323). Since communication between cerebellum and cortex takes place through thalamus, and having in mind the existence of important non-motor cerebellar functions, those changes are to be expected, and play an important part in developing models of the disruption in widely distributed networks underlying schizophrenia pathology.

In line with cognitive and other changes found in first-degree relatives and those at risk for psychosis, assumptions have been made about the existence of the same thalamic connectivity change patterns in those populations. MRI showed reduced volume of the anterior limb of the internal capsule in the population at increased risk for developing schizophrenia (324). Probabilistic tractography study by Cho et al. (325) revealed reduced thalamo-OFC connectivity in FEP patients, while individuals at risk showed the same but attenuated pattern, identifying connectivity changes as possible biomarker candidates.

Thalamic pathology and symptoms

There are no consistent findings regarding the relationship between clinical correlates and thalamic pathology, which is to be expected given the reported inconsistencies in the pathology itself stemming from numerous methodological limitations and the heterogeneity of the disorder being investigated. Reduced thalamic volume has been associated with reduced cognitive performance, thought disorder, bizarre behavior, impaired integration of sensory information, and hallucinations (279). Bilateral thalamic volume reduction showed significant correlation with the total scores of the Positive and Negative Syndrome Scale in FEP, and it was suggested that decreased thalamic volumes might serve as a biomarker in discriminating

FEP patients with and without auditory verbal hallucinations (326). The already mentioned probabilistic tractography study (325) found that the strength of the thalamo-OFC connectivity correlated with the Global Assessment of Functioning (GAF) score in those at risk for developing schizophrenia, while FA in the anterior limb of the internal capsule correlated with cognitive performance of the patients (316). In another already mentioned DTI study of SCZ patient population (318), thalamo-cortical connectivity with lateral PFC predicted performance on a working memory task.

Lower relative glucose metabolism in the pulvinar was correlated with positive symptoms and hallucinations, and lower relative glucose metabolism in MD showed association with negative symptoms, and the relationship was globally also found with total symptom severity as measured by Brief Psychiatric Rating Scale (327). On the other hand, volumetric FEP study by Coscia et al. (328) found no correlation between volume reduction in the pulvinar and positive or negative symptoms, but the association was found with impairment in language and executive functioning.

1.4. Functional magnetic resonance imaging (fMRI) in Schizophr Res

1.4.1. Basic principles of MRI and functional magnetic resonance imaging

In attempts to identify possible underlying biological changes in psychiatric disorders, and potentially move away from dependence on solely a descriptive diagnostic approach, different neuroimaging methods have been developed and utilized in psychiatry. Neuroimaging has become common in the diagnostic process in clinical psychiatry, allowing us to identify neurological/medical conditions that can present with different psychiatric syndromes (e.g. frontal and temporal lobe tumors, developmental and traumatic lesions), but has also found its place in identifying treatment targets and drug discovery (329). As outlined by Phillips (330), development of neuroimaging modalities and their application in psychiatry has the potential:

1. To provide a tool in differential diagnosis process;
2. To provide information on risk of developing mental disorder in at-risk population; and
3. To help identify those most likely to respond to a specific treatment modality.

Neuroimaging has also been combined with genetics in order to elucidate genetic/molecular underpinnings of observed structural and functional neural changes in psychiatric disorders (329). Neuroimaging modalities can be divided into structural and functional neuroimaging techniques. Most commonly used structural techniques are CT and MRI, whereas most commonly used functional techniques include PET, single photon emission

computed tomography (SPECT), and functional magnetic resonance imaging (fMRI). Neuroimaging modalities using radioligands (PET, SPECT) are still widely used to determine receptor density and distribution, release of specific neurotransmitters, neurotransmitter receptor binding and changes with regards to changed conditions, but also changes in the local metabolism and blood flow (330). Those techniques, however, are tied to the requirement of specific facilities and services, which led to fMRI taking front place among functional neuroimaging modalities in psychiatry but also for imaging of normal brain activity (331).

MRI signal formation is based on the specific magnetic properties of certain nuclei in the human body. Atomic nuclei with magnetic moment and angular momentum (spins) placed in the strong magnetic field show precession axis that is mainly parallel (longitudinal magnetizations) to the magnetic field (labeled as low-energy state) but with some remaining perpendicular (transversal magnetization) to the magnetic field (high-energy state). Those nuclei can be excited through application of resonant frequency energy causing some of them to change to the high-energy state. Returning to low-energy longitudinal magnetization state following removal of the energy source results in energy being emitted, which can be measured in the receiver coil and represents the MRI signal to be used in imaging (332). Decay of transverse net magnetization takes place due to loss of coherence of the spins, owing to interaction of proximate spins with different precession frequencies, but also to additional effect of inhomogeneity of the magnetic field that causes different spin precessions. Changes in net magnetization over time are known as relaxation, and can be conceptualized as:

- Loss of transverse net magnetization coherence after removal of the energy source – *transverse relaxation*
- Return to the longitudinal net magnetization – *longitudinal recovery*.

Those changes, based on the previous conceptualization of relaxation and recovery, and causes for the transverse decay, can be characterized by three time constants:

- T_1 – recovery of longitudinal magnetization over time;
- T_2 – decay of transverse magnetization due to interactions of spins with differing precession frequencies;
- T_2^* - decay of transverse magnetization due to both spin precession frequency differences and inhomogeneity of local magnetic field (333).

By using different sequences that differentially affect one of these aspects of decay/recovery, it is also possible to target tissue with specific properties.

Selection of the area to be imaged is done through a specific match between static magnetic field gradient and the excitation pulse, enabling specific excitation of spins in the desired region and, in order to achieve spatial encoding, additional two gradient fields along

orthogonal axes are applied. In fMRI, those two gradients (phase and frequency encoding) are both applied during data acquisition, alternating rapidly. Spatial resolution is defined by the size of voxels (three-dimensional element of the volume being imaged), and depends on slice thickness (selected by specific frequency of excitation pulse), field-of-view (FOV), and the matrix defined by phase and frequency encoding steps. Most clinical MRI scanners use magnets able to create 1.5 Tesla (T) magnetic fields, and 3T scanners although also used in clinical practice, are widely used in research (7T and >7T ultra-high field systems are also used in research). With 3T systems, resolution for structural MRI imaging is at about 1 mm isotropic, and resolution is lower for functional imaging. Higher strength of the magnetic field improves the strength of the signal relative to other sources of variability (signal-to-noise ratio SNR), spatial and temporal resolution, but also leads to higher magnetic field instabilities, artifacts, and more significant magnetic susceptibility (which, however, can be used in functional imaging) (332, 334).

MRI allows for different types of intrinsic contrasts to be used in image generation, which can yield significantly differing images. Two elements of image formation that influence utilizing different intrinsic contrast are specific timings of the image collection:

- Repetition time (TR) – time between repeated excitation impulses;
- Echo time (TE) – time between excitation and the signal sampling.

Static contrasts (related to spin numbers and types, as well as relaxation specificity) are important in imaging tissues with different characteristics, and protocols taking advantage of those contrasts (e.g. proton density contrast based on number of protons in a voxel) can yield, among others, proton-density-weighted images, as well as most commonly used T_1-weighted (based on the T_1 value of the tissue being imaged) and T_2-weighted images (333). T_2^* contrast represents the basis for the fMRI because of the sensitivity to the levels of deoxygenated hemoglobin in a specific area, and intermediate TE is used in order to make the image sensitive not just to the number of protons but also to field inhomogeneity caused by deoxygenated hemoglobin (333). Another factor influencing the signal is the local chemical environment. Difference in resonance frequency of specific molecules, some of which are important for brain functions, gives rise to phenomenon called chemical shift, and that can be used in magnetic resonance spectroscopy (MRS) for creating spatial maps of resonance peaks that reflect concentrations of the investigated molecules (332). Some of the most important peaks in MRS spectrum reflect concentrations of N-acetyl aspartate (NAA), a putative marker for neuronal loss and dysfunction, as well as choline (Cho), creatine (Cr), and the combined peak for glutamate and glutamine (Glx) (332).

BOLD fMRI

Functional MRI uses principles of MRI with subjects being placed in scanners able to create strong magnetic fields and radiofrequency pulses, and conceptually rests on the fact that oxygenated and deoxygenated hemoglobin possess different magnetic properties, with deoxygenated hemoglobin showing significant magnetic moment, which can be used in T_2*-weighted images to measure changes in blood oxygenation. Ogawa et al. (335) showed the specific effect of deoxygenated blood in MRI, and hypothesized that this blood-oxygenation-level dependent (BOLD) contrast could help in identifying areas of increased activity through coupling of neural activity and hypothesized changes in blood flow that follow it (336). As there is an increased neural activity in a specific brain area (e.g. caused by specific cognitive task), there is also an increased flow of the oxygenated blood that reaches the same area displacing deoxygenated hemoglobin that was previously suppressing the signal that is received in the MRI (337, 338). Neurovascular coupling that represents the basis for the fMRI depends on a number of factors (e.g. factors influencing blood flow) and is described by hemodynamic response function (HRF), the change in the BOLD signal following beginning of the neuronal activity and reduction of the amount of deoxygenated hemoglobin present in the specific region. It was postulated that assumed HRF can be used to determine predicted fMRI signal following neural activity, and Poisson and gamma functions were used to describe it (339). BOLD can be generally conceptualized in a series of phases including:

1. Initial dip lasting for 1-2 seconds – initial low-intensity reduction in signal present only in certain voxels, especially seen in higher-strength magnetic fields, that could be explained through increased initial oxygen extractions (337, 340);
2. Peak reached usually 3-5 seconds after the onset of neural activity initiation/stimulus presentation. If there is a prolonged neural activity the peak extends into a plateau (337, 341, 342);
3. BOLD signal decrease with undershoot (fall below baseline) 6-10 seconds after the end of neural activity/stimulus, due to slower return to baseline of the increased blood volume but also due to changes in oxygen metabolism (337, 343).

As already mentioned, the initial dip is not present universally, and even the canonical HRF consisting of the peak and post-stimulus undershoot, because of the complex underlying physiology, shows significant variability related to a number of factors including age, brain region, neural activity difference, vasculature differences, baseline blood flow, specifics of image acquisition, magnetic susceptibility, differences in respiration and heart-rate, but also ingestion of caffeine and alcohol (339, 344, 345). Lindquist et al. (346) summarized issues

complicating conceptualization of the coupling between neural activity and the BOLD response:

- Complexity of the neural activity (that includes glial activity as well) following a specific stimulus, due to its dependence on the stimulus type itself and change over time;
- Significant lag of the hemodynamic response (peak reached at approximately 5 seconds after the stimulus) with consequent integration of different neural/glial activity over time;
- Nature of BOLD response as a non-linear integrator.

Nonetheless, Logothetis et al. (347) did report a simultaneous recording of cortical neural activity and fMRI, clearly linking BOLD and neural activity, and Ogawa et al. (348) reported that repeated neuronal activation can produce changes in fMRI signal amplitude on a time scale of 100 milliseconds. Simultaneous recording of fMRI (TR = 100 ms) and magnetoencephalography (MEG) during a visuomotor reaction-time task showed the same sequence of activations across five regions (349). Richter et al. (350) demonstrated that with regard to time course, duration of hemodynamic response can be used as an estimate of the duration of a neural activity. Furthermore, it is also hypothesized that BOLD with its closer connection to local filed potentials more closely reflects information input and intracortical processing than neural output characterized by spiking activity (347).

Imaging sequences, spatial, and temporal resolution

Because of the need for fast imaging that could capture functional changes, fast pulse sequences sensitive to T_2^* contrast have been developed in order to capture a large number of images in a short time period. Images are usually collected rapidly using one of the following approaches (351):

- Echo-planar imaging (EPI);
- Spiral imaging.

The two approaches differ in the way gradients change and consequently in the way they fill k-space. K-space differs from the normal image space, as it is a Fourier transform of the MRI signal, and all points of that space contain information from all locations of the actual image (352). We can envision it as a raw data matrix that is filled during the image acquisition, and after the entire k-space is filled, inverse Fourier transform can be used to reconstruct the actual image from those data. Previously mentioned additional gradients (perpendicular phase and frequency encoding gradients) are applied to specifically alter spins of different voxels,

and information can therefore be coded in a matrix using those axes (i.e. k_x, k_y, and k_z). In EPI, there is a rapid strong gradients switching (alternating directions of the sequential lines being scanned) used to fill the k-space after a single excitation with 90° and 180° RF pulses (352). Spiral imaging, on the other hand, uses sinusoidal gradient changes to fill the k-space starting at its center, improving the acquisition rate but requiring another analytical step before using Fourier transform to reconstruct images (353).

Spatial resolution of BOLD fMRI depends on a number of factors, such as slice thickness, FOV, and matrix size but, generally, reducing the size of voxels in BOLD fMRI is limited by the fact that smaller voxel size means reduction in SNR and simultaneously increase in time of the image acquisition (337). Lower SNR presents a problem in situations where we do not have a significant neural response, and prolonging image acquisition time leads to significant T_2^* decay and therefore blurring of the image. Spatial resolution of BOLD fMRI at usually 3-4 mm is significantly better than that of PET and SPECT, but research on ocular dominance columns in primary visual cortex has also managed to produce resolution of under 1 mm (354, 355). Larger voxels carry with them the issue of inclusion of different tissues and loss of spatial specificity in the vascular system (contribution to the signal from larger vessels), which is, however, minimized in spin-echo sequences that use second 180° pulse to generate signal changes and can eliminate BOLD signal from extravascular components of larger blood vessels (337). Ultra-fast imaging was made possible by advances in gradients technology, allowing for complete image data acquisition in under 1 s (50-100 ms), but results in significant loss of resolution (356). Ultra-fast imaging, however, would allow for better sampling of the different hemodynamic responses, even repeated ones. As seen from previous points, in trying to visualize neural activity that often lasts for less than 1 s, with fMRI we measure the signal linked to the hemodynamic response that lasts for over 10 s. With regard to temporal resolution, BOLD fMRI could be said to have intermediate temporal resolution given that it can discriminate well events that are a few seconds apart, and the estimate of the highest temporal resolution in fMRI lies at a few hundred milliseconds (337). Temporal resolution is determined by TR and vascular system limitations, opening the path for TR manipulation during the BOLD fMRI, but very short TRs can require smaller flip angles and consequently reduction in the signal received (337). Flip angle reflects the change towards transverse plane following excitation, and with longer TRs a 90° flip angle can provide for maximum signal.

Another factor limiting our ability in predicting hemodynamic response is the deviation from the expected linearity of the BOLD response. While we might expect scaling and superposition of individual events to be present, as supported by experimental evidence, there is also deviation from the linearity at shorter intervals (< 6 s) due to reduced response to a quick subsequent stimulus (337, 343). Dependency on refractory effect and consequently

deviation from linearity can also vary in different brain regions as evidenced by differences between primary brain motor regions and higher motor regions reported by Birn et al. (357). With advances in event-related trial design, such as the use of selective trial averaging, it is possible to measure even activations closer apart in time (358).

Data preprocessing in fMRI

Signal changes in the cortex during common stimulation tasks are usually only under 3%, and visually resulting images would seem virtually identical, which makes it clear that any additional factors introducing variability can significantly affect the results (359). It is because of that, and because of a significant number of factors affecting BOLD fMRI signal, that computational preprocessing steps of fMRI data are done prior to initiating statistical analyses. We define functional SNR as quantitative relation between intensity of the signal linked to neural activity and the variability introduced by all sources of the noise (360). Even the strength of the magnetic field can present an issue. Although higher field strength intuitively means a higher functional SNR, the relationship is not linear, and there is also an increase in the number of voxels being activated, as well as decrease in T_2^*, which means the signal must be acquired more quickly. Peters et al. (361) showed an approximately linear increase in relaxation rate T_2^* (shorter T_2^* value) with increasing field strength. In addition, there is a significant loss of signal with higher field strengths in brain areas where air and tissue border each other (e.g. ventral frontal regions), which is termed *susceptibility artifact*.

Main causes of noise in fMRI are (360):

- Intrinsic thermal noise (increasing linearly with the field strength);
- System noise linked to scanner functioning;
- Head motion artifacts;
- Physiological noise (e.g. heart rate, breathing, fluctuations in blood flow, oxygen metabolism);
- Variability introduced by neural activity not related to the task;
- Variability introduced by specific cognitive and behavioral patterns of task performance.

As mentioned previously, increase in field strength is not followed by linear increase in SNR, and one of the reasons for that is the fact that physiological noise increases significantly at higher field strengths, becoming the dominant noise and influencing SNR (362). Although there are different approaches and protocols of preprocessing BOLD fMRI data prior to statistical analyses, we can generally include the following steps in fMRI data preprocessing (360):

- Quality assurance identifying common artifacts;
- Correction of slice acquisition time for interleaved acquisition (odd-even acquisition where adjacent slices are not collected at adjacent time points) through methods such as temporal interpolation;
- Head motion correction through coregistration (spatial alignment) to a reference volume by methods like rigid-body transformation (using three translations along x, y, and z axes, and three rotations through all planes). Filtering methods can also be used to remove motion related artefacts;
- Distortion correction by using magnetic field mapping, or in case field maps are not available, by bias field estimation;
- Functional-structural images coregistration;
- Spatial normalization (compensating for shape differences) into a common space enabling inter-subject comparisons;
- Temporal filtering used to remove specific frequency components (e.g. low-pass filter removing physiological oscillations, or prewhitening procedure for removing autocorrelations in a data time series);
- Spatial filtering used to smooth fMRI data across adjacent voxels and increase functional SNR as well as to improve the validity of statistical tests used.

The use of different preprocessing steps is also related to a number of methodological issues. For example, in case of spatial filtering, filter's width might not match activation extent adequately (e.g. too wide filter) leading to attenuation of meaningful activations below the selected threshold (360). Spatial smoothing, temporal filtering, and motion correction have been shown to have significant impacts on fMRI results, and it was additionally demonstrated that those effects might be subject-dependent, leading to suggestions of creating individually-optimized preprocessing pipelines (363).

FMRI study designs and analyses

There are two main task-based experimental paradigms used in fMRI research, blocked design and event-related studies. Blocked design studies include presentation of stimuli or experimental conditions in alternating blocks, allowing for good detection of significant signal provided the blocks are not too short and there is sufficient difference in BOLD signal between the blocks (364). Event-related design, on the other hand, can present stimuli (events) one at a time and in a random order. Averaging responses from several epochs (time segments linked to the stimuli) can identify stimuli-induced signal changes (hemodynamic response). Although blocked design is better at detecting activations, event-related design will

show advantages in estimating shape and the timing of hemodynamic responses (364). Mixed designs combine the characteristics of the two described designs, using discrete blocks but with multiple types of stimuli presented within each block, theoretically allowing us to distinguish between different activations caused by different designs. As reported by Casey et al. (354), design and interpretation of results depend on duration of the event/stimulus, rate of presentation, its intensity, but also on the type of stimulus, and the affected brain region.

In addition to studies aiming at localization of function to a specific brain region, most often achieved through tasks specifically targeting certain function, in fMRI research there is also an approach focusing on functional connectivity between different brain regions. One of the designs commonly used in functional connectivity studies is the resting-state connectivity that requires administration of no tasks or experimental paradigms but aims at identifying intrinsic task-independent neural activity. Low-frequency synchronous BOLD oscillations (signal changes) are detected while subjects lie awake in the scanner with no administered task, and are used to infer functional connectivity of the brain areas. Biswal et al. (365) reported that low frequency (< 0.1 Hz) fluctuations in resting state showed significant temporal correlation within sensorimotor cortex as well as with time courses in other regions associated with motor function. Using that approach, Raichle et al. (366) described the so-called *default network* that showed significant baseline activity at rest (without performing a task) that decreased during activation due to the variety of tasks. Although initially dismissed by some as artifacts, synchronized oscillations in BOLD fMRI were robustly confirmed by later studies and the fact that they followed structural connectivity pathways and were dependent on their integrity (367, 368). Physiological oscillations (respiration and heart activity) have a different frequency pattern compared to the low frequencies of interest in in resting-state fMRI (0.01–0.1 Hz) (369). As mentioned previously, data preprocessing steps allow us to regress out physiological noise, or aliasing of high frequencies into the lower resting-state frequencies can be prevented by using high-sampling rate (369-371). In recognition of the importance of the fact that synchronized BOLD fluctuations reflect the underlying functional connectivity of the brain regions, resting-state fMRI was finally also identified as one of the core techniques used in the Human Connectome Project (371-373).

A number of different methods for interpreting resting-state fMRI data and elucidating functional connectivity between different regions have been proposed, but they can roughly be divided into:

- Model-dependent approaches;
- Model-free approaches.

Model-dependent methods are also called region-of-interest (ROI)-based connectivity analyses, as they are based on *a priori* selection of ROI. ROI can be selected based on the well defined anatomical boundaries or taken from traditional task-based fMRI analysis. Correlation of time series of the selected seed region with time series of voxels in other brain regions can be done through different methods such as partial correlations, multiple regressions, and cross-correlation coefficient in order to create the functional connectivity map. Even though seed-based analyses are simple in terms of the computations, there is inherent bias in the seed selection (374).

Model-free methods were developed to avoid *a priori* assumptions or definitions of specific regions to focus on, and to allow for data-driven identification of whole-brain connectivity patterns. These methods look for patterns of connectivity across different brain regions, and some of the methods used include independent component analysis (ICA), principal component analysis (PCA), and clustering methods (371). In ICA, multivariate decomposition is used to separate BOLD signal into spatial maps of independent functional networks, populated by z scores resulting from the correlation between the time series of each voxel and that network's mean time series (374). Clustering methods aim at grouping data points into non-overlapping subclusters of high-level and low-level similarity. Regardless of points of distinction and specificity, seed-based methods, ICA, and clustering-based methods all show a significant overlap supporting the existence of functionally connected networks in the human brain at rest (371). Graph theory and graph analytical methods have recently been used to gain additional insights into the organization of local and global brain functional networks. Computing functional connectivity between node pairs and identifying significant functional connectivity (by using predefined threshold or weighting), yields a graph representation of functional networks and forms the basis for subsequent analyses of its organization by using graph theory (371). As an example of the previously stated, identifying the nodes with a higher degree (total number of connections) points to locations vital for information flow within a specific investigated network (375).

An important statistical approach in analyzing BOLD fMRI data from different experiment types and research models is the *general linear model (GLM)* used in multiple regression analysis. GLM has the potential of incorporating other tests like t-test and correlation analyses, allowing for significant flexibility in answering research questions (376). GLM is based on a set of matrices including non-spatial data matrix representing fMRI data, and design matrix specifying linear model to be evaluated. In addition to regressor of interest that predicts hemodynamic changes in the brain, GLM design matrix can include various nuisance regressors assigning additional variance to those specific regressors and leading to an increase in significance of results. Creation of different contrast weights in the matrix allows

for testing of predictions with regard to different regressors in the matrix and the research hypothesis, and different contrasts can additionally all be entered together into an F-test. Another important element pertaining to fMRI data analysis is the multiple comparisons issue giving rise to Type I errors (false positive results increasing with the number of statistical tests). The most common way of dealing with this issue are methods such as the Bonferroni correction and false discovery rate (376).

BOLD fMRI offers numerous additional opportunities of combining that research modality with others that might complement it at different levels (e.g. DTI, electroencephalogram - EEG), or of using it with therapeutic interventions such as transcranial magnetic stimulation of the brain. In addition, it has recently been often combined with machine learning techniques through pattern classification algorithms. Multi-voxel pattern analysis (MVPA) identifies various patterns of voxel activations to predict certain categories through a number of steps including the use of pattern classification algorithms, and has already been utilized in research of different nosological categories as well as phenomena like moral intentions and consciousness (377-379). In line with the growing interest and attempts of using fMRI data and machine learning for identification of different psychiatric traits, Madsen et al. (380) supported the use of that approach in classification of schizotypy.

1.4.2. Previous fMRI research in schizophrenia, and on thalamic connectivity changes in schizophrenia

Schizophrenia has extensively been researched using BOLD fMRI given the technique's non-invasive nature, temporal resolution, and computational possibilities. That line of research confirmed the previous structural findings and other functional neuroimaging research (e.g. PET), but additionally significantly facilitated research into SCZ biology and our understanding of it, opening new avenues of research. Initial fMRI findings provided mixed results. While previous research found no pathognomonic findings, several regions were consistently identified as involved in schizophrenia and even linked to certain symptom domains, like DLPFC (linked to negative symptoms), ACC, thalamus, and hippocampus (129, 381-384). Functional MRI SCZ research produced some conflicting results (e.g. on similar working memory tasks different laboratories reported both increased and decreased frontal blood flow), possibly at least partly due to better spatial resolution of this technique (194). Tamminga & Medoff (194) reported changes in ACC/medial frontal cortex in SCZ subjects during auditory recognition task in a practiced condition, postulating a 'circuit failure' in limbic cortex and areas of prefrontal cortex influenced by ACC. On the same task, the same authors (194) reported that the hippocampus of SCZ patients has greater blood flow across different

task conditions, and that administration of ketamine reduces that flow in SCZ patients but not in healthy volunteers, in line with possible effects of postmortem findings of reduced NMDA receptor NR1 subunits in schizophrenia. As reported by Anticevic et al. (385), PFC hyperconnectivity seen in early-course SCZ patients is predictive of symptoms, and also showed longitudinal changes that predicted symptom improvement.

SCZ research has benefited significantly from research in cognitive neuroscience, applying previously developed paradigms. Research has shown changes compared to healthy population in motor tasks, working memory, attention, word fluency, emotion processing, and decision-making (386). The most pronounced impairment was found in functions related to frontotemporal systems, memory, learning, and executive functions (386-388). Although certain studies found no deviations in activations following stimuli such as a flashing checkerboard with a simple motor response, changes in activation were found in more complex stimuli requiring information integration (387). Interestingly, changes were shown in FEP patients, as well as in at-risk population. Recent-onset SCZ patients showed DLPFC activation changes during a number of cognitive tasks including working memory (389), and FEP antipsychotic-naïve patients being presented with simultaneous auditory and visual stimuli showed reduction in activation in parietal lobes bilaterally, right thalamus, and right PFC (390). Population at an increased genetic risk shows activation changes generally similar to those seen in SCZ across different tasks (391). Differences in activations associated with emotion processing were reported in both patients and their relatives (392). Generally, as reported by Ruiz et al. (393), SCZ was found to be associated with wide-spread changes in connectivity that affected, in addition to frontotemporal connections, also the connectivity between DLPFC and the temporal lobe, hippocampal formation, parietal lobe, thalamus and cerebellum, cingulate cortex, and limbic regions.

Along with changes seen in different task-induced brain activity, as measured by BOLD fMRI, changes were also seen in SCZ patients with regard to default mode network (DMN) that is active during resting-state and includes posterior cingulate, ventromedial PFC, and angular gyrus and inferior parietal lobe (366). It is hypothesized that executive control disruption can affect DMN activity and cause disturbances of thought (394). Since suppression of DMN is necessary for successful task performance, as expected, SCZ patients and first-degree relatives showed reduced suppression during working memory tasks, and DMN connectivity correlated with psychopathology (395).

BOLD fMRI is also used in combination with pharmacological interventions and computer modeling to elucidate the underlying SCZ pathology even further and bridge the cellular, system and clinical changes as reported by our group (396). Anticevic et al. (397) reported changes in healthy volunteers administered ketamine (PFC hyperconnectivity) that

reflect more closely early-course SCZ, allowing us to postulate the specific role of glutamate system dysfunction in early-course and FEP patients. Functional MRI has also become an integral part of imaging genetics studies that investigate the way genetic variation affects the brain function, activations and connectivity. As stated by Birnbaum and Weinberger (398), initial expectation that SCZ susceptibility genes would be more penetrant at the level of neuroimaging intermediate phenotypes than at the level of psychopathology proved true, and maps of genetic vulnerability showing those intermediate phenotypes have become more common. Almost all major susceptibility genes for SCZ found their place in imaging genetics. Schleifer et al. (176) reported dissociable disruptions in thalamic and hippocampal resting-state functional connectivity in patients with 22q11.2 deletion syndrome, with thalamo-cortical connectivity increased in somatomotor areas and reduced with associative networks. The 22q11.2 deletion syndrome represents a translational models for psychotic disorders and as such serves as a good example of the role of fMRI in detecting large-scale connectivity changes linked to specific underlying causes.

Thalamic functional connectivity changes in SCZ

A number of studies using BOLD fMRI have investigated the changes in thalamic connectivity and yielded relatively consistent region-specific findings (399). Welsh et al. (400) utilized BOLD fMRI resting-state paradigm in a study of 11 SCZ patients and 12 healthy controls, and the seed-based analysis demonstrated existence of thalamo-cortical MD nucleus functional connectivity as well as reduction of that connectivity in the patient population. A larger study by Woodward et al. (401), comparing 62 SCZ patients and 77 healthy control subjects, divided the thalamus functionally based on its connections to selected cortical areas of interest (PFC, somatosensory cortex, motor cortex/supplementary motor area, temporal lobe, posterior parietal cortex, and occipital lobe), and found that the selected areas correlated with mostly non-overlapping thalamic regions. Also, the same study showed a reduced connectivity between the thalamus and prefrontal areas, and at the same time an increased connectivity between the thalamus and sensorimotor regions (401). Wang et al. (402) also reported a pattern of over- and under-connectivity in a resting-state fMRI study of 72 SCZ patients and 73 healthy controls, with over-connectivity found with bilateral precentral gyrus, dorsal medial frontal gyrus, middle occipital gyrus, and lingual gyrus, and under-connectivity with bilateral superior frontal gyrus, anterior cingulate cortex, inferior parietal lobe, and cerebellum.

Resting-state study on thalamo-cortical disturbances in SCZ and BD by our research group, as reported by Anticevic et al. (403), compared 90 SCZ patients with the same number

of matched controls, and converged on the similar findings of bilateral increased connectivity between the thalamus and sensorimotor cortex, as well as reduced connectivity with prefrontal, striatal, and cerebellar regions. The findings of over- and under-connectivity were not independent but strongly negatively correlated, suggesting a common underlying mechanism, and additionally, significant positive correlation was found between over-connectivity with sensory cortex and psychopathology as measured by PANSS total score. Data-driven clustering of thalamus signal performed in the same study (including both between-groups difference clustering and voxel-wise approach using dissimilarity index) showed the dysconnectivity focused on the thalamic area nuclei with significant projections with PFC. Additionally, in the same study (403), the finding was replicated on an independent 23-patient sample to demonstrate its robustness, and similar findings were then confirmed in remitted BD patients. Finally, in order to investigate this finding's utility as a biomarker, MVPA was performed. SCZ patients were classified correctly using thalamo-cortical dysconnectivity patterns with 73.9% accuracy, and the same was seen for BD patients, but with lower accuracy (61.7%).

As indicated by above chance classification of both SCZ and BD using thalamo-cortical connectivity changes, the presence of those changes across different disorders was postulated and indeed proven in other studies. Skåtun et al. (404) examined resting-state fMRI data from 96 SCZ and 57 BD patients compared to 280 healthy control subjects, and reported thalamic connectivity changes in both groups postulating the role of thalamic connectivity across psychosis spectrum. Results of that study showed reduction in within-thalamus connectivity (especially in regions projecting to frontal areas) and in connectivity between the thalamus and left frontoparietal area in SCZ, with increased thalamic connectivity with somatomotor regions in BD patients (404). Furthermore, the same study found that one thalamic sub-region had over-connectivity with sensory areas, while eight other exhibited under-connectivity with frontal and posterior areas in SCZ, and reduced connectivity was negatively correlated with the symptoms. Another study comparing different diagnostic categories compared resting-state data for 50 FEP patients, 50 patients with major depressive disorder, 50 posttraumatic stress disorder patients (all patients medication-naïve), and 122 healthy subjects, and reported that connectivity changes between MD nucleus and prefrontal and parietal regions were transdiagnostic (405). The only finding specific to SCZ in that study was over-connectivity between right MD and right pallidum. Another study by our group, using resting-state data to compare thalamic connectivity patterns of 90 SCZ patients with 73 remitted BD patients, of which 33 had history of psychosis, suggested that BD subjects with psychosis history show thalamic connectivity effects more consistent with SCZ, which points to the possibility of importance of thalamic connectivity patterns in psychosis spectrum (406).

In addition to showing transdiagnostic nature of thalamic disturbances, a study by Gong et al. (405) pointed also to the presence of thalamic connectivity changes early in the course of schizophrenia, which was confirmed in other studies. Woodward and Heckers (407) performed a study on 148 subjects with psychosis, of which 53 in the early-stage psychosis, and 105 healthy control subjects, demonstrating inversely correlated thalamic under-connectivity with DLPFC, medial PFC, and cerebellar areas, and over-connectivity with motor cortex for all psychosis subjects regardless of the stage. The same study also reported that connectivity changes with fronto-parietal network correlated with cognitive functioning (407). A multi-center 2-year follow-up study by Anticevic et al. (408) was performed on 243 subjects identified as at a high clinical risk of psychosis, and found significantly correlated patterns of thalamic over-connectivity with sensorimotor areas and under-connectivity with prefrontal and cerebellar areas that were more pronounced in those who converted to psychosis. The same study also showed correlation between dysconnectivity and the Scale of Prodromal Symptoms score. In line with the suggestion that thalamic connectivity patterns can be used as predictors of psychosis conversion, Cao et al. (409) reported that in the prodromal population the pattern of over-connectivity in cerebello–thalamo–cortical circuitry is more pronounced in those who convert to psychosis, and correlates with disorganization symptoms and time to conversion. Buchy et al. (410) found a correlation between attenuated connectivity between the thalamus and left sensorimotor cortex and younger age at onset of cannabis use in a population at high clinical risk for psychosis.

A recent study by Ferri et al. (411), using resting-state multi-site data from 183 SCZ patients and 178 matched healthy controls, reported thalamic under-connectivity with cerebellum and ACC bilaterally, and over-connectivity with sensorimotor regions (bilateral precentral and postcentral gyrus, middle/inferior occipital gyrus, and middle/superior temporal gyrus). Even more importantly, in the same study positive correlation was found between thalamic-middle temporal gyrus connectivity and delusions and hallucinations, and negative correlation between thalamo-cerebellar connectivity and delusions and bizarre behavior (411).

Task-based fMRI studies, especially targeting cognitive functioning, also reveal clear changes in thalamic activation and connectivity (412). A significant difference was observed between SCZ patients and healthy subjects in activation of the thalamus during procedural learning (413), and some studies have also shown reduced activation of the thalamus in tasks examining working memory (414). Ragland et al. (415) reported increased activation of the thalamus with worse performance on episodic memory encoding phase. Reduced activation of the thalamus in attentional tasks was reported, except in the case of auditory sensory gating tasks, confirming contradictory patterns of over- or under-activation on different cognitive tasks (412). Huang et al. (416) additionally demonstrated, using Dual task condition, that SCZ

patients showed less modulation in MD activation and connectivity with PFC with higher cognitive demand.

2. Hypothesis

Patients with schizophrenia will, using resting-state functional magnetic resonance imaging, show stable and specific patterns of thalamic functional connectivity changes that will correlate differently with specific symptoms of the disorder.

3. Aims of the research

General aim:

To characterize changes in thalamo-cortical connectivity and their relationship with symptom clusters and specific symptoms in patients with schizophrenia.

Specific aims:

1. Using resting-state functional magnetic resonance imaging, to identify in more details the changed patterns of thalamo-cortical connectivity (over- /under-connectivity) in schizophrenia;

2. To determine the relationship of identified changes in thalamo-cortical connectivity with specific positive and negative symptoms of schizophrenia;

3. To determine and quantify the differences in within-thalamus activity and compare results with previous anatomically defined thalamus nuclei subdivision.

4. Subjects and methods

Examination of relationship between changes in thalamic functional connectivity in psychosis spectrum population, measured by BOLD fMRI, was done in a cross-sectional manner across multiple sites, under the combined protocol. Study subjects data pooling and subsequent analyses were performed under the project *Examining Cognition, Emotion, and Individual Differences in Schizophrenia*, extended under name *Characterizing Clinical and Pharmacological Neuroimaging Biomarkers* (Principal Investigator Alan Anticevic, approved by Yale University's Institutional Review Board, Human Investigation Committee number 1111009332). Subject recruitment and the related procedures, as well as assessments, were done as part of the Bipolar-Schizophrenia Network on Intermediate Phenotypes (B-SNIP) consortium initiative, which was created in an attempt to investigate intermediate phenotypes across psychotic disorders (199). Details on recruitment, neuroimaging protocols, and non-imaging data gathered and used for the present analysis are presented separately below.

4.1.   Subjects recruitment procedures

Subjects were recruited and assessed under B-SNIP consortium protocols, with subject recruitment starting in 2008, and the procedures were done across five sites (199, 417):

- Hartford – Yale University/Institute of Living;
- Boston and Detroit – Harvard University/Wayne State University;
- Chicago – University of Chicago/University of Illinois at Chicago;
- Dallas – University of Texas–Southwestern;
- Baltimore – Maryland Psychiatric Research Center.

As per B-SNIP consortium's framework, recruitment focused on probands with SCZ and spectrum disorders (SCAD and BD with psychosis history), their first-degree relatives and healthy controls (199). Probands, non-acute and mostly medicated patients, were recruited through clinical or community referrals, as well as through advertising, whereas healthy controls were recruited through advertising and research registries. Recruitment and consenting procedures were approved by the Institutional Review Boards, and written informed consent was obtained from all participants after explanation of study details. Diagnosis was confirmed through collection of medical and psychiatric histories, and finally using Structured Clinical Interview for DSM-IV Axis I Disorders, Patient Edition (SCID) (418). As already described by Tamminga et al. (199), the collected information went through a review process with at least two experienced clinicians, and cross-site diagnostic conferences were held on a

monthly basis. Additional demographics data was gathered (age, sex, race, level of parental education), and for patients data on duration of illness was gathered as well.

For current analyses, study population was pooled from the B-SNIP study population based on specific criteria and divided into two groups:

- Psychosis probands (diagnosed according to DSM-IV criteria with SCZ and spectrum disorders including SCAD and psychotic BD – BDp);
- Healthy controls with no history of any psychotic (including BD) or depressive disorder (as determined by SCID), and no family history of those disorders.

In order to account for drop out due to fMRI quality issues and matching of two research populations, initial more stringent criteria regarding age and handedness were relaxed and the original B-SNIP criteria were used regarding those two variables, which resulted in the following inclusion criteria for both groups:

- Age 15 – 65;
- Age-corrected Wide-Range Achievement Test (WRAT) reading test score > 65;
- Negative urine drug screening for common illicit psychoactive substances prior to testing;
- Sufficient knowledge of English to participate in testing procedures.

Exclusion criteria shared for both groups, based on B-SNIP exclusion criteria and specific criteria linked to current analyses, were:

- History of significant medical or neurological condition that could affect symptom presentation or cognitive abilities;
- History of seizures or loss of consciousness lasting longer than 10 minutes;
- Any history indicating learning disability, mental retardation, or attention deficit disorder;
- Diagnosis of substance abuse in the past 30 days or substance dependence in the past 6 months;
- Any condition precluding participation in MRI scanning arm (e.g. metallic foreign objects in the body, such as aneurysm clips or pacemakers) and subsequently non-participation in MRI scanning procedures.

As reported by Tamminga et al. (199, 419), B-SNIP at the time of initial reports recruited 933 probands (397 SCZ, 224 SCAD, and 312 BDp) and 459 healthy controls. However, the final study population for presented analyses was selected based on the availability of neuroimaging data, and those data passing quality assessment, as well as group matching of

probands and healthy control groups based on age, sex, handedness, SNR, and information on parental education (comparison of matched populations is reported in more details in the Results section). Study population identified to have neuroimaging data that passed stringent quality control, and to satisfy other inclusion criteria, finally included 655 subjects divided into two groups:

- Probands (N = 436);
- Healthy controls (N = 219).

Five healthy control subjects satisfied the outlined criteria, and passed the neuroimaging data quality control, but were removed during the matching with proband population. Probands included psychosis spectrum patients diagnosed with SCZ (N = 167), SCAD (N = 119), and BDp (N = 150).

Additionally, the population of patients diagnosed with SCZ according to DSM-IV criteria (N = 167) was looked at separately from the entire proband population, and a subgroup of demographically matched healthy control subjects was formed (N = 153) for SCZ-specific follow-up analyses.

Table 1 shows the number of variables that were used for demographics matching and group comparison and that had missing data, as well as the number of subjects with missing data.

Table 1 | Missing values

Variable	N of subjects missing data
Father's years of education	75
Mother's years of education	33
Duration of illness	19
WRAT score	6

There was no discernable pattern to the missing data. Missing data were imputed using IBM SPSS 20.0's fully conditional specification, iterative Markov chain Monte Carlo (MCMC) method with 10 iterations and 5 imputations. As part of the MCMC method, linear regression was used.

For all patients, dosage of administered antipsychotics was converted into chlorpromazine (CPZ) equivalents in order to be used as covariate in statistical analyses (420).

4.2. Symptom assessments

Clinical assessment training for raters was done prior to the initiation of the study, with required reliability set at > 0.85, and rater re-training was done yearly to ensure stabile reliability (199).

Subjects were evaluated after having consented and the testing was done in a cross sectional manner, at one time point, with no follow-up longitudinal clinical data points.

Psychosis symptoms were evaluated using the Positive and Negative Syndrome Scale (PANSS) that consists of 30 items rated on a 1-7 scale (24, 25). Numerical scale used to rate individual PANSS items reflects an increasing level of psychopathology from 1 – absent to 7 – extreme, with clear rating procedures and anchor points used to ensure inter-rater reliability, and data collected through observation during the interview and from reports. Given the number of items and the lowest possible score for each item, the lowest possible total PANSS score is 30, but can be higher even for healthy population since the rating of 2 on any item designates minimal or questionable pathology that, if present, might mean upper levels of the normal range. PANSS items are divided into three domains, positive, negative, and general psychopathology.

Positive:

- P1 – Delusions
- P2 – Conceptual disorganization;
- P3 – Hallucinatory behavior;
- P4 – Excitement;
- P5 – Grandiosity;
- P6 – Suspiciousness/persecutory ideations;
- P7 – Hostility.

Negative:

- N1 – Blunted affect;
- N2 – Emotional withdrawal;
- N3 – Poor rapport;
- N4 – Passive/apathetic social withdrawal;
- N5 – Difficulty in abstract thinking;
- N6 – Lack of spontaneity and flow of conversation;
- N7 – Stereotyped thinking.

General:

- G1 – Somatic concerns;
- G2 – Anxiety;
- G3 – Guilt feelings;
- G4 – Tension;
- G5 – Mannerism and posturing;
- G6 – Depression;
- G7 – Motor retardation;
- G8 – Uncooperativeness;
- G9 – Unusual thought content;
- G10 – Disorientation;
- G11 – Poor attention;
- G12 – Lack of judgement and insight;
- G13 – Disturbance of volition;
- G14 – Poor impulse control;
- G15 – Preoccupation;
- G16 – Active social avoidance.

In addition to calculating scores of each of the three subscales, and in line with alternative 5-dimension symptom conceptualization and recognition of complex nature of some of the items, alternative loading of PANSS items was done according to Van Der Gaag et al. (26), yielding 5 symptom clusters: positive symptoms, negative symptoms, disorganization, excitement, and emotional distress.

Loading of PANSS items algorithm according to Van Der Gaag (26):

- Positive symptoms: P1 + P3 + G9 + P6 + P5 + G1 + G12 + G16 − N5;
- Negative symptoms: N6 + N1 + N2 + N4 + G7 + N3 + G16 + G8 + G13 − P2;
- Disorganization: N7 + G11 + G10 + P2 + N5 + G5 + G12 + G13 + G15 + G9;
- Excitement: G14 + P4 + P7 + G8 + P5 + N3 + G4 + G16;
- Emotional distress: G2 + G6 + G3 + G4 + P6 + G1 + G15 + G16.

Cognitive functioning was evaluated using the Brief Assessment of Cognition in Schizophrenia (BACS), developed for clinical trials to test for major areas of cognitive functioning, all of which have been found to be impaired in schizophrenia: working memory, verbal memory, motor speed, attention, executive functions, and verbal fluency (20). Tests were scored by two independent evaluators, and some tests were randomly selected for scoring accuracy review at NeuroCog Trials (417).

BACS Tests (421):

- List learning (verbal memory)
- Digit sequencing task (working memory)
- Token motor task (motor speed)
- Verbal fluency (processing speed)
- Tower test (executive functions, reasoning, and problem solving)
- Symbol coding (attention and processing speed).

Normative data stratified on age and sex as reported by Keefe et al. (421) are used to calculate total BACS score and score for every individual subtest. Standardized scores (z-scores) are calculated for each measure and for the composite score. As reported by Hill et al. (417), total scores anchored to B-SNIP controls and those anchored to Keefe normative data are highly correlated with r values >0.98.

4.3. fMRI acquisition protocols

MRI scanning procedure was performed at a single time point, with no follow-up neuroimaging scans. Both structural and functional images were collected during one imaging session using 3T scanners at all sites. As already described by Wang et al. (422), foam pads were used to minimize head motions, and ear plugs to reduce scanner noise. There was no task-based paradigm implemented, so subjects were instructed to keep as calm as possible during the scanning procedures, not to think about anything in particular, and to keep their eyes fixated on a crosshair projected onto the scanner screen. Table 2 and Table 3 list details of structural and functional imaging parameters respectively across sites, as already published in Wang et al (422).

Table 2 | Structural MRI Parameters

Site	Scanner Model	TR (ms)	TE (ms)	Flip Angle (degrees)	Slices	Matrix	Voxel Size
Hartford	Siemens Allegra	2300	2.91	9	160	256x240	1x1x1.2
Boston	GE Signa HDX	6.98	2.84	8	166	256x256	1x1x1.2
Detroit	Siemens TrioTim	2300	2.94	9	160	256x240	1x1x1.2
Chicago	GE Signa HDX	6.98	2.84	8	166	256x256	1x1x1.2
Dallas	Philips	6.6	2.8	8	170	256x256	1x1x1.2
Baltimore	Siemens TrioTim	2300	2.91	9	160	256x240	1x1x1.2

Table 3 | Functional MRI Parameters

Site	Scanner Model	TR (ms)	TE (ms)	Flip Angle (degrees)	Slices	Matrix	Voxel Size
Hartford	Siemens Allegra	1500	27	70	29	64x64	3.4x3.4x5
Boston	GE Signa HDX	3000	27	60	30	64x64	3.4x3.4x5
Detroit	Siemens TrioTim	1570	22	60	29	64x64	3.4x3.4x4
Chicago	GE Signa HDX	1775	27	60	29	64x64	3.4x3.4x4
Dallas	Philips	1500	27	60	29	64x64	3.4x3.4x4
Baltimore	Siemens TrioTim	2210	30	70	36	64x64	3.4x3.4x3

4.4. Preprocessing neuroimaging data

Neuroimaging data preprocessing was done according to established protocols, but with specific in-house modifications of the process described previously (176). Following open-source Human Connectome Project (HCP) algorithms, final standard space utilizes the Connectivity Informatics Technology Initiative (CIFTI) file format, allowing for combined cortical surface and subcortical volume analyses yielding high-resolution data (both spatial and temporal) such as in Dense Connectome while minimizing processing requirements (423). CIFTI format supports gray matter modelling both on cortical surface and as subcortical voxels, and spatial dimensions in combined coordinate system are designated as 'grayordinates' (423). HCP-optimized surface and volume visualization platform Connectome Workbench was used for current analyses (424). As in Glasser et al. (423), processing steps followed minimal preprocessing pipeline for both structural and functional data in order to achieve correction of spatial artifacts, cross-modal registration, creation of surface, and alignment to standard space.

Steps followed during data preprocessing, with specific minimal optimizations applied, were already described in detail by Schleifer et al. (176), and included:

1. Correction for bias-field distortions was performed, and FMRIB (Functional Magnetic Resonance Imaging of the Brain) Software Library's (FSL) linear image registration tool (FLIRT) and FSL nonlinear registration tool (FNIRT) were used to register T1-weighted images to standard Montreal Neurological Institute (MNI) 152 coordinate system (425);

2. Segmentation of whole-brain gray and white matter was done to produce individual cortical and subcortical segmentation using FreeSurfer (open source software used to process and analyze brain MRI images) pipeline (426, 427);

3. Cortical ribbon was created using pial and white-matter boundaries, yielding cortical surface, and masks for subcortical gray matter were generated, and both were combined to form CIFTI individual grayordinates matrix (including both surface and volume) (423);

4. Cortical surfaces and subcortical volumes were registered, with surfaces being registered to the HCP atlas group average using surface-based registration (linked to cortical landmark features), and nonlinear registration used for subcortical volumes (423);

5. BOLD data preprocessing included, after being motion corrected, alignment to middle frames of each run using FLIRT, and brain mask was applied to exclude non-brain signals;

6. Conversion of BOLD data to CIFTI format (initial processing for BOLD data done in Neuroimaging Informatics Technology Initiative – NIFTI format) and inclusion into CIFTI gray matter surface/volume matrix, sampling from cortical ribbon, and for subcortical voxels using FreeSurfer segmentation;

7. BOLD data cortical surface was registered to HCP atlas using nonlinear warping based on features of sulci, and subcortical volumes were registered during NIFTI processing in a single step integrating transform matrices for all previous preprocessing steps.

In addition to this minimal preprocessing pipeline, subsequent preprocessing 'de-noising' steps were undertaken, also previously reported by Schleifer et al. (176):

- MATLAB tools (in-house developed) were used for computing signals from the ventricles, white matter, as well as from across gray matter voxels as approximation of global signal regression (GSR) to deal with spatially widely distributed artifacts (428);

- High-pass filter (> 0.008 Hz) was applied to BOLD time series to remove low-frequency noise and possible scanner drift.

Both previous elements were modelled as nuisance variables and regressed out, with all following analyses using BOLD time series that survived these two de-noising steps (176). BOLD SNR was calculated individually using signal's mean and standard deviation (SD) for any slice across the BOLD run, excluding non-brain voxels.

One further step was applied aimed at reducing the effect of movement artifact, following recommendations from Power et al. (429). This 'movement scrubbing' included removing frames that were flagged based on one of the two criteria (176):

- Total displacement across all 6 rigid-body parameters exceeding 0.5 mm (assuming 50 mm cortical sphere radius);
- Root mean square of difference in intensity between current and preceding frame divided by mean intensity and normalized to time series median exceeding a value of 3.

Flagged frame as well as a preceding frame and two subsequent frames were flagged for exclusion, and subjects with more than 50% flagged frames were excluded from analyses (176). Percentage of removed frames was introduced into statistical models as a covariate and was found not to affect the results.

4.5. Data and statistical analyses

Comparison of demographics variables for the two groups of study population (probands and healthy controls) during matching on age, sex, handedness, parental education, SNR, and WRAT, was done using independent samples t-test, and chi-squared test. Statistical significnce was set at $p < 0.05$. Testing of demographics data was performed using statistical program IBM SPSS Statistics 20.0.

As previously mentioned, GLM is the most common approach in analyzing fMRI data, and as such was used as the basis for our thalamic connectivity analyses. GLM, as multivariate regression model, is based on multiple regression with its assumption that the value of observed data (y) could be attributed to linear combination of several regressors (x) and parameter weight linked to a specific regressor (β), and to uncorrelated noise (ε) (376). Expressing that in an equation, linear regression could be conceptualized as:

$$y = \beta_0 + \beta_1 x_1 + \beta_2 x_2 + \ldots + \beta_p x_p + \varepsilon$$

Parameter weight (β) represents how much a specific factor contributes to the observed data, and β_0 reflects contribution of factors that are held constant (376). However, taking into account complexity of fMRI data, when explaining GLM we need to use a set of matrices as described in Figure 1. The model looks for the values in parameter matrix for a specific design matrix that best describe fMRI data with smallest values in the error matrix.
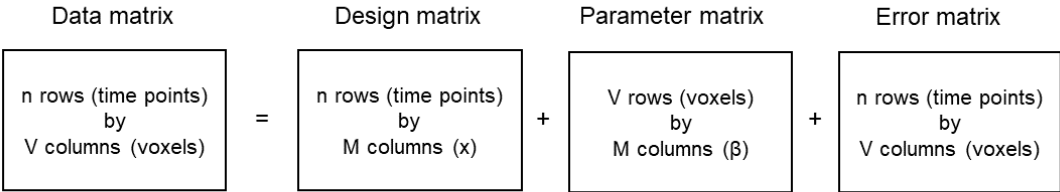
Data matrix		Design matrix		Parameter matrix		Error matrix
n rows (time points) by V columns (voxels)	=	n rows (time points) by M columns (x)	+	V rows (voxels) by M columns (β)	+	n rows (time points) by V columns (voxels)

Figure 1. The basic principle of GLM in fMRI data analysis as described in Huettel et al. (376).

Analyses were performed using FSL's Permutation Analysis of Linear Models (PALM) and numerical computing platform MATLAB (matrix laboratory) (430). PALM allows for a range of regression and permutation strategies, while at the same time being robust to heteroscedasticity (differing distributions of noise) and able to work with non-imaging data and both surface-based and volume-based neuroimaging data. PALM also utilizes robust permutation methods to assess classical multivariate statistics and allows the control of family-wise error rate.

Seed-based connectivity analyses

Our group, utilizing FreeSurfer to achieve individual anatomical segmentation of high-resolution structural images, and the whole-brain seed-based approach, already examined and reported thalamus whole-brain connectivity changes in clinical populations (176, 403). This seed-based approach, looking at the whole thalamus as a single seed, was replicated in the present analyses in order to confirm the previous findings. Thalamus connectivity map was calculated using bilateral thalamus voxels BOLD time series that were averaged to yield single thalamus value. This mean thalamic time series was then correlated with every other cortical or subcortical value in the CIFTI grayordinates space, yielding Pearson's coefficient value. Finally, using Fisher *r*-to-*Z* transform, correlation values were transformed into Fisher-*Z*-values

(Fz) for each voxel, and included into a map in which every voxel value in fact represents its connectivity to the seed region (whole thalamus).

Testing of the main Group effect (probands vs. controls) was done using FSL's Permutation Analysis of Linear Models (PALM) with one-way analysis of variance (ANOVA) where BOLD resting-state connectivity data were the dependent measure. Significance was set at $p < 0.05$. Type I error protection was done utilizing nonparametric permutation testing with PALM algorithm with 1000 permutations (430), and the whole-brain correction was done using family-wise error rate by Threshold-Free Cluster Enhancement method to create spatially contiguous voxels clusters that are above given statistical criterion (431).

In addition, as per specific aim of a more detailed thalamus parcellation, thalamus subdivision was achieved using a recent work from our group by Ji et al. (432) on functional connectivity networks. Identified thalamic subdivision was then used in subsequent seed-based analyses, but this time with results of thalamic parcellation as separate seeds (nine seeds). Ji et al. (432) used previously developed cortical parcellation containing 180 symmetrical cortical parcels per hemisphere (433), extracted average BOLD time series from all 360 parcels, and created functional connectivity matrix that was used to identify linked networks by Louvain clustering algorithm. Using Pearson correlation, voxels were assigned to the network with which they shared the highest mean connectivity, resulting in nine thalamic sub-regions (seeds) as shown in Figure 2. Visualization was done using Connectome Workbench platform.
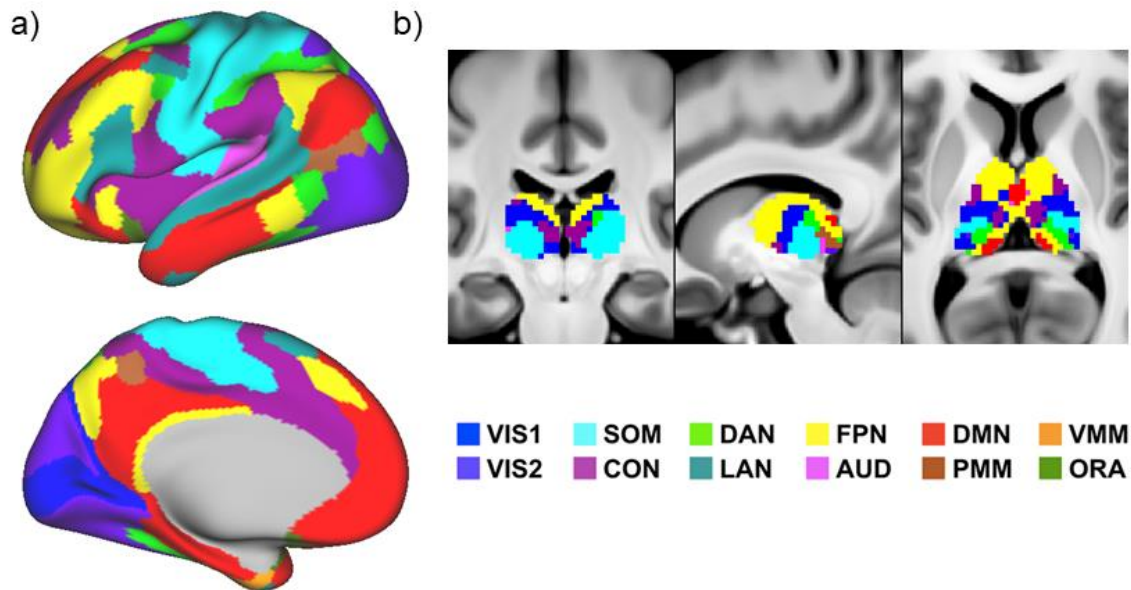
Figure 2. Functional networks parcellation based on Ji et al. (432). a) Cortical networks used to assign subcortical voxels, shown on the rendered image of the left hemisphere (lateral and medial surfaces); b) Thalamic functional subdivision based on voxel assignment to cortical parcels in coronal, sagittal, and axial planes respectively.
VIS1 primary visual, VIS2 secondary visual, SOM somatomotor, DAN dorsal attention, FPN frontoparietal cognitive control, DMN default-mode, VMM ventral multimodal, CON cingulo-opercular, LAN language, AUD auditory, PMM posterior multimodal, and ORA orbito-affective network.

Seed-based analyses were repeated with nine separate thalamic seeds. Time frames from each of those nine seeds were separately averaged across all voxels in *a priori* defined seeds to yield nine seed-specific average values that were then correlated to every other cortical and subcortical value in CIFTI grayordinates space, giving us Pearson's coefficient value. Following Fisher's *r*-to-*Z* transform, Fz maps reflected connectivity of every other cortical and subcortical voxel with specific thalamic sub-region. PALM was used again, now with nine seeds to test group-by-seed interaction effect. Seed-based BOLD resting state fMRI data were analyzed with factors of group (probands and controls) and seeds (nine thalamic subdivisions as separate seeds). As stated for the whole-thalamus analysis, Type I error protection was done through multiple permutations (1000) in nonparametric permutation testing in PALM, and family-wise Type I error correction was additionally applied through Threshold-Free Cluster Enhancement method.

Both whole-thalamus (one seed) and nine-seed analyses were repeated using only a subset of patients (SCZ) and matched healthy controls to examine the possible differences between SCZ effects and effects of the wider spectrum (probands group including SCZ, SCAD, and BDp).

Additional PALM GLMs were computed, to account for possible confounders. GLMs were modeled to include separately age, sex, CPZ equivalents, and duration of illness as predictors to evaluate their effects.

To test the hypothesis that detailed subdivision of the thalamus into nine functionally defined seeds would actually yield little additional information, nine thalamic seeds were finally lumped into two thalamic seeds:

- Sensorimotor – VIS1, VIS2, SOM, AUD;
- Associative – CON, DAN, FPN, DMN, PMM.

All of the previously reported PALM analyses were then performed with this reduced number of seeds (two) with the aim of testing 2x2 group-by-seed interaction, using resting-state fMRI as dependent measure, both with the entire psychosis proband group and the SCZ group separately, with appropriate matched healthy controls.

Clustering

In order to look at thalamic connectivity changes without depending on *a priori* defined subregions, data driven clustering analysis was performed agnostic to prior anatomical or functional parcellations of the thalamus. Between-group resting state fMRI difference in connectivity for all thalamic voxels was used to group those voxels. The method of *k*-means clustering was performed using correlation distance matrix of group-difference resting-state fMRI (176). Given the previous *a priori* 9-seed solution, which was based on previous functional parcellation of the thalamus, data driven clustering was done for k = 1 through k = 9. Clustering steps followed the protocol already published by our group (403):

1. Individual identification of all thalamic voxels using FreeSurfer;
2. Registration using FNIRT (434), after identification of the subject with segmentation that was most similar to the entire group and using that segmentation for non-linear registration of all thalamic voxels across all subjects;
3. Application of non-linear transformation matrix to BOLD voxels that corresponded to individually segmented thalamus volumes;
4. Creation of seed-based connectivity fMRI for each thalamic voxel with all other gray matter voxels yielding connectivity map for each thalamic voxel in each subject;
5. Application of Fisher *r*-to-*Z* transform and calculation of group averaged value for each group;

6. Calculation of group difference map, and dysconnectivity maps for each voxel, to be used as input value for *k*-means clustering;
7. Whole-brain voxel dysconnectivity maps were converted into one-dimensional vectors and used to compute correlation between each pair of thalamic voxels (reflecting similarity in dysconnectivity between those two voxels);
8. Applying *k*-means clustering algorithm that found *k* clusters by grouping voxels with most similar whole-brain dysconnectivity patterns between two groups (1-r was used as the dissimilarity measure).

As already reported by Anticevic et al. (403), in order to avoid the algorithm being caught in local minima, clustering was repeated 10 times for each *k*, but with different random starting point. Solution that yielded smallest distances within a cluster was finally accepted.

In addition to *k*-means clustering, thalamic connectivity was examined to determine which voxels would show the greatest connectivity pattern differences between the two groups. To do so, we used eta^2 index that quantifies similarity between fMRI connectivity maps (ranging from 0 to 1) (435). Similar to steps preceding *k*-means clustering, dysconnectivity maps were converted into one-dimensional vectors, and $1-eta^2$ (measure of dissimilarity between two groups' averaged seed functional connectivity maps) was calculated. Creation of 'dissimilarity map' with $1-eta^2$ value calculated for each thalamic voxel helped in identifying voxels/areas that drive the between-group difference in thalamic connectivity. Voxels with higher $1-eta^2$ were defined as those with the greatest difference in thalamo-cortical connectivity between probands and healthy controls.

Symptoms and functional connectivity patterns

In order to evaluate a possible link between connectivity changes patterns (both over- and under-connectivity) and symptoms, composite scores for PANSS were separately entered in GLM and analyzed using linear regression. Mean Fz was calculated for over-connectivity and under-connectivity effects separately and entered into the model.

Following our previous finding of correlation between thalamic dysconnectivity and total PANSS score, as well as General Psychopathology subscale (403), in addition to total score, General Psychopathology PANSS subscale score was evaluated in a similar linear model. With the aim of a finer parsing of the psychopathology, five symptom dimensions resulting from the alternative Van Der Gaag loading of PANSS items (Positive, Negative, Disorganization, Emotional Distress, and Excitation) were also entered separately in GLM. Furthermore, based on the assumption that biological mechanisms underlying specific PANSS items might differ, linear models for thalamic subnucleus proved to show most specific/prominent changes were

also populated with five specifically chosen items from PANSS scale – delusions (P1), conceptual disorganization (P2), hallucinations (P3), blunted affect (N1), difficulty in abstract thinking (N5), depression (G6), and disorientation (G10). Wider item-based analysis was avoided since, even with applied safeguards, the number of PANSS items would make it difficult to completely control for the Type I error. Five items were chosen to cover different psychopathology aspects, and additionally based on expected reduced rater variability in rating of those items.

Visualization of connectivity data analyses

Statistical results from each voxel in the brain combined formed a statistical map of connectivity changes. Maps that were created are therefore not a direct representation of the brain activity, but a statistical map color-coded according to alpha probability value for voxels (376). Maps were provided with color bars that link specific color palette and values of the statistical test used in the analysis.

Statistical maps were overlaid for visualization purposes on the image representing brain anatomy, either using a two-dimensional structural image of higher resolution (i.e. T_1 image), or three-dimensional rendered images with smooth and high-resolution images formed on the basis of structural images. Depending on the location of the finding that reached statistical significance, underlying structural image can be from either of the three planes (axial, coronal, and sagittal).

For current analyses Connectome Workbench protocols were used. Connectome Workbench is an open source resource written in C++ used for visualization of surface- and volume-based neuroimaging data, especially data that is in line with HCP imaging protocols (424). In addition to visualization platform, Connectome Workbench offers also wb_command for performing a variety of algorithmic tasks on both surface and volume, as well as on grayordinate space data.

Linear regression results were visualized using R, a free software platform for data analysis and visualization.

5. Results

5.1. Study population and demographics

As previously stated, B-SNIP study population initially reported by Tamminga et al. (199, 419) included 933 probands (397 SCZ, 224 SCAD, and 312 BDp) and 459 healthy controls. Following already described pooling of subjects with neuroimaging data that passed quality control and matching of groups, our final study population included 655 subjects divided into two groups (436 probands and 219 healthy controls).

Details of the final study population and matching according to age, handedness, sex, race, parental education, and SNR are reported in Table 4. Table 4 compares proband and matched healthy controls, with reported means and standard deviations or percentage (depending on the variable). Depending on the type of variable, groups were compared using independent samples t-test or chi-square test.

Since follow-up analyses were performed using only SCZ subpopulation and a matched subset of healthy controls, clinical and demographic details of those two matched populations are presented in Table 5. Table 5 compares SCZ and matched healthy controls, with reported means and standard deviations or percentage (depending on the variable). Depending on the type of variable, groups were compared using independent samples t-test or chi-square test.

Group of probands consisted of psychosis spectrum patients diagnosed according to DSM-IV criteria:

- SCZ (N = 167);
- SCAD (N = 119);
- BDp (N = 150).

Table 6 reports differences in clinical variables between these three groups that make up proband population. One-way ANOVA was used for comparison of three proband subgroups, with statistical significance set at the level of $p < 0.05$.

Table 4 | Clinical and Demographic Characteristics - Whole sample

Characteristic	Controls (N=219)		Probands (N=436)		Significance	
	M / %	S.D.	M / %	S.D.	T Value / Chi-Square	P Value (two-tailed)
Age (in years)	37.22	12.18	35.33	12.31	1.87	.062
Gender (% male)	41.55	-	48.62	-	2.93	.087
Father's Education (in years)	13.50	3.57	13.74	3.81	0.75	.454
Mother's Education (in years)	13.16	3.22	13.59	3.05	1.58	.114
Handedness (% right)	84.93	-	85.78	-	1.08	.783
Race (%)	-	-	-	-	8.88	.261
African American	29.68	-	33.49	-	-	-
Native American	0.46	-	0.00	-	-	-
Asian	4.57	-	2.06	-	-	-
Caucasian	61.19	-	59.86	-	-	-
Native Hawaiian	0.46	-	0.00	-	-	-
Mixed Race	1.83	-	2.75	-	-	-
Signal-to-noise	231.40	83.04	218.36	93.45	1.71	.087
Antipsychotic (% yes)	0.00	-	84.17	-	-	-
AP 1st Gen (% yes)	0.00	-	9.17	-	-	-
AP 2nd Gen (% yes)	0.00	-	74.77	-	-	-
Antipsychotic Medication (CPZ equiv.)	-	-	443.19	402.91	-	-
Antidepressant (% yes)	1.83	-	44.27	-	127.51	<.001*
Mood Stabilizer (% yes)	0.00	-	46.33	-	-	-
Anxiolytic/Hypnotic (%yes)	2.74	-	27.29	-	-	<.001*
Anticholinergic (% yes)	0.00	-	12.84	-	-	-
Duration of illness (in years)	-	-	15.24	11.89	-	-
Participant's BACS Z score	0.02	1.15	-1.38	1.35	-13.41	<.001*
Participant's WRAT score	102.28	13.64	98.78	15.00	-2.88	.004*
PANSS Positive Symptoms	-	-	15.67	5.35	-	-
PANSS Negative Symptoms	-	-	14.60	5.11	-	-
PANSS General Psychopathology	-	-	31.46	8.68	-	-
PANSS Total Psychopathology	-	-	61.67	16.34	-	-
PANSS 5-factor Positive Domain	-	-	16.29	6.19	-	-
PANSS 5-factor Negative Domain	-	-	15.23	6.03	-	-
PANSS 5-factor Emotional Distress	-	-	18.58	5.98	-	-
PANSS 5-factor Disorganization	-	-	18.80	5.94	-	-
PANSS 5-factor Excitation	-	-	14.52	4.58	-	-

M - Mean, S.D. - Standard deviation, * - statistically significant difference at the level of p < 0.05

Table 5 | Clinical and Demographic Characteristics - SCZ vs Controls

Characteristic	Controls (N=153)		SCZ (N=167)		Significance	
	M / %	S.D.	M / %	S.D.	T Value / Chi-Square	P Value (two-tailed)
Age (in years)	34.01	11.18	34.09	11.99	0.64	.949
Gender (% male)	59	-	67	-	2.33	.127
Father's Education (in years)	13.78	3.53	13.71	3.05	0.17	.865
Mother's Education (in years)	13.45	3.22	13.53	2.81	0.24	.809
Handedness (% right)	82.35		86.23		1.17	.761
Race (%)	-	-	-	-	16.02	.025*
African American	27.45	-	43.71	-	-	-
Native American	0.65	-	0.00	-	-	-
Asian	5.23	-	1.20	-	-	-
Caucasian	62.74	-	49.70	-	-	-
Native Hawaiian	0.65	-	0.00	-	-	-
Mixed Race	1.96	-	2.99	-	-	-
Signal-to-noise	210.73	70.96	198.10	83.09	1.42	.157
Antipsychotic (% yes)	0	-	90.42	-	-	-
AP 1st Gen (% yes)	0	-	10.78	-	-	-
AP 2nd Gen (% yes)	0	-	79.64	-	-	-
Antipsychotic Medication (CPZ equiv.)	-	-	490.64	395.79		-
Antidepressant (% yes)	0.65	-	37.13	-	69.87	<.001*
Mood Stabilizer (% yes)	0	-	20.96	-	-	-
Anxiolytic/Hypnotic (%yes)	1.96	-	22.16	-	31.57	<.001*
Anticholinergic (% yes)	0	-	15.57	-	-	-
Duration of illness (in years)	-	-	12.93	11.14	-	-
Participant's BACS Z score	0.14	1.10	-1.64	1.39	-12.77	<.001*
Participant's WRAT score	103.43	14.14	95.85	15.67	-4.50	<.001*
PANSS Positive Symptoms	-	-	16.38	5.15	-	-
PANSS Negative Symptoms	-	-	16.25	5.67	-	-
PANSS General Psychopathology	-	-	31.68	8.30	-	-
PANSS Total Psychopathology	-	-	64.26	16.04	-	-
PANSS 5-factor Positive Domain	-	-	17.47	5.98	-	-
PANSS 5-factor Negative Domain	-	-	16.31	6.43	-	-
PANSS 5-factor Emotional Distress	-	-	18.10	5.44	-	-
PANSS 5-factor Disorganization	-	-	20.58	6.33	-	-
PANSS 5-factor Excitation	-	-	14.05	4.24	-	-

M - Mean, S.D. - Standard deviation, * - statistically significant difference at the level of $p < 0.05$

Table 6 | Clinical characteristics of proband subgroups

Characteristic	SCZ (N=153)		SCAD (N=119)		BDp (N=150)		Significance	
	M	S.D.	M	S.D.	M	S.D.	F Value / (df)	P Value
Age (in years)	34,09	11,99	36,00	11,90	36,12	12,41	1.42 (2, 433)	0,24
Antipsychotics (CPZ eq)	490,64	395,79	509,21	466,44	323,13	327,39	6.47 (2, 276)	0.002*
Duration of illness (yrs)	12,93	11,14	16,58	12,44	16,17	12,10	5.04 (2, 414)	0.007*
BACS Z score	-1,64	1,39	-1,53	1,28	-0,94	1,31	15.51 (2, 433)	<.001*
WRAT score	95,85	15,67	97,15	14,08	102,42	13,10	0.35 (2, 433)	0,70
PANSS Positive	16,38	5,15	18,27	4,75	12,82	4,08	42.04 (2, 433)	<.001*
PANSS Negative	16,25	5,67	16,15	4,52	12,02	3,87	42.18[a] (2, 433)	<.001*
PANSS General	31,68	8,30	35,03	8,41	28,33	7,66	16.33 (2, 433)	<.001*
PANSS Total	64,26	16,04	69,31	14,96	53,17	12,84	34.83 (2, 433)	<.001*
PANSS 5-factor Pos.	17,47	5,98	19,26	5,34	12,68	4,28	58.77[a] (2, 433)	<.001*
PANSS 5-factor Neg.	16,31	6,43	17,27	6,26	13,32	5,15	15.90[a] (2, 433)	<.001*
PANSS 5-factor Emo.	18,10	5,44	21,31	6,34	17,10	5,87	8.752 (2, 433)	<.001*
PANSS 5-factor Disorg.	20,58	6,33	19,94	5,56	15,54	4,13	36.96[a] (2, 433)	<.001*
PANSS 5-factor Exc.	14,05	4,24	16,21	4,83	13,74	4,33	14.97 (2, 433)	<.001*

M - Mean, S.D. - Standard deviation; * - Statistically significant at the level of p < 0.05; [a] – Welch's Statistics, after violation of Levene's test for homogeneity of variances.

Using Levene's test it was shown that the assumption of homogeneity of variances did not hold for the PANSS Negative Subscale, F(2,432)=9.54, p<0.001; Van Der Gaag loading for the Positive Subscale, F(2, 432)=5.12, p=0.006; the Negative Subscale, F(2, 432)=3.97, p=0.02; and the Disorganization Subscale, F(2, 432)=6.98, p=0.001. Due to the violation of assumption of homogeneity of variances, Welch's test was used for those items.

Post hoc multiple comparison using Turkey's HSD (honestly significant difference) tests showed that the BDp population's mean for BACS composite score was significantly different from the scores of SCZ and SCAD populations, but that the SCZ and SCAD means did not differ significantly. The same pattern was also seen for the PANSS Negative Subscale, the PANSS total score, Van Der Gaag's Negative Symptoms Subscale and Disorganization Subscale, and CPZ equivalent doses of antipsychotics.

Means for the duration of illness differed significantly between the SCZ and BDp group, whereas the mean duration of illness of the SCAD group was between those two values, just reaching the level of significance (p = 0.05) when compared to SCZ, but not significantly different from BDp.

All three groups differed significantly on the PANSS Positive Subscale, PANSS General Psychopathology Subscale, and Van Der Gaag's loading for Positive Subscale.

Van Der Gaag's loading for Emotional Distress Subscale showed significant difference in means for SCZ and SCAD, and SCAD and BDp population. There was no significant difference between SCZ and BDp populations. The same pattern was seen in Van Der Gaag's loading for Excitation.

5.2. Whole-thalamus seed-based connectivity analysis

Figure 3 and Figure 4 show unthresholded main effect of participant groups (probands with psychosis and healthy controls) for the whole thalamus used as the single seed in functional connectivity analysis. Results of thresholding at $p < 0.05$ are shown in Figure 5 and Figure 6. Visualization was done using Connectome Workbench platform. Figure 7 reports mean over- and under-connectivity (Fz) between thalamic voxels and the rest of the brain for healthy control sample and probands (psychosis spectrum disorders).
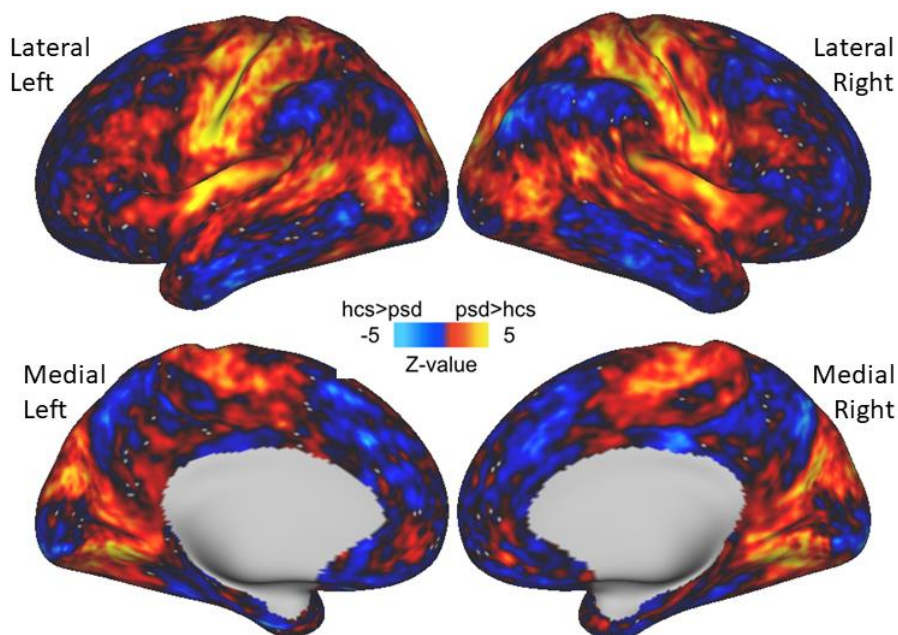

Figure 3. Unthresholded whole thalamus seed-based functional connectivity analysis for probands vs. hcs – cortical surface view; hcs – healthy control subjects, psd – psychosis spectrum disorders.

Figure 4. Unthresholded whole thalamus seed-based functional connectivity analysis for probands vs. hcs – volume-based subcortical view (axial plane); A – Anterior, P – Posterior; L – Left; R – Right.

Figure 5. Thresholded whole thalamus seed-based functional connectivity analysis for probands vs. hcs – cortical surface view; hcs – healthy control subjects, psd – psychosis spectrum disorders.
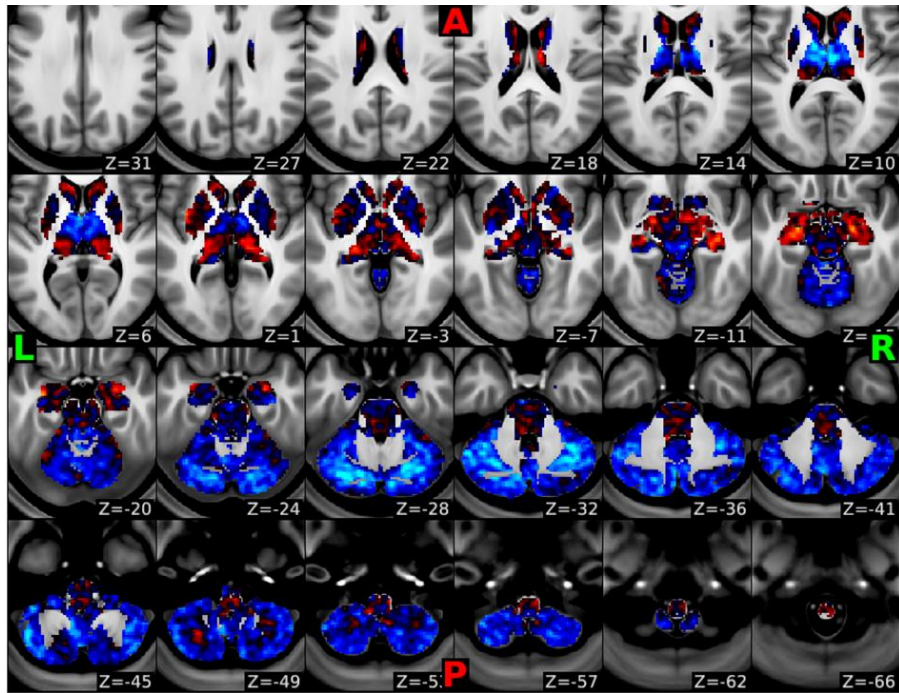
Figure 6. Thresholded whole thalamus seed-based functional connectivity analysis for probands vs. hcs – volume-based subcortical view (axial plane); A – Anterior, P – Posterior; L – Left; R – Right.
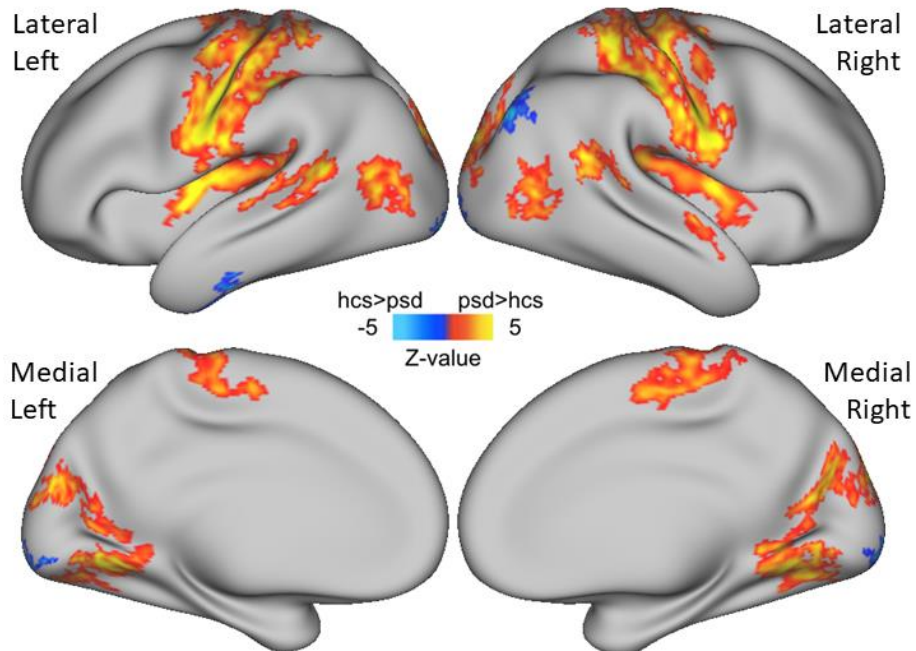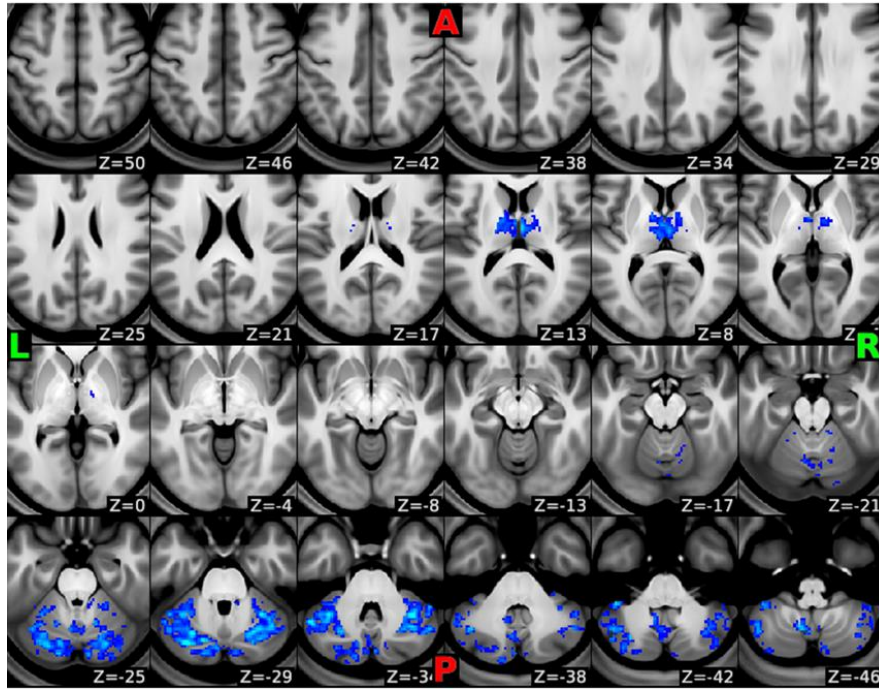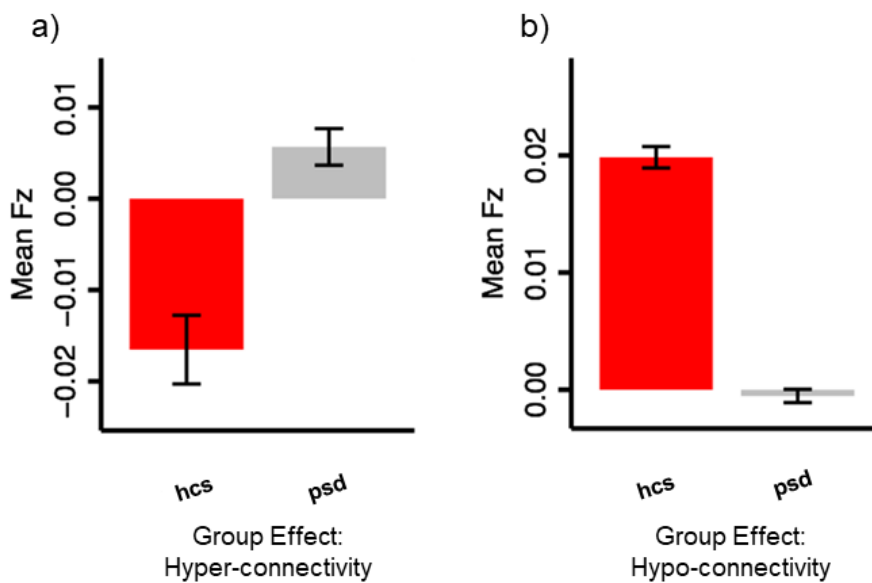

Figure 7. Mean connectivity averaged across all thalamic voxels in over- (a) and under-connected (b) areas (psychosis probands vs. healthy controls), with 95% confidence interval;
hcs – healthy control subjects, psd – psychosis spectrum disorders.

Wide swathes of primary and secondary sensory and motor cortex survived the thresholding and were shown to have increased connectivity with the thalamus, as well as primary and secondary visual cortex, primary gustatory cortex, auditory cortex, Supplementary motor area, insular cortex, posterior cingulate cortex, fusiform gyrus, supramarginal gyrus.

Table 7 lists all regions showing statistically significant connectivity differences (over-connectivity) with whole thalamus between probands and healthy controls. List of regions with significant thalamic under-connectivity for probands compared to healthy controls is reported in Table 8. The nearest anatomical landmark, the number of voxels, and Brodmann area (if available) are reported as well. Regions with over 100 voxels are reported.

Table 7 | Regions showing thalamic over-connectivity for probands vs. hcs

X	Y	Z	Number of voxels	Hemisphere	Anatomical landmark	Brodmann area
53	-23	39	461	Right	Postcentral gyrus	BA 3
-50	-25	50	452	Left	Postcentral gyrus	BA 2
32	-38	52	443	Right	Postcentral gyrus	BA 3
37	-31	19	355	Right	Insula	BA 13
-30	-42	56	350	Left	Inferior parietal lobule	BA 40
-62	-15	24	346	Left	Postcentral gyrus	BA 3
-44	-14	31	335	Left	Precentral gyrus	BA 6
40	-23	48	335	Right	Postcentral gyrus	BA 3
-50	-49	14	325	Left	Superior temporal g.	BA 13
20	-88	24	310	Right	Cuneus	BA 18
-45	-79	6	301	Left	Middle occipital g.	BA 19
-37	-14	14	274	Left	Insula	BA 13
18	-59	-6	273	Right	Lingual gyrus	BA 19
45	-18	51	257	Right	Precentral gyrus	BA 4
5	-24	68	256	Right	Medial frontal g.	BA 6
-21	-85	25	249	Left	Cuneus	BA 18
-37	-23	45	246	Left	Postcentral gyrus	BA 3
48	-46	17	234	Right	Superior temporal g.	BA 13
45	-64	6	230	Right	Middle temporal g.	BA 37
52	-10	32	226	Right	Precentral gyrus	BA 6
58	-14	32	214	Right	Precentral gyrus	BA 4
-38	-37	15	205	Left	Superior temporal g.	BA 41
61	-6	22	202	Right	Precentral gyrus	BA 4
-6	-25	74	178	Left	Medial frontal g.	BA 6
-5	-85	24	174	Left	Cuneus	BA 18
37	-7	10	173	Right	Claustrum	-
-21	-70	7	170	Left	Cuneus	BA 17
35	-34	64	168	Right	Postcentral gyrus	BA 3
-15	-66	-5	167	Left	Lingual gyrus	BA 18
5	-9	53	166	Right	Medial frontal g.	BA 6
13	-73	26	164	Right	Precuneus	BA 31
-26	-19	71	160	Left	Precentral gyrus	BA 6
29	-23	64	159	Right	Precentral gyrus	BA 6
10	-34	67	155	Right	Paracentral lobule	BA 6
25	-64	-6	155	Right	Lingual gyrus	BA 19
-55	-9	21	152	Left	Postcentral gyrus	BA 43
17	-89	26	151	Right	Cuneus	BA 18
20	-53	0	148	Right	Parahippocampal g.	BA 30
-21	-74	-7	138	Left	Lingual gyrus	BA 18
-5	-25	54	135	Left	Medial frontal g.	BA 6
-28	-27	52	133	Left	Precentral gyrus	BA 4
-15	-61	-4	132	Left	Lingual gyrus	BA 19
-37	-8	9	121	Left	Claustrum	-
-58	-8	26	117	Left	Precentral gyrus	BA 4
-42	-11	56	113	Left	Precentral gyrus	BA 6

Table 8 | Regions showing thalamic under-connectivity for probands vs. hcs

X	Y	Z	Number of voxels	Hemisphere	Anatomical landmark	Brodmann area
40	-64	-52	250	Right	Superior parietal lobule	BA 7
36	-52	-32	250	Right	Cerebellum, culmen	-
22	-68	-28	250	Right	Cerebellum, declive	-
-26	-62	-60	250	Left	Cerebellum, inf. semi-lunar	-
-30	-74	-30	250	Left	Cerebeelum, declive	-
-32	-76	-40	250	Left	Cerebellum, tuber	-
-34	-50	-32	250	Left	Cerebellum, culmen	-
-44	-64	-44	244	Left	Cerebellum, pyramis	-
-38	-54	-58	237	Left	Cerebellum, tonsil	-
18	-62	-60	232	Right	Cerebellum, inf. semi-lunar	-
-48	-56	-34	227	Left	Cerebellum, tuber	-
-26	-64	-32	214	Left	Cerebellum, uvula	-
-8	-60	-46	208	Left	Cerebellum, inf. semi-lunar	-
10	-82	-28	199	Right	Cerebellum, declive	-
10	-8	4	175	Right	Thalamus, ventral lat. n.	-
-8	-16	10	175	Left	Thalamus, medial dors. n.	-
-2	-70	-38	172	Left	Cerebellum, pyramis	-
30	-70	-30	166	Right	Cerebellum, declive	-
-8	-76	-30	163	Left	Cerebellum, declive	-
-14	-88	-38	156	Left	Cerebellum, tuber	-
-22	-98	-8	155	Left	Lingual gyrus	BA 18
38	-58	-44	153	Right	Cerebellum, tonsil	-
-10	-6	10	153	Left	Thalamus, anterior n.	-
32	-62	-32	152	Right	Cerebellum, uvula	-
6	-16	10	138	Right	Thalamus, medial dors. n.	-
-14	-80	-28	138	Left	Cerebellum, declive	-
48	-62	-34	131	Right	Cerebellum, tuber	-
19	-98	-8	131	Right	Lingual gyrus	BA 17
-16	-72	-30	123	Left	Cerebellum, declive	-
10	-78	-50	118	Right	Cerebellum, inf. semi-lunar	-
42	-74	-44	113	Right	Cerebellum, pyramis	-
-36	-56	-34	112	Left	Cerebellum, culmen	-
-6	-62	-26	109	Left	Cerebellum, declive	-
8	-68	-34	102	Right	Cerebellum, pyramis	-

Schizophrenia sample

Results for the whole thalamus seed-based analyses are reported in Figure 8 and Figure 9 (unthresholded results), and Figure 10 and Figure 11 (thresholding at p < 0.05).
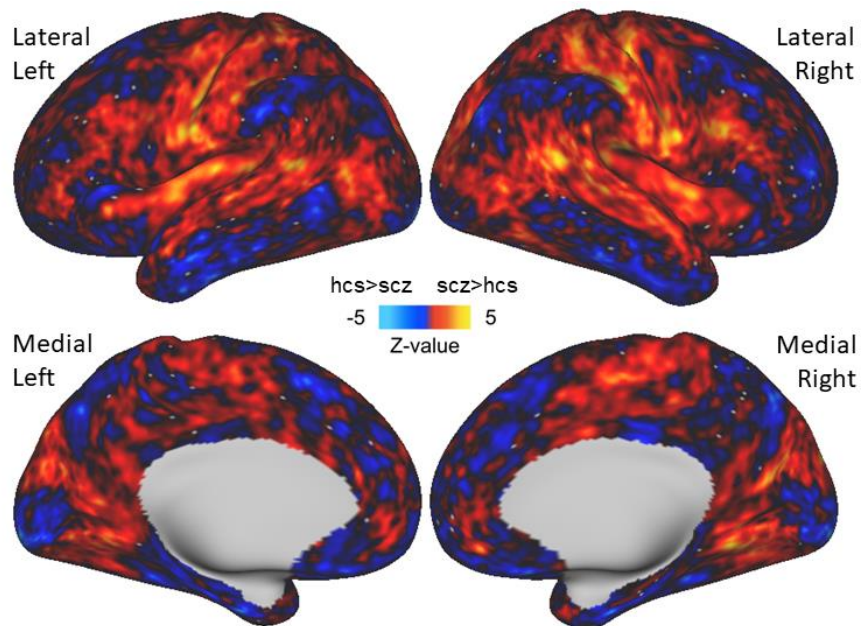

Figure 8. Unthresholded whole thalamus seed-based functional connectivity analysis for scz vs. hcs – cortical surface view; hcs – healthy control subjects, scz – schizophrenia subjects.
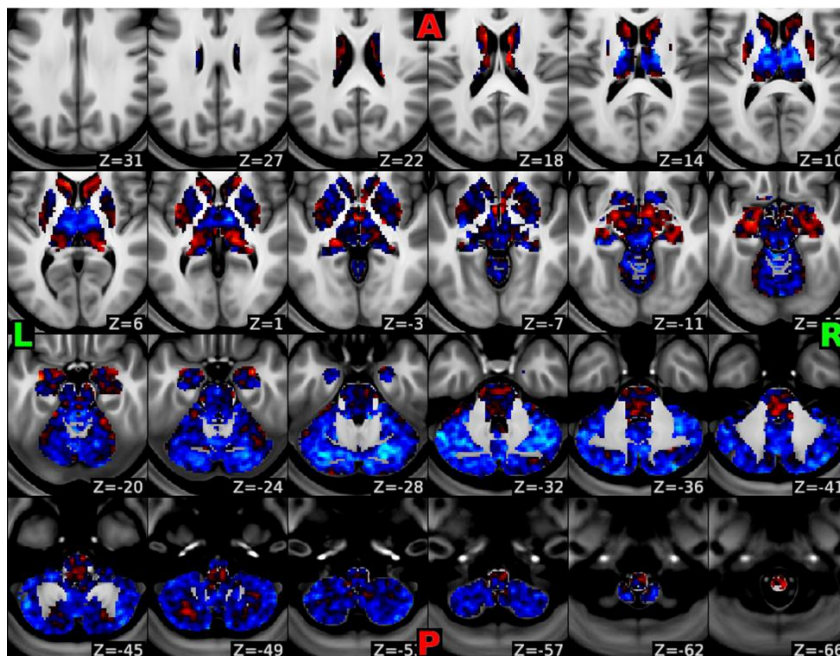

Figure 9. Unthresholded whole thalamus seed-based functional connectivity analysis for scz vs. hcs – volume-based subcortical view (axial plane); A – Anterior, P – Posterior; L – Left; R – Right.

Figure 10. Thresholded whole thalamus seed-based functional connectivity analysis for scz vs. hcs – cortical surface view; hcs – healthy control subjects, scz – schizophrenia subjects.

Figure 11. Thresholded whole thalamus seed-based functional connectivity analysis for scz vs. hcs – volume-based subcortical view (axial plane); A – Anterior, P – Posterior; L – Left; R – Right.
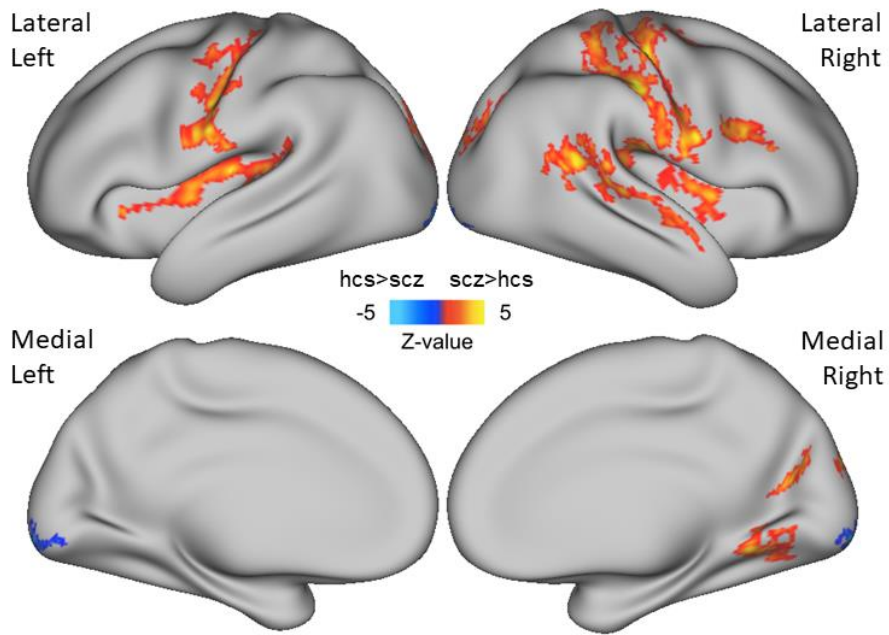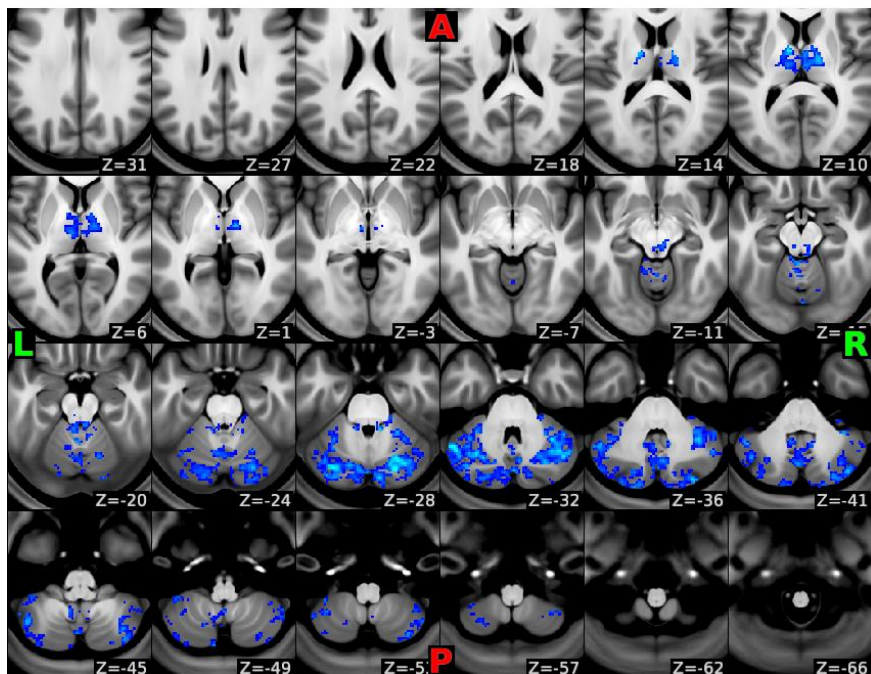
Pattern similar to the one seen for the psychosis spectrum emerged, although with somewhat spatially restricted results. Missing from SCZ over-connectivity findings (when compared to wider psychosis spectrum) were gustatory cortex, primary visual cortex, posterior cingulate and fusiform gyrus. Cortical and subcortical regions showing statistically significant difference in thalamic connectivity (over-connectivity) between schizophrenia sample and healthy controls are reported in Table 9. In Table 10, regions of significant reduction in thalamic connectivity in SCZ patients are reported. As in previous tables reporting regions with increase/reduction in connectivity, the nearest anatomical landmark, the number of voxels, and Brodmann area (if available) are reported as well. Regions with over 100 voxels are reported.

Table 9 | Regions showing thalamic over-connectivity for scz patients vs. hcs

X	Y	Z	Number of voxels	Hemisphere	Anatomical landmark	Brodmann area
53	-23	39	501	Right	Postcentral gyrus	BA 3
48	-43	16	400	Right	Superior temporal g.	BA 13
37	-31	18	258	Right	Insula	BA 13
40	-21	46	245	Right	Precentral gyrus	BA 4
16	-53	-7	243	Right	Lingual gyrus	BA 19
-35	-19	39	239	Left	Precentral gyrus	BA 4
32	-37	52	236	Right	Postcentral gyrus	BA 3
-37	-8	8	229	Left	Claustrum	-
-60	-7	26	229	Left	Precentral gyrus	BA 4
-45	-14	31	218	Left	Precentral gyrus	BA 6
37	-22	58	207	Right	Precentral gyrus	BA 4
32	-70	25	179	Right	Middle temporal g.	BA 39
-36	-32	14	168	Left	Superior temporal g.	BA 41
45	-17	50	161	Right	Precentral gyrus	BA 4
52	-10	32	149	Right	Precentral gyrus	BA 6
40	0	7	143	Right	Insula	BA 13
57	-3	20	139	Right	Precentral gyrus	BA 6
-18	-86	24	119	Left	Cuneus	BA 18

Table 10 | Regions showing thalamic under-connectivity for scz patients vs. hcs

X	Y	Z	Number of voxels	Hemisphere	Anatomical landmark	Brodmann area
50	-58	-50	250	Right	Cerebellum, tonsil	-
12	-12	4	250	Right	Thalamus, ventral lat. n.	-
-8	-16	8	250	Left	Thalamus, medial dors. n.	-
-26	-82	-30	250	Left	Cerebellum, declive	-
-42	-62	-44	250	Left	Cerebellum, pyramis	-
-34	-76	-38	238	Left	Cerebellum, tuber	-
30	-82	-38	232	Right	Cerebellum, tuber	-
36	-50	-36	231	Right	Cerebellum, anterior lobe	-
30	-70	-30	214	Right	Cerebellum, declive	-
-2	-72	-40	208	Left	Cerebellum, pyramis/vermis	-
-34	-56	-52	202	Left	Cerebellum, tonsil	-
10	-42	-28	197	Right	Cerebellum, culmen	-
-2	-44	-16	192	Left	Cerebellar lingual	-
-48	-56	-32	192	Left	Cerebellum, tuber	-
-2	-56	-36	185	Left	Cerebellum, nodule	-
-30	-62	-32	171	Left	Cerebellum, uvula	-
-22	-98	-7	170	Left	Lingual gyrus	BA 18
24	-66	-28	147	Right	Cerebellum, declive	-
40	-76	-42	142	Right	Cerebellum, pyramis	-
-4	-62	-26	139	Left	Cerebellum, declive	-
10	-82	-28	138	Right	Cerebellum, declive	-
-30	-74	-30	126	Left	Cerebellum, declive	-
44	-64	-32	121	Right	Cerebellum, tuber	-
-16	-80	-24	116	Left	Cerebellum, declive	-
6	-68	-34	115	Right	Cerebellum, pyramis	-
24	-97	-9	111	Right	Lingual gyrus	BA 18
22	-74	-28	110	Right	Cerebellum, declive	-
34	-46	-38	105	Right	Cerebellum, anterior lobe	-
-16	-72	-30	100	Left	Cerebellum, pyramis	-

Figure 12 reports mean over- and under-connectivity (Fz) between averaged thalamic voxels values and the rest of the brain for schizophrenia patients and matched healthy control sample.
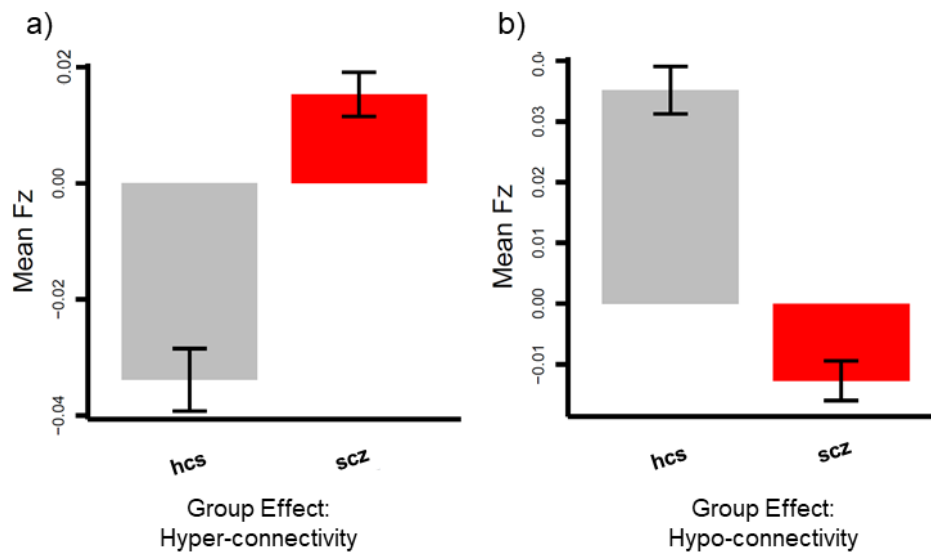

Figure 12. Mean connectivity averaged across all thalamic voxels in over- (a) and under-connected (b) areas (schizophrenia vs. healthy controls), with 95% confidence interval;
hcs – healthy control subjects, scz – schizophrenia patients.

In order to assess whether age, sex, duration of illness, or antipsychotic medication (CPZ equivalents) alter the permuted analyses, all were included formally as a covariate in the PALM whole-brain GLM. Inclusion of these covariates did not change the general pattern of thalamic connectivity changes.

5.3. Nine-seed group-by-seed interaction

Seed-based analyses were repeated using nine thalamic functional seeds identified by our group and previously reported by Ji et al. (432). Cortical functional networks, as well as associated thalamic functional subdivision, are shown in Figure 2 in Subjects and methods section. As seen from Figure 2, there was no significant correlation of thalamic voxels with ventral multimodal, language, and orbito-affective networks, while other nine networks charted onto the thalamus.

Figure 13 and Figure 14 show group-by-seed interaction for two groups (probands and healthy controls) and nine thalamic seeds using Connectome Workbench platform.
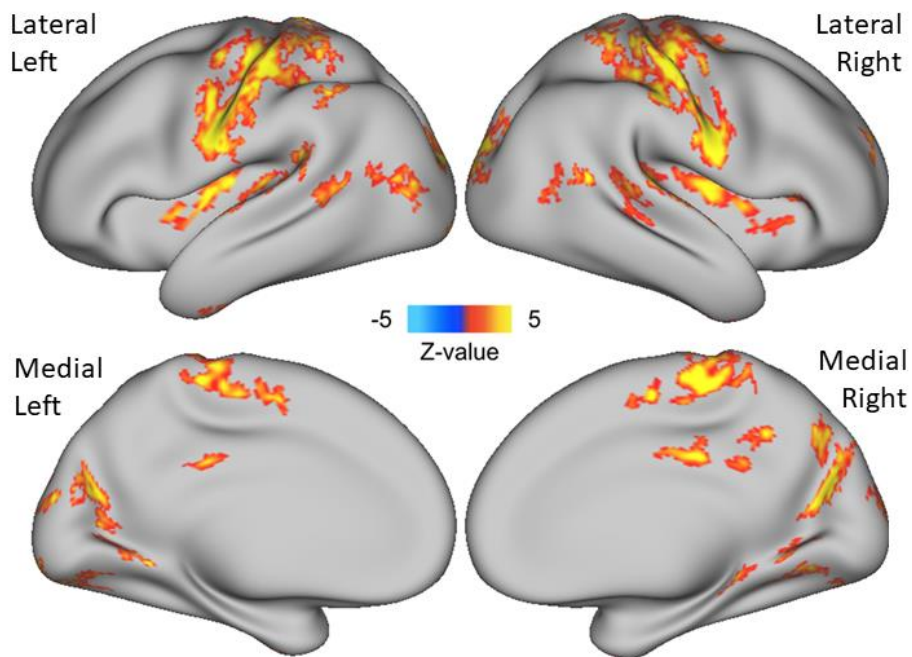
Figure 13. Interaction effect, showing the 2x9 interaction between two groups (psychosis spectrum and healthy control subjects) and the nine thalamic seeds on cortical surface.
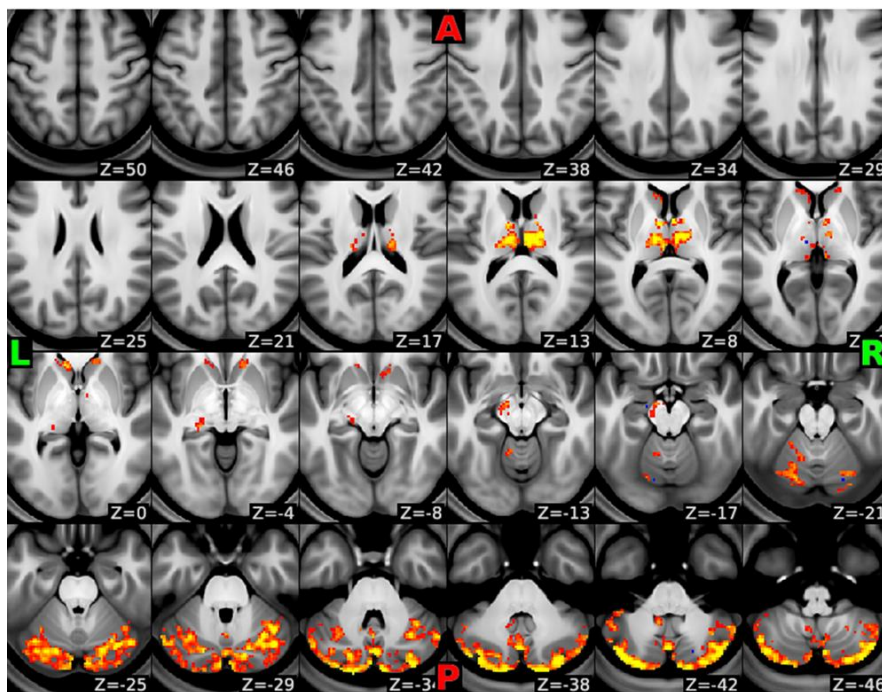

Figure 14. Interaction effect, showing the 2x9 interaction between two groups (psychosis spectrum and healthy control subjects) and the nine thalamic seeds using volume-based view (axial plane); A – Anterior, P – Posterior; L – Left; R – Right.

For all nine thalamic seeds identified according to functional connectivity with cortical networks, individual seed-based whole-brain connectivity analyses were conducted in order to specifically investigate which of those seeds drove the effect. For three of the seeds/functional networks, no effects survived thresholding and stringent type I error protection/correction (frontoparietal cognitive control, cingulo-opercular, and posterior multimodal). Surface-based maps of connectivity differences between psychosis probands and matched healthy controls for the remaining six seeds are shown in Figure 15.
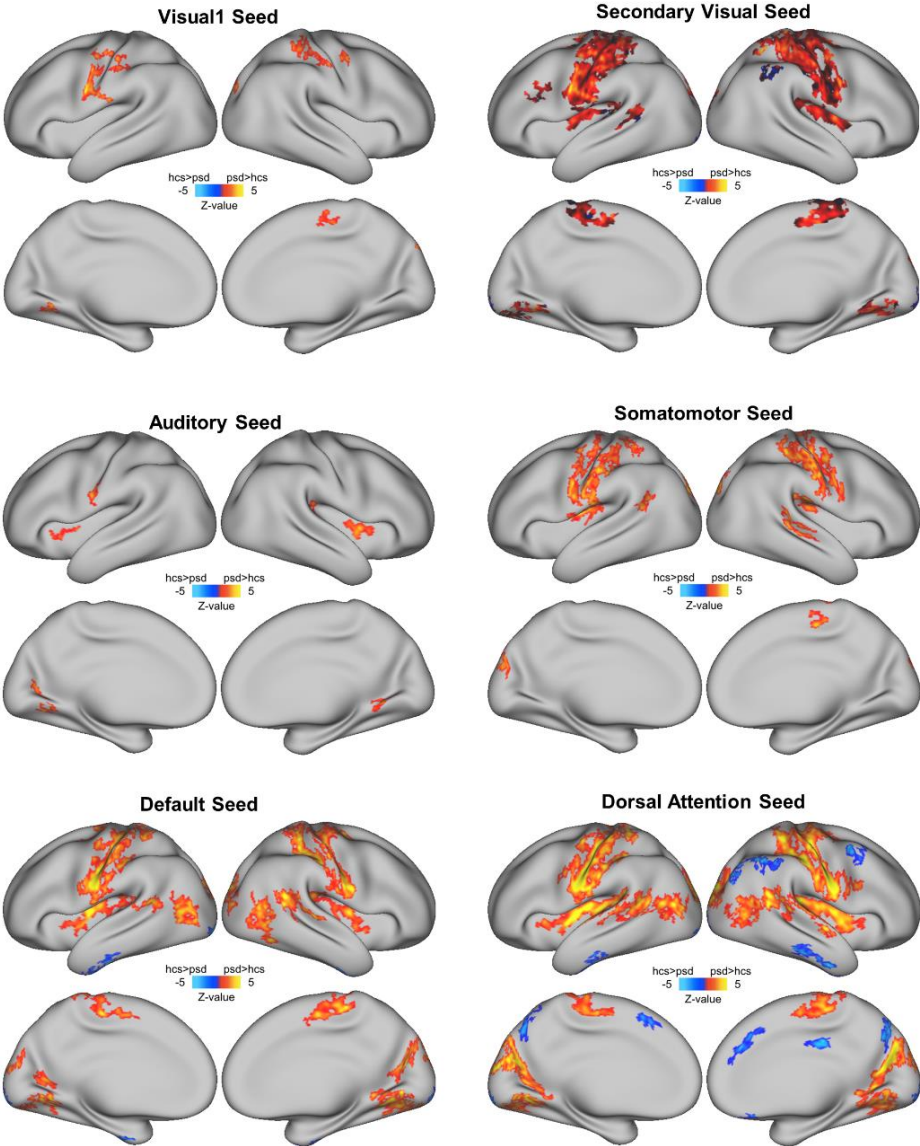

Figure 15. Thresholded surface seed-based analyses results for six thalamic seeds that survived p < 0.05 thresholding. Visualization follows previously used convention with left and right lateral cortical surfaces in the first row, and left and right medial cortical surfaces in the second row for each of the seeds.

Although a similar pattern of over-connectivity with sensory and motor regions emerged across seeds, with significant differences in the extent, dorsal attention seed showed most noticeable results, with the greatest number of regions surviving thresholding. In addition to dorsal attention seed's between-group connectivity differences being spatially most extensive, it was also the only seed for which prefrontal under-connectivity effects survived permutation analyses.

Table 11 and Table 12 report cortical and subcortical regions that show statistically significant difference in connectivity (over- and under-connectivity respectively) between thalamic dorsal attention seed and the rest of brain voxels for psychosis probands vs. matched healthy controls. Only regions with over 100 voxels are reported in tables, which means that some of the effects seen on Figure 15 (e.g. under-connectivity for orbitofrontal cortex and dorsolateral prefrontal regions) are not explicitly listed.

Table 11 | Regions showing over-connectivity for probands vs. hcs (dorsal attent. seed)

X	Y	Z	Number of voxels	Hemisphere	Anatomical landmark	Brodmann area
-55	-9	23	652	Left	Postcentral gyrus	BA 43
39	-24	48	626	Right	Postcentral gyrus	BA 3
22	-87	23	532	Right	Cuneus	BA 18
53	-47	13	520	Right	Superior temporal g.	BA 22
-49	-49	13	472	Left	Superior temporal g.	BA 13
32	-38	52	461	Right	Postcentral gyrus	BA 3
50	-25	40	427	Right	Postcentral gyrus	BA 3
-37	-21	43	372	Left	Precentral gyrus	BA 4
58	-6	21	366	Right	Precentral gyrus	BA 4
45	-64	6	348	Right	Middle temporal g.	BA 37
-45	-72	14	332	Left	Middle temporal g.	BA 39
21	-54	1	309	Right	Lingual gyrus	BA 18
-12	-72	19	291	Left	Cuneus	BA 18
-28	-42	56	290	Left	Inferior parietal lobule	BA 40
-49	-13	30	283	Left	Precentral gyrus	BA 6
-45	-33	40	280	Left	Inferior parietal lobule	BA 40
-45	-28	62	258	Left	Postcentral gyrus	BA 3
-5	-26	56	219	Left	Medial frontal gyrus	BA 6
-48	-40	21	214	Left	Insula	BA 13
6	-27	57	211	Right	Medial frontal gyrus	BA 6
39	-31	15	205	Right	Superior temporal g.	BA 41
-9	-37	76	200	Left	Postcentral gyrus	BA 3
38	-16	13	200	Right	Insula	BA 13
-23	-88	19	191	Left	Cuneus	BA 18
-33	-26	9	190	Left	Insula	BA 13
55	-13	50	189	Right	Postcentral gyrus	BA 3
-15	-66	-5	187	Left	Lingual gyrus	BA 18
-38	-9	7	186	Left	Claustrum	-
-19	-75	-8	183	Left	Lingual gyrus	BA 18
17	-74	25	179	Right	Precuneus	BA 31
-14	-88	27	162	Left	Cuneus	BA 18
19	-64	15	161	Right	Posterior cingulate	BA 31
46	-18	55	159	Right	Precentral gyrus	BA 4
-23	-67	7	155	Left	Posterior cingulate	BA 30
58	9	24	142	Right	Inferior frontal gyrus	BA 9
9	-70	1	140	Right	Lingual gyrus	BA 18
54	-9	4	135	Right	Superior temporal g.	BA 22
6	-23	62	134	Right	Medial frontal gyrus	BA 6
41	-3	3	125	Right	Claustrum	-
-8	-92	15	123	Left	Cuneus	BA 18
26	-28	53	119	Right	Precentral gyrus	BA 4
-55	-34	13	118	Left	Superior temporal g.	BA 42
26	-66	-5	118	Right	Lingual gyrus	BA 19
-57	-11	4	108	Left	Superior temporal g.	BA 22

Table 12 | Regions showing under-connectivity for probands vs. hcs (dorsal attent. seed)

X	Y	Z	Number of voxels	Hemisphere	Anatomical landmark	Brodmann area
40	-58	-30	500	Right	Cerebellum, declive	-
-10	-78	-30	432	Left	Cerebellum, declive	-
-36	-78	-42	429	Left	Cerebellum, pyramis	-
-28	-74	-28	390	Left	Cerebellum, declive	-
0	-72	-42	360	Left	Cerebellum, uvula of vermis	-
40	-66	-54	342	Right	Cerebellum, inf. semi-lunar	-
-26	-66	-30	330	Left	Cerebellum, declive	-
51	-53	45	330	Right	Inferior parietal lobule	BA 40
32	-70	-30	313	Right	Cerebellum, declive	-
6	-16	10	304	Right	Thalamus, medial dors. n.	-
-46	-64	-46	304	Left	Cerebellum, inf. semi-lunar	-
-42	-72	-42	282	Left	Cerebellum, pyramis	-
42	-74	-42	274	Right	Cerebellum, pyramis	-
20	-72	-28	260	Right	Cerebellum, declive	-
-10	-54	-60	243	Left	Cerebellum, tonsil	-
-32	-68	-58	239	Left	Cerebellum, inf. semi-lunar	-
2	-76	-34	200	Right	Cerebellum, tuber of vermis	-
14	-50	-60	191	Right	Cerebellum, tonsil	-
28	-84	-38	190	Right	Cerebellum, tuber	-
22	-66	-60	185	Right	Cerebellum, declive	-
52	-60	-42	183	Right	Cerebellum, pyramis	-
18	-84	-24	183	Right	Cerebellum, declive	-
12	-80	-28	181	Right	Cerebellum, declive	-
-44	-64	-30	181	Left	Cerebellum, declive	-
-10	-16	10	177	Left	Thalamus, medial dors. n.	-
14	-90	-38	173	Right	Cerebellum, tuber	-
-34	-50	-32	166	Left	Cerebellum, culmen	-
-22	-66	-60	157	Left	Cerebellum, inf. semi-lunar	-
59	-26	-23	138	Right	Inferior temporal gyrus	BA 20
-14	-82	-26	132	Left	Cerebellum, declive	-
-30	-86	-36	125	Left	Cerebellum, uvula	-
-18	-72	-30	123	Left	Cerebellum, declive	-
34	-76	-26	121	Right	Cerebellum, declive	-
-54	-18	-33	121	Left	Fusiform gyrus	BA 20
4	-76	-16	120	Right	Cerebellum, declive	-
9	34	30	120	Right	Cingulate gyrus	BA 32
40	-58	-44	115	Right	Cerebellum, tonsil	-
38	-68	-44	113	Right	Cerebellum, pyramis	-
18	-98	-1	111	Right	Cuneus	BA 17
18	-14	12	109	Right	Thalamus, ventral lat. n.	-
40	-52	-50	105	Right	Cerebellum, tonsil	-
-8	-52	-44	105	Left	Cerebellum, tonsil	-

5.4. Two-seed group-by-seed interaction

In order to simplify the analyses, and assuming that effects would converge across associative and sensorimotor seeds, nine thalamic regions that were identified based on functional thalamic connectivity with specific cortical regions (seen in Figure 2) were finally lumped into two groups: associative and sensorimotor. Results of 2x2 group-by-seed interaction analysis that survive thresholding at $p < 0.05$ are reported in Table 13. We report regions with over 100 voxels. The effect of interaction for both associative and sensorimotor thalamic areas is reported in Figure 16.

Table 13 | Regions identified in 2x2 group-by-seed interaction

X	Y	Z	Number of voxels	Hemisphere	Anatomical landmark	Brodmann area
Over-connectivity regions						
-46	-19	43	135	Left	Precentral gyrus	BA 4
Under-connectivity regions						
-6	-86	-30	108	Left	Cerebellum, declive	-
-30	-70	-22	139	Left	Cerebellum, declive	-
-38	-72	-44	101	Left	Cerebellum, pyramis	-
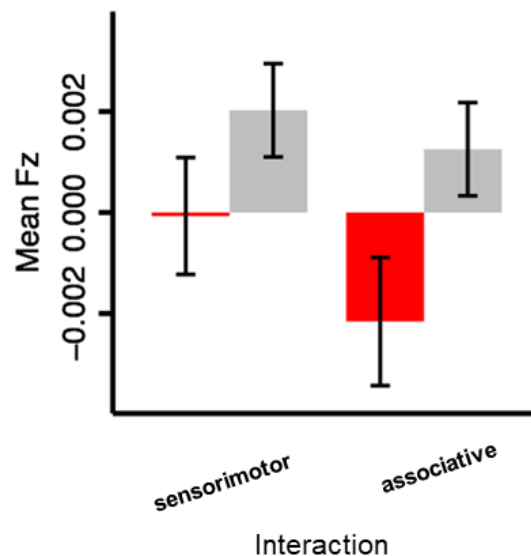
Figure 16. The effect of interaction (psychosis probands vs. healthy controls) for both sensorimotor and associative seeds, with 95% confidence interval; red – controls, grey – psychosis probands.

Group differences (psychosis spectrum probands vs. healthy controls) for associative seed are reported in Figure 17 and Figure 18, and for sensorimotor seed in Figure 19 and Figure 20. Thresholding was done at p < 0.05.
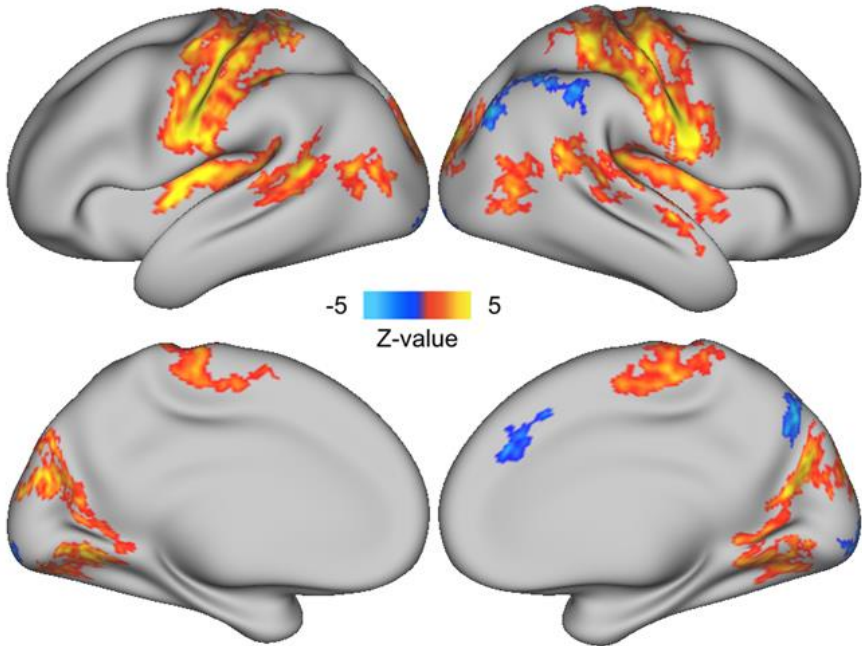

Figure 17. Thresholded group difference (psychosis probands vs. healthy controls) for associative seed – cortical surface.
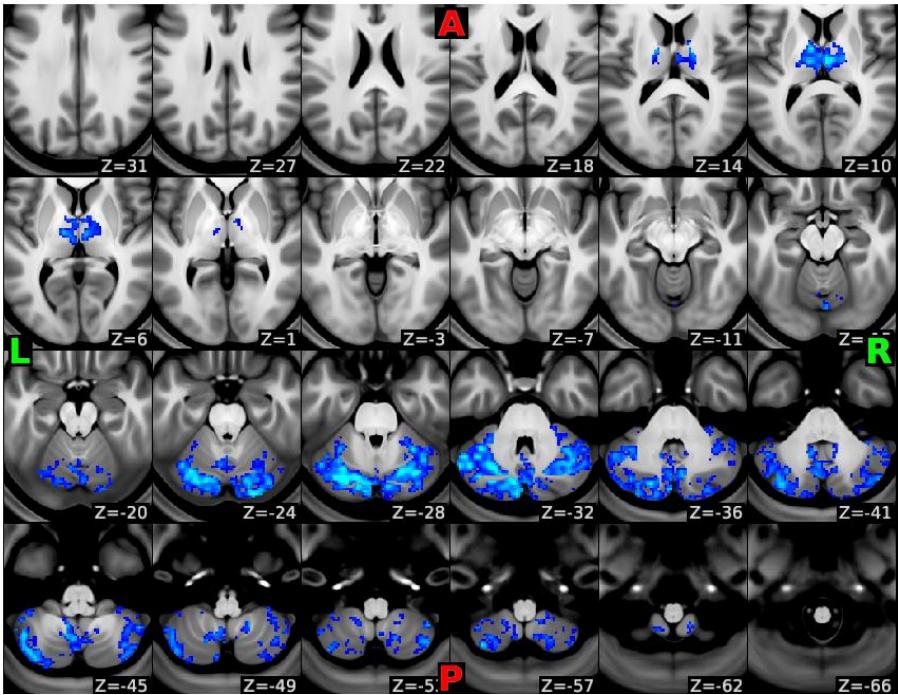

Figure 18. Thresholded group difference (psychosis probands vs. healthy controls) for associative seed – subcortical volume.
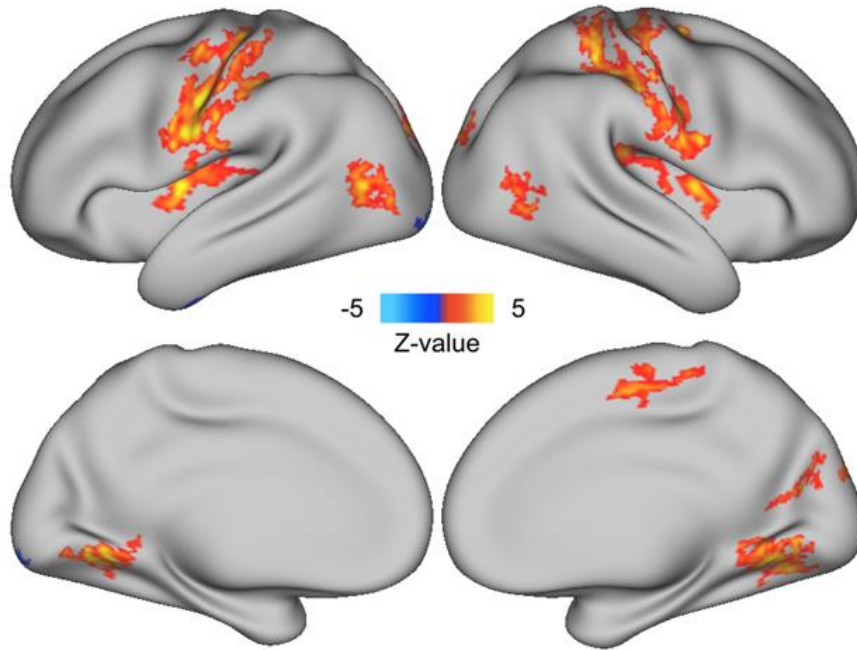
Figure 19. Thresholded group difference (psychosis probands vs. healthy controls) for sensorimotor seed – cortical surface.
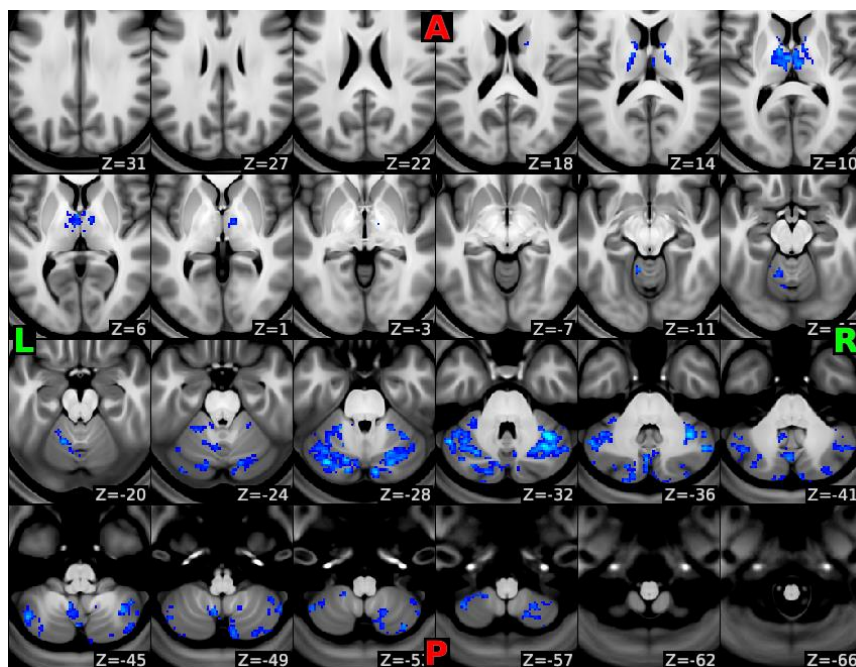
Figure 20. Thresholded group difference (psychosis probands vs. healthy controls) for sensorimotor seed – subcortical volume.

Group-by-seed 2x2 interaction was repeated for schizophrenia subsample (N = 167) and matched healthy controls (N = 153). No cortical regions or over-connectivity effects survived thresholding in the 2x2 interaction. Table 14 reports under-connected regions with over 100 voxels.

Table 14 | Regions identified in 2x2 group-by-seed interaction (scz vs. controls)

X	Y	Z	Number of voxels	Hemisphere	Anatomical landmark	Brodmann area
Under-connectivity regions						
24	-68	-22	148	Right	Cerebellum, declive	-
-30	-72	-20	106	Left	Cerebellum, declive	-

Group differences for schizophrenia patients vs. matched healthy controls for associative thalamic seed are reported in Figure 21 and Figure 22, and for sensorimotor thalamic seed in Figure 23 and Figure 24. Thresholding was set at $p < 0.05$.

Table 15 and Table 16 report brain regions showing over- and under-connectivity (respectively) group differences (schizophrenia patients vs. healthy control subjects) for associative thalamic seed.
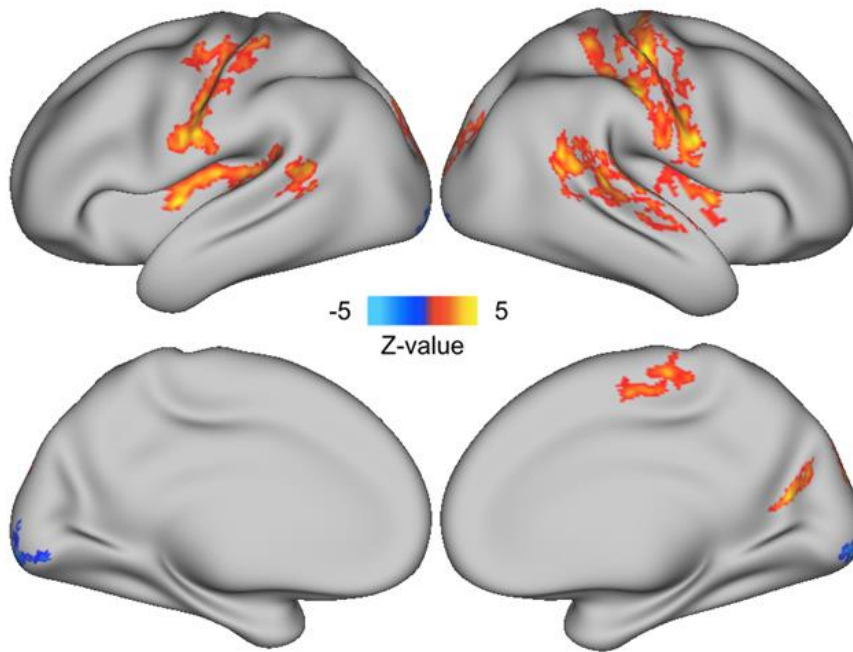
Figure 21. Thresholded group difference (schizophrenia vs. healthy controls) for associative seed – cortical surface.
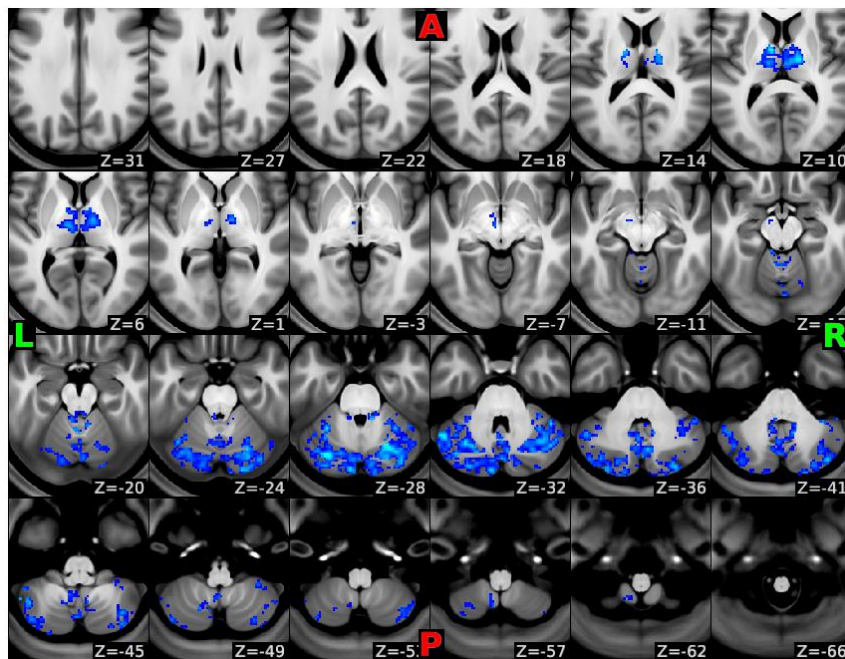

Figure 22. Thresholded group difference (schizophrenia vs. healthy controls) for associative seed – subcortical volume.
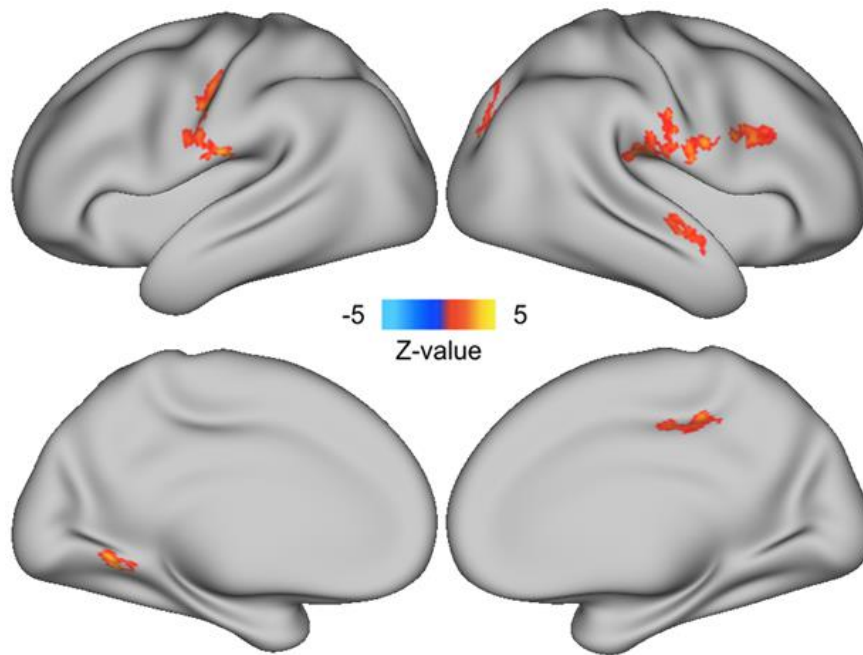
Figure 23. Thresholded group difference (schizophrenia vs. healthy controls) for sensorimotor seed – cortical surface.
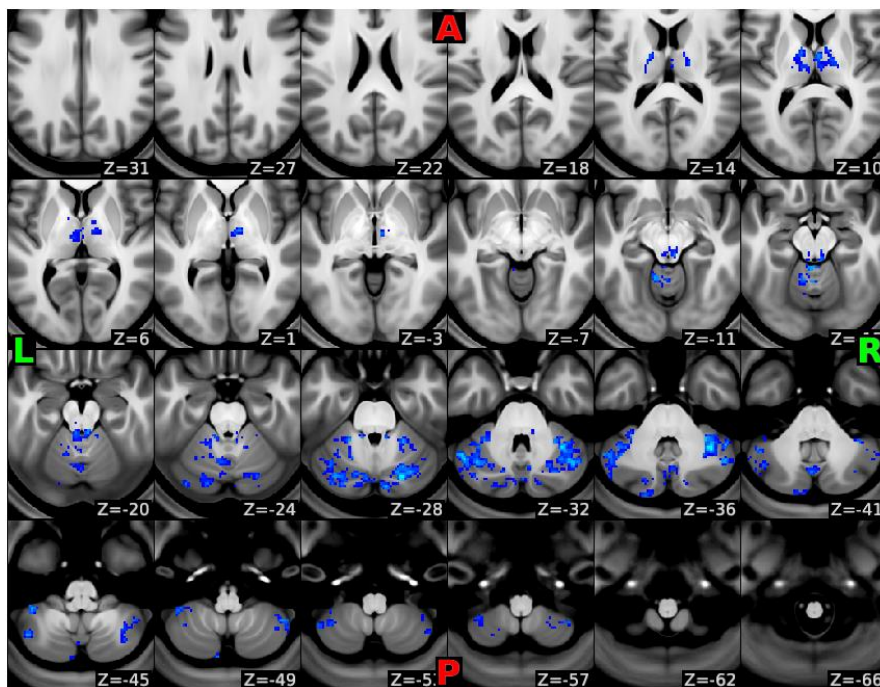

Figure 24. Thresholded group difference (schizophrenia vs. healthy controls) for sensorimotor seed – subcortical volume.

Table 15 | Regions showing over-connectivity for scz vs. hcs (associative seed)

X	Y	Z	Number of voxels	Hemisphere	Anatomical landmark	Brodmann area
54	-23	39	536	Right	Postcentral gyrus	BA 3
39	-22	46	303	Right	Postcentral gyrus	BA 3
57	-5	20	289	Right	Precentral gyrus	BA 6
-60	-7	26	250	Left	Precentral gyrus	BA 4
48	-44	16	242	Right	Superior temporal gyrus	BA 13
-33	-30	16	194	Left	Insula	BA 13
44	-17	48	194	Right	Precentral gyrus	BA 4
59	-35	8	193	Right	Superior temporal gyrus	BA 22
-48	-18	43	191	Left	Precentral gyrus	BA 4
-37	-21	41	184	Left	Precentral gyrus	BA 4
-41	-36	59	177	Left	Postcentral gyrus	BA 40
6	-23	62	168	Right	Medial frontal gyrus	BA 6
42	-25	61	164	Right	Postcentral gyrus	BA 3
-36	-18	15	159	Left	Insula	BA 13
22	-86	24	135	Right	Cuneus	BA 18
-20	-85	22	129	Left	Cuneus	BA 18
38	-12	14	117	Right	Insula	BA 13
19	-64	15	106	Right	Posterior cingulate	BA 31

Table 16 | Regions showing under-connectivity for scz vs. hcs (associative seed)

X	Y	Z	Number of voxels	Hemisphere	Anatomical landmark	Brodmann area
38	-64	-52	250	Right	Cerebellum, inf. semi-lunar	-
38	-60	-32	250	Right	Cerebellum, tuber	-
24	-66	-28	250	Right	Cerebellum, declive	-
14	-14	10	250	Right	Thalamus, ventral lat. n.	-
-10	-16	8	250	Left	Thalamus, medial dors. n.	-
-40	-74	-44	250	Left	Cerebellum, pyramis	-
-48	-56	-34	242	Left	Cerebellum, tuber	-
-30	-64	-34	223	Left	Cerebellum, uvula	-
28	-82	-36	221	Right	Cerebellum, uvula	-
-28	-74	-30	221	Left	Cerebellum, declive	-
-6	-78	-30	219	Left	Cerebellum, declive	-
-18	-64	-48	207	Left	Cerebellum, inf. semi-lunar	-
10	-80	-28	203	Right	Cerebellum, declive	-
-28	-82	-30	193	Left	Cerebellum, declive	-
-2	-60	-36	168	Left	Cerebellum, uvula	-
-20	-99	-8	168	Left	Lingual gyrus	BA 18
-34	-76	-36	165	Left	Cerebellum, tuber	-
-20	-80	-34	158	Left	Cerebellum, uvula	-
-4	-50	-20	151	Left	Cerebellum, culmen	-
6	-68	-34	148	Right	Cerebellum, pyramis	-
36	-44	-40	133	Right	Cerebellum, culmen	-
42	-66	-32	127	Right	Cerebellum, tuber	-
-14	-78	-22	126	Left	Cerebellum, declive	-
22	-74	-26	113	Right	Cerebellum, declive	-
0	-62	-26	107	Right	Cerebellum, declive	-
-2	-72	-42	107	Left	Cerebellum, uvula of vermis	-

5.5. Clustering

Figure 25 shows the nine-cluster solution of the data-driven clustering of thalamic voxel connectivity. The k=9 clustering solution reflects configuration of thalamic connectivity differences between patients with psychosis and healthy controls. The nine clusters were grouped together based on similarities in pattern of group difference. For purpose of visual comparison, functional subdivision of the thalamus yielding nine areas, as reported by Ji et al. (432), was added to Figure 25. The results of the voxel-level between-group connectivity differences are reported in Figure 26.
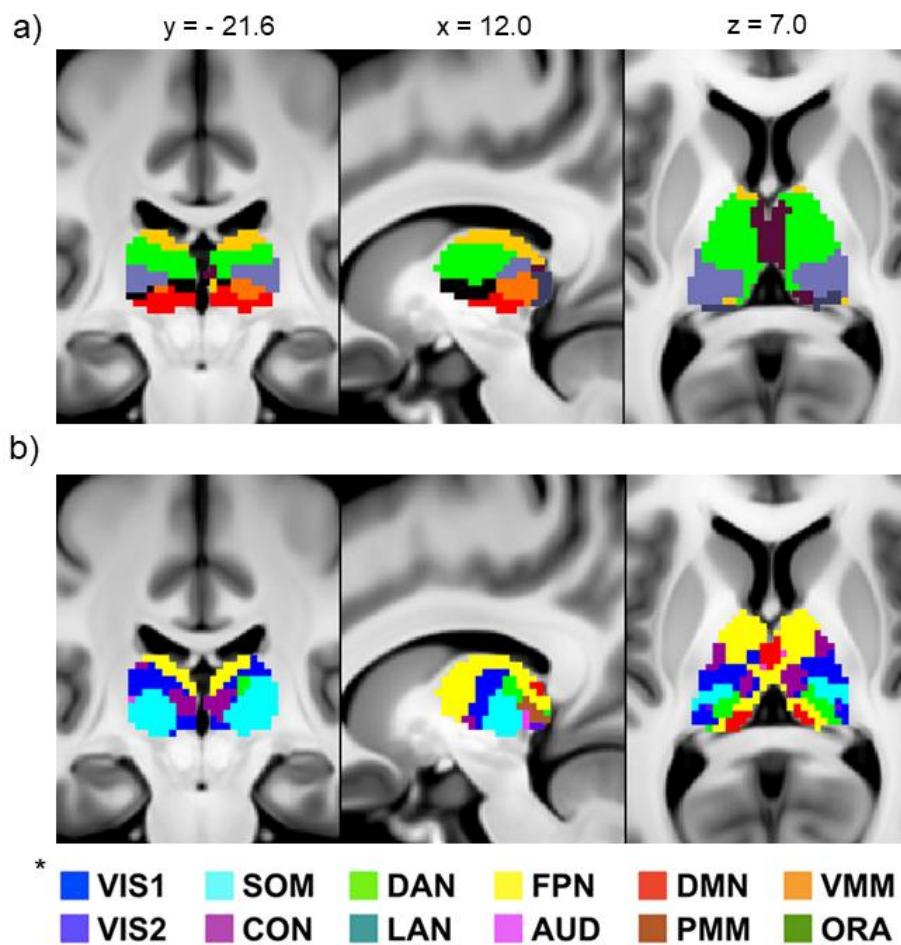
Figure 25. Data driven thalamic clustering compared to *a priori* functional subdivision. a) k=9 data-driven cluster solution based on subject groups difference patterns; (b) Functional connectivity thalamic subdivision according to Ji et al. (432); * - color-coding labels refer specifically to panel b.
VIS1 primary visual, VIS2 secondary visual, SOM somatomotor, DAN dorsal attention, FPN frontoparietal cognitive control, DMN default-mode, VMM ventral multimodal, CON cingulo-opercular, LAN language, AUD auditory, PMM posterior multimodal, and ORA orbito-affective network.
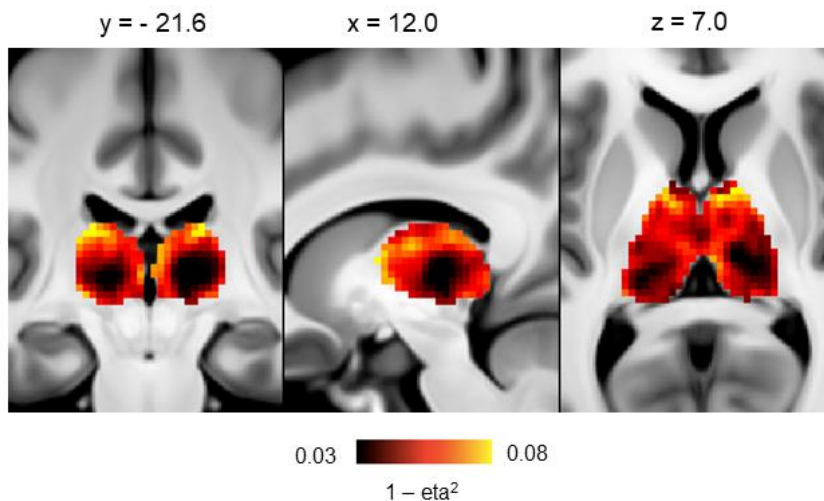
Figure 26. 1-eta^2 dysconnectivity map, demonstrating the areas of the thalamus driving the between group effects. Brightest voxels identify the highest between-group differences.

Figure 27 reports the two-cluster k-means clustering solution for the connectivity differences between psychosis spectrum probands and healthy control subjects.
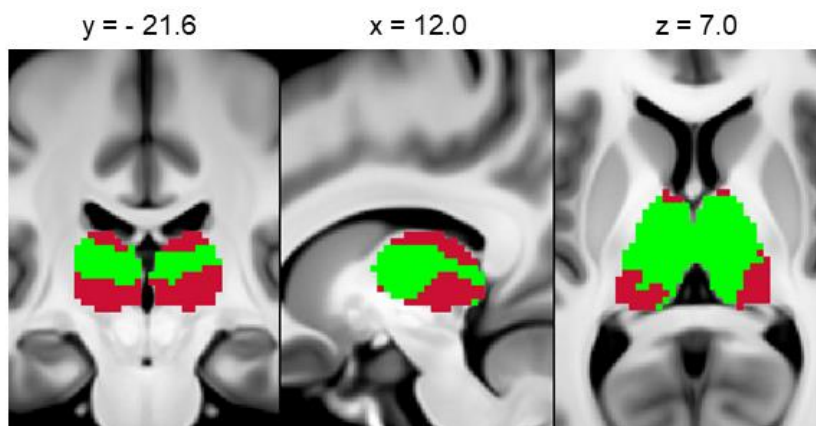

Figure 27. Two-cluster solution of between-group (psychosis probands vs. healthy controls) connectivity differences (k-means clustering).

Schizophrenia sample clustering

Clustering procedures were repeated for the schizophrenia sample and compared to the matched healthy controls population. Figure 28 shows the nine-cluster solution for group differences of connectivity between SCZ patients and matched healthy controls. Figure 29 shows voxel-level differences in connectivity between SCZ sample and healthy controls.
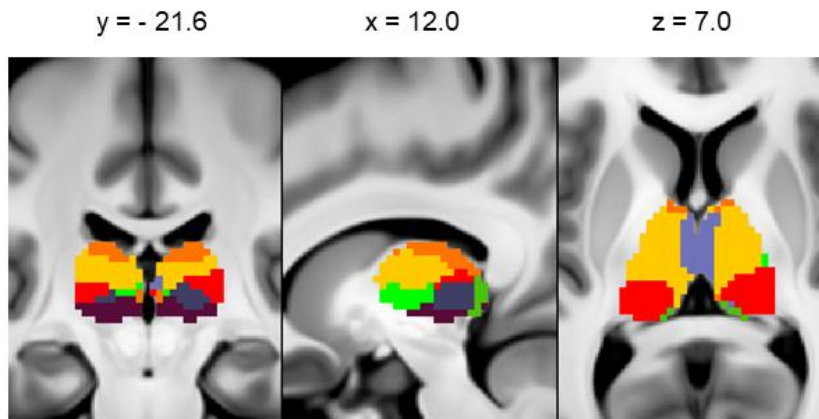
Figure 28. Data driven thalamic clustering of group connectivity differences between SCZ and healthy control participants groups, 9-cluster solution (for comparison see Figure 25 panel a; similar colors do not designate specific comparable networks).
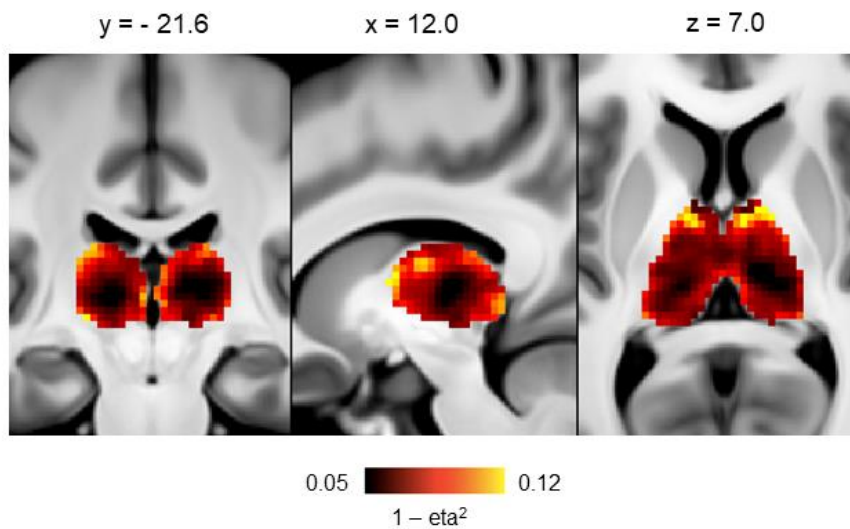

Figure 29. 1-eta^2 dysconnectivity map for SCZ vs. matched healthy controls group, demonstrating the areas of the thalamus driving the between group effects. Brightest voxels identify the highest between-group differences (for comparison see Figure 26).

For SCZ sample, two-cluster solution resulting from k-means clustering is shown in Figure 30.
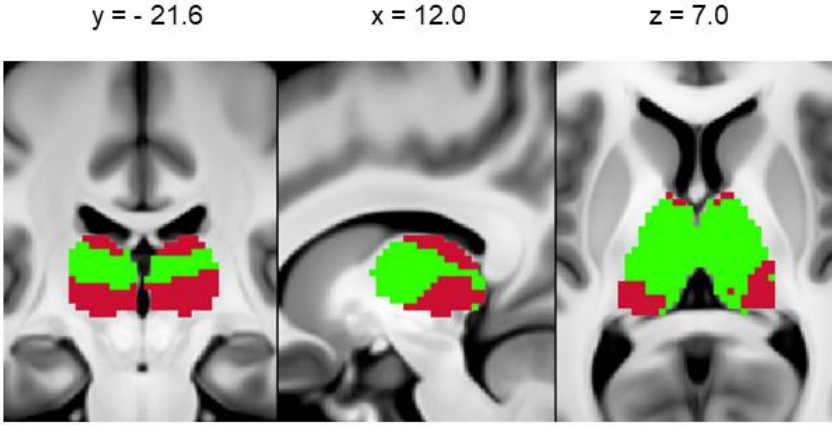

y = - 21.6   x = 12.0   z = 7.0

Figure 30. Two-cluster solution (k-means clustering) of between-group (SCZ vs. healthy controls) connectivity differences (for comparison see Figure 27).

5.6. Relationship with symptoms

Averaged thalamic connectivity across all voxels was used as the independent measure while different psychopathology scores were entered separately into GLM as dependent measures for regression analyses. Table 17 reports results for psychosis probands group using whole-thalamus seed-based analysis for both over-connectivity and under-connectivity in relationship with total PANSS score, General Psychopathology score, and scores of Van der Gaag symptom cluster loadings (Positive, Negative, Disorganization, Emotional distress, Excitation).

Table 17 | Relationship with symptoms / whole-thalamus connectivity

Symptom clusters	Over-connectivity (Fz) F statistic (dF) / p		Under-connectivity (Fz) F statistic (dF) / p	
PANSS Total	0.67 (1, 434)	0.413	2.5 (1, 434)	0.115
PANSS General	0.63 (1, 434)	0.428	5.12 (1, 434)	0.024*
vd Gaag Positive	0.70 (1, 434)	0.404	0.16 (1, 434)	0.686
vd Gaag Negative	1.77 (1, 434)	0.184	1.83 (1, 434)	0.177
vd Gaag Disorganization	0.14 (1, 434)	0.711	0.92 (1, 434)	0.338
vd Gaag Emotional Distress	1.07 (1, 434)	0.301	3.13 (1, 434)	0.078
vd Gaag Excitation	0.27 (1, 434)	0.599	3.61 (1, 434)	0.058

* - statistically significant difference at the level of $p < 0.05$ with adjusted R-squared = 0.00886.

Table 18 reports relationship between symptom clusters and averaged thalamic connectivity (over- and under-connectivity) for schizophrenia sample only (N = 167).

Table 18 | Relationship with symptoms / whole-thalamus connectivity (SCZ)

Symptom clusters	Over-connectivity (Fz) F statistic (dF) / p		Under-connectivity (Fz) F statistic (dF) / p	
PANSS Total	10.63 (1, 165)	0.001**	4.16 (1, 165)	0.043*
PANSS General	8.88 (1, 165)	0.003**	5.64 (1, 165)	0.019*
vd Gaag Positive	1.36 (1, 165)	0.245	0.02 (1, 165)	0.884
vd Gaag Negative	11.85 (1, 165)	<.001**	5.33 (1, 165)	0.022*
vd Gaag Disorganization	9.34 (1, 165)	0.002**	3.54 (1, 165)	0.062
vd Gaag Emotional Distress	1.52 (1, 165)	0.219	1.58 (1, 165)	0.210
vd Gaag Excitation	10.55 (1, 165)	0.001**	7.21 (1, 165)	0.008**

* - statistically significant difference at the level of $p < 0.05$;
** - statistically significant difference at the level of $p < 0.01$

Figures 31-35 show statistically significant relationship between specific psychopathology score (total score and subscales) and mean thalamic over- and under-connectivity Fz for SCZ patients. Figures include 95% confidence interval and report adjusted R-squared, in addition to information provided in Table 17.
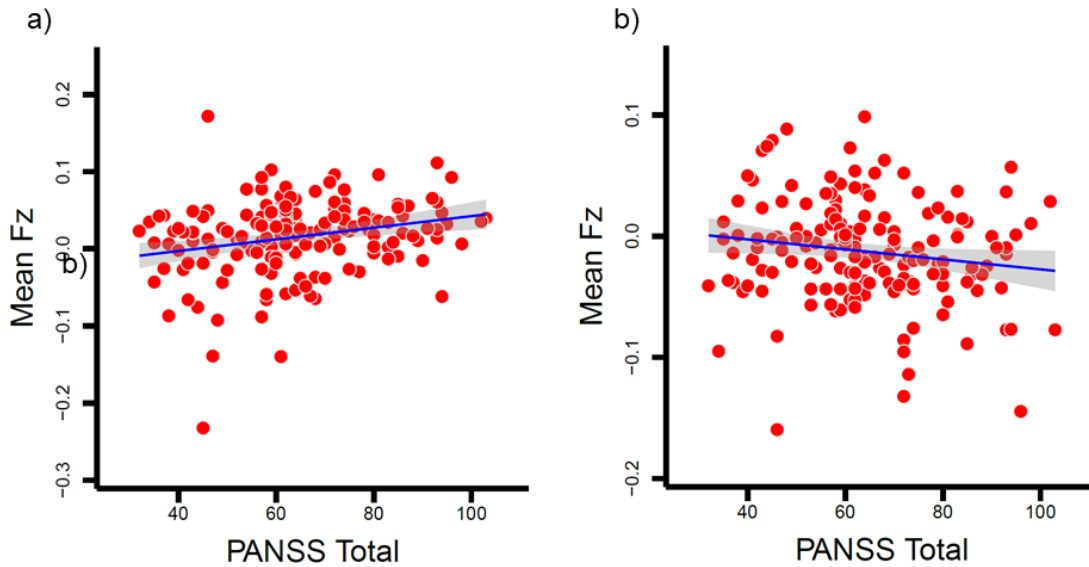

Figure 31. Linear regression with PANSS Total score and mean thalamic Fz for SCZ patients, including 95% confidence interval; a) thalamic over-connectivity effect with adjusted R-squared = 0.02718, and b) under-connectivity effect with adjusted R-squared = 0.01866.
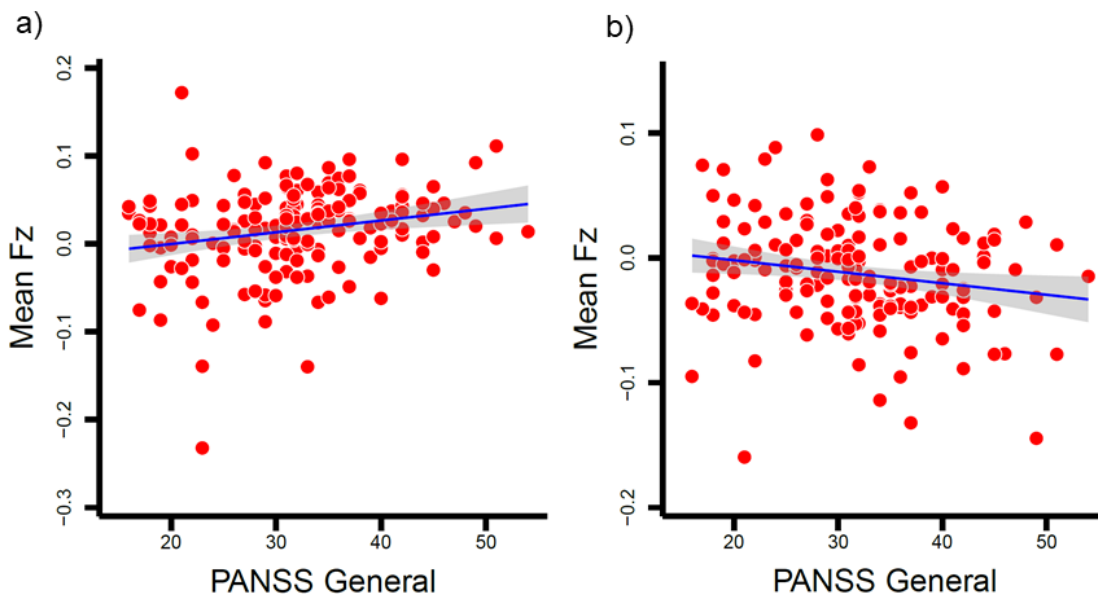

Figure 32. Linear regression with PANSS General Psychopathology score and mean thalamic Fz for SCZ patients, including 95% confidence interval; a) thalamic over-connectivity effect with adjusted R-squared = 0.04532, and b) under-connectivity effect with adjusted R-squared = 0.02718.
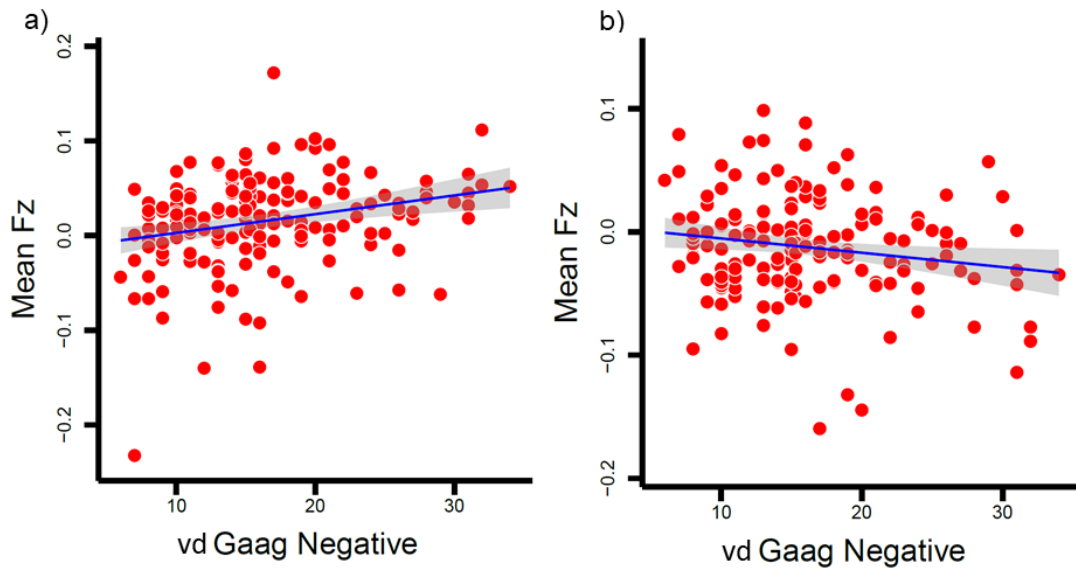
Figure 33. Linear regression with PANSS Negative Psychopathology (Van der Gaag loading) score and mean thalamic Fz for SCZ patients, including 95% confidence interval; a) thalamic over-connectivity effect with adjusted R-squared = 0.06137, and b) under-connectivity effect with adjusted R-squared = 0.02543.
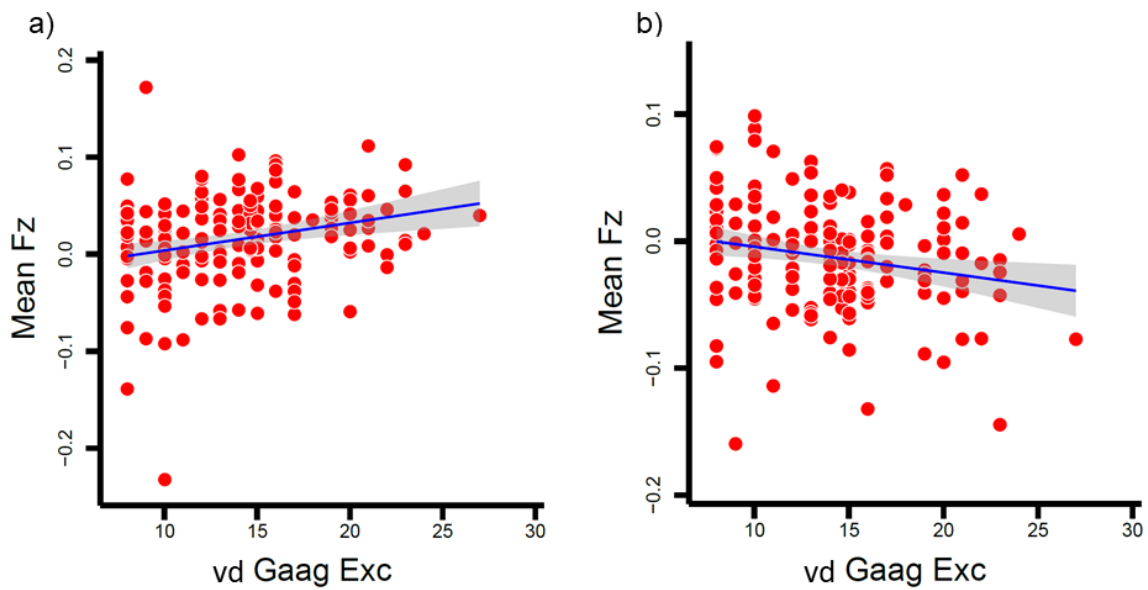

Figure 34. Linear regression with PANSS Excitation (Van der Gaag loading) score and mean thalamic Fz for SCZ patients, including 95% confidence interval; a) thalamic over-connectivity effect with adjusted R-squared = 0.05442, and b) under-connectivity effect with adjusted R-squared = 0.03607.
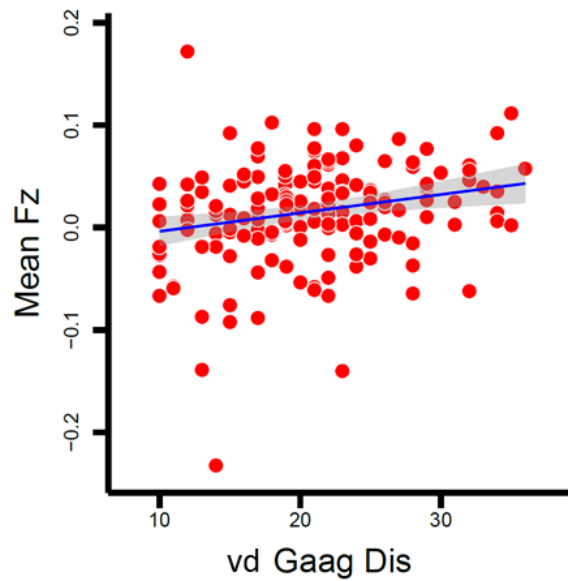
Figure 35. Linear regression with PANSS Disorganization (Van der Gaag loading) score and mean thalamic Fz for SCZ patients, including 95% confidence interval; Thalamic over-connectivity effect with adjusted R-squared = 0.04785.

In an attempt to take a closer look at possible links between specific, more finely grained, connectivity, and PANSS item-level psychopathology in psychosis, connectivity patterns of the dorsal attention network were correlated with delusions (P1), conceptual disorganization (P2), hallucinations (P3), blunted affect (N1), difficulty in abstract thinking (N5), depression (G6), and disorientation (G10). The only significant link with one of the major symptom clusters was found between dorsal attention network's over-connectivity effect and Van der Gaag's loading for negative symptom cluster ($F_{(1, 434)} = 4.89$, $p = 0.027$, R-squared = 0.00886). Table 19 reports details for each of the specific PANSS items.

Table 19 | Relationship with specific symptoms (dorsal attent. network seed)

Symptom clusters	Over-connectivity (Fz) F statistic (dF) / p		Under-connectivity (Fz) F statistic (dF) / p	
P1 Delusions	0.15 (1, 434)	0.695	0.06 (1, 434)	0.806
P2 Conceptual Disorg.	0.53 (1, 434)	0.466	0.005 (1, 434)	0.941
P3 Hallucinations	0.29 (1, 434)	0.593	1.85 (1,434)	0.174
N1 Blunted Affect	1.32 (1, 434)	0.250	0.23 (1, 434)	0.629
N5 Abstract Thinking	0.74 (1, 434)	0.387	0.09 (1, 434)	0.760
G6 Depression	2.22 (1, 434)	0.137	0.174 (1, 434)	0.676
G10 Disorientation	1.11 (1, 434)	0.293	4.87 (1, 434)	0.028*

* - statistically significant difference at the level of $p < 0.05$ with adjusted R-squared = 0.00881

6. Discussion

6.1. The sample

Thalamic connectivity pattern changes have previously already been identified in schizophrenia (273, 401, 403, 407), but also across psychosis spectrum (403), as well as across different stages of the illness (408). We published findings on thalamo-cortical connectivity changes in schizophrenia and bipolar disorder, measured by resting-state fMRI, which confirmed over-connectivity with large bilateral sensorimotor cortical regions, and under-connectivity with prefrontal, striatal, and cerebellar regions (403). Over- and under-connectivity effects were found to be correlated, suggesting a related system-wide disturbance, and a similar pattern of connectivity changes was found in bipolar patients population, enabling the use of those specific thalamo-cortical disturbances in diagnostic classification using MVPA for both SCZ and BD (although with difference in accuracy) (403). Also, we published fMRI findings suggesting that MD and LGB dysconnectivity patterns in SCZ show similarities, regardless of their different cortical and subcortical projections, but also that BD patients with history of psychosis showed thalamic dysconnectivity patterns similar to those seen in SCZ patients (406).

In the current analysis, by examining one of the largest clinical samples so far (436 psychosis spectrum subjects and 219 healthy controls) and the resting-state fMRI paradigm, we have confirmed the existence of thalamic over- and under-connectivity across a number of cortical and subcortical brain regions. The final clinical sample, reduced due to stringent fMRI quality-check requirements and the need for careful matching of clinical and healthy control samples, finally included 167 patients diagnosed with schizophrenia, 119 patients diagnosed with schizoaffective disorder, and 150 patients diagnosed with bipolar disorder with a history of psychosis. Psychosis sample was matched with 219 healthy control individuals, based on age, sex, handedness, parental education, and race, as reported in Table 4. The matching was, however, not attempted for WRAT scores, as lower achievement is expected for schizophrenia population (especially with longer illness duration), and WRAT scores were found to correlate with cognitive functions that might be specific for clinical populations and show association with specific symptoms (436). Furthermore, reading deficits correlate with both visual and auditory sensory measures in schizophrenia (437), and, given the expected connectivity changes between the thalamus and sensory areas in schizophrenia, forcing the matching on WRAT scores might end up removing the crucial effects when comparing probands and the healthy population. The use of psychosis spectrum in defining clinical population for this study reflected the current attempts at 'deconstructing' schizophrenia and conceptualizing it as only the far end of the wider psychosis spectrum with poorer outcome

(156, 195, 197). The existence of the psychosis spectrum and the overlap between disorders (e.g. SCZ, SCAD, and BD) has been repeatedly confirmed by family aggregation, overlapping clinical phenomena and presentations, as well as shared genetic susceptibility of those disorders (88, 180, 191, 200). Research in schizophrenia that fails to acknowledge that fact is also at a danger of falling victim to Berkson's bias, resulting from the focus on the worst-outcome population, and resulting in misleading correlations (156). If we accept the existence of a wider psychosis spectrum, research into biological underpinnings of clinical phenomena that are shared transdiagnostically cannot be undertaken adequately by focusing on just one of the diagnostic entities. Clinical phenomena/symptoms shared between disorders would then be expected to either follow the same 'biological pathways', or to at least show similar patterns possibly modified by additional condition-specific factors. Either way, elucidating the exact biological nature of clinical phenomena/symptoms and all of the factors influencing them would consequently require a look into wider transdiagnostic spectra that exhibit those symptoms.

Psychosis spectrum-focused approach notwithstanding, all of the fMRI connectivity analyses that were undertaken for the psychosis sample were also repeated specifically for SCZ patient group (N = 167) and matched healthy controls (N = 153), in order to compare connectivity effects seen when treating SCZ as part of the psychosis spectrum, and when analyzing it separately. Given that a comparison of thalamic connectivity differences among three different psychotic disorders was not a goal of the current analyses, no formal comparison among them was undertaken. Such comparison remains, however, an important goal for follow-up analyses.

As seen from Table 6, SCZ, BDp, and SCAD populations were similar with regard to age, but differed among each other on most clinical variables. As expected, BDp sample showed better cognitive functioning (as measured by BACS score), whereas SCZ and SCAD patients had comparable cognitive changes. BDp sample was also overall less symptomatic (as measured by total PANSS score), had less negative symptoms, and scored lower on Disorganization PANSS Van der Gaag subscale loading. SCZ and SCAD were not significantly different on any of those variables. Interestingly, SCAD differed from the two other clinical subgroups on Emotional Distress and Excitation Van der Gaag PANSS loading (higher scores), whereas BDp and SCZ patients had similar scores on those scales. The fact that comparable results were found on Emotional Distress and Excitation for both SCZ and BDp groups lets us tentatively question the dichotomy between those two disorders based solely on affectivity, although we must keep in mind the limitations of approximation of those two symptom clusters using alternative PANSS items loadings we utilized. All three groups differed significantly on positive symptoms scales, with SCAD population having most positive symptoms, followed by SCZ and then BDp patients. Graded sloping (up- or downward) effect,

which we might expect to find when looking at 'extended schizophrenia' spectrum that extends into bipolar disorder with a history of psychosis (SCZ – SCAD – BDp), was actually present only for cognitive functioning, negative, and disorganization scores (with SCZ showing worst results, BDp group performing better, and SCAD lying somewhere between those two groups).

6.2. fMRI as a tool in psychiatric research

Magnetic resonance imaging, with its various modalities, offers numerous opportunities for elucidating structural, functional, and neurochemical underpinnings of different mental disorders. As we have previously reported (438), MRS offers a promising non-invasive tool for development of possible predictors of illness course and relapse in mental disorders. Although using fMRI offers numerous advantages in psychiatric research, like its non-invasive nature, good temporal and improving spatial resolution, flexibility of research paradigms (task-based or task-independent), and the ability to combine it with other techniques, due to complexity of the data structure and the size of information gathered analyzing fMRI data is still linked to a number of methodological issues. Even using a no-task paradigm (resting-state), in which subjects are expected to lie still during the scanning procedures and not to engage in any specific mental activity, which ultimately avoids the burden of modelling based on task structure and assumed neural responses, carries with it a number of significant methodological issues.

The current analyses were based on the state-of-the-art HCP preprocessing pipeline that deals with image registration, distortion correction, and achieving higher SNR, with minor in-house modifications. The discussions are, however, still ongoing with regard to GSR step of the preprocessing pipelines. Global signal regression is a very efficient step in removal of common and problematic respiration, cardiac, and motion artifacts, increasing the variance explained by other factors, but it also removes any globally distributed neurological component, and is said to potentially introduce negative correlations between brain regions. In a recent paper, Li et al. (439) reported that the explained behavioral variance increased by an average of 40% across multiple behavioral measures for resting-state functional connectivity analyses, although benefitting more task-based performance than self-reported measures. Our previously published analyses of thalamo-cortical disturbances in schizophrenia showed that the discovered connectivity patterns did not change when omitting GSR step during preprocessing (403), which has been confirmed also by a more recent work from the same group investigating thalamic connectivity (176). In line with these facts and a relative consensus on GSR allowing better delineation of subcortical nuclei, showing closer link to the DTI-defined anatomy, and improving specificity of positive correlations (440), we opted for inclusion of the GSR step. All negative correlations resulting from the present analyses were

reported, and did not deviate from previously discovered and reported anti-correlations, additionally suggesting appropriateness of using the GSR preprocessing step.

The general linear model, used for fMRI data analyses, is a flexible model that can incorporate a number of different statistical models such as ordinary linear regression, t-test, F-test, analysis of variance (ANOVA), analysis of covariance (ANCOVA), multivariate analysis of variance (MANOVA), and multivariate analysis of covariance (MANCOVA). Additionally, the tool used for applying permutation analyses of linear models (PALM) allows for a range of regression and permutation strategies, while at the same time being robust to heteroscedasticity (differing distributions of noise), and able to work with non-imaging data and both surface-based and volume-based neuroimaging data. PALM also utilized robust permutation methods to assess classical multivariate statistics and allowed the control of family-wise error rate. As already reported by Schleifer et al. (175), this Type I error correction method avoids making assumptions on distribution, which has been found to inflate Type I error according to Eklund et al. (432). FSL's PALM tool utilizes Threshold-Free Cluster Enhancement (431), and significance was assessed using nonparametric permutations, with subsequent analyses benefitting from the initial Type I error protection.

Another important aspect of fMRI connectivity data needs to be continuously emphasized when presenting/interpreting or discussing related findings. Results of fMRI analyses used by themselves do not reflect the existence of anatomical connections or changes in those connections, but simply changes in co-activation and synchronous signal oscillation (spontaneous or task-induced) of different brain regions – functional connectivity. Interpretation of fMRI connectivity results will thus include the need to take into account possible wider-distributed interrelated processes, moving away from the more simplistic 'linear two-region communication' interpretations. Also, importantly, fMRI signal does not directly represent a neural activation, but is an indirect blood-oxygenation-related measure (BOLD signal) that approximates a neural activity based on the assumed model of hemodynamic response. While a more detailed elaboration of these issues would clearly exceed the scope of this discussion, in the Introduction section it has already been outlined that simultaneous recording of a neural activity and fMRI clearly links BOLD and neural activity (345). In addition to that, repeated neuronal activation produces changes in fMRI signal (346), and the duration of hemodynamic response can be used as an estimate of the duration of a neural activity (348).

Regardless of the need for careful interpretation and the mindfulness about methodological limitations, fMRI offers an extremely valuable and flexible tool to be utilized in research of various mental disorders. Inherent usefulness of fMRI research lies in its non-invasive nature and good spatial and temporal resolution characteristics, as well as the ability

to be combined with other modalities (e.g. EEG) and to be used in the context of computational psychiatry.

6.3. Seed-based thalamic connectivity analyses and the pattern of thalamic dysconnectivity

Functional connectivity analyses looking at the thalamus as a single seed, and differences between psychosis patients and matched healthy control group, showed general effects that have previously been reported by our and other research groups, with over-connectivity between the thalamus and large sensorimotor regions, but also the associative cortex. After stringent Type I error protection and thresholding at $p < 0.05$, increased thalamic connectivity effect survived for: large areas of bilateral primary motor and sensory cortex, associative sensory cortex, bilateral Supplementary motor area, left primary and bilateral secondary and associative visual cortex, auditory cortex, gustatory cortex, insular cortex, right fusiform gyrus, right posterior cingulate, and left supramarginal gyrus (Figure 5 and Table 7). Areas showing significant thalamic under-connectivity when comparing psychosis probands and healthy controls, unsurprisingly, included large cerebellar areas, but also right primary visual cortex, left secondary visual cortex, right superior parietal lobule, and bilateral MD nucleus, along with right VL nucleus, and left anterior thalamic nucleus (Figure 6 and Table 8).

Restricting analysis to just schizophrenia patients and comparing them to a specifically matched subset of healthy controls, a similar overall pattern of thalamic over-connectivity with sensorimotor regions, and under-connectivity primarily with cerebellum survived. As shown in Figure 10 and listed in Table 9, in schizophrenia patients there was significant thalamic over-connectivity with bilateral primary and secondary sensorimotor cortical areas, including bilateral Supplementary motor area, as well as right insular cortex, left auditory cortex, right middle temporal gyrus (BA 39), and left secondary and right associative visual cortex. Interestingly, while insular cortex was primarily connected to disorders with significant emotion regulation impairment, over-connectivity with insular cortex robustly appear in analyses comparing SCZ population with healthy controls. Areas showing functional under-connectivity with the thalamus (Figure 11 and Table 10), in addition to the cerebellum, included bilateral secondary visual cortex, right VL and left MD thalamic nucleus.

It should be noted that in both wider psychosis sample and the schizophrenia patient population thalamic connectivity shows pronounced reduction in variation when compared to that in the healthy controls, and then a shift towards over- or under-connectivity.

The overall pattern seems to be strikingly similar when we look at schizophrenia separately and when we examine it as part of the psychosis spectrum, with SCZ conceptualized as just the far end that is characterized not by any pathognomonic signs or symptoms but by increased severity of symptoms and more pronounced functional impairments. Some differences were noted, however, including over-connectivity with primary visual cortex, gustatory cortex, fusiform gyrus, and posterior cingulate. We could explain these differences by the fact that inclusion of SCAD and BDp population is bound to result in changed connectivity with brain regions modulating mood or providing emotional salience and context like posterior cingulate and fusiform gyrus. Both regions, however, also play an important part in wider network implicating cognitive functions and intrinsic control networks. Another way of explaining differences in connectivity maps is the increased power in detecting regions with the larger sample, suggesting that the same regions might be identified even with an increase in size of the SCZ-only sample. Elements possibly supporting the latter explanation are non-significant difference in Emotional Distress scores between BD and SCZ populations (difference in scores on Emotional Distress was driven by SCAD population), and identifications of networks in SCZ sample that have previously primarily been linked to BD (i.e. insular cortex) (406).

Results of the current analyses are in line with our previously published findings (403), but also with the results from other research groups (401, 402, 404, 407), of likely correlated patterns of thalamic over-connectivity with sensorimotor areas and under-connectivity with the cerebellum. Cortical areas affected by connectivity changes, along with primary sensory and motor areas, include almost without exception areas taking part in the higher-order processing of sensory information. It is, therefore, not surprising that among areas showing thalamic over-connectivity we found the fusiform gyrus that plays a role in higher processing of visual information, faces, word recognition and reading (441-443), and the insular cortex that receives sensory input via the thalamus and is believed to play a role in sensorimotor processing, but also in providing emotional context to sensory information, and in higher cognitive functions (e.g. salience, attention, social cognition) (444). Another region centering on temporoparietal junction exhibited significant thalamic over-connectivity, and includes structures thought to be linked with Wernicke's area, and, like angular gyrus, thought to play an important role in attention, semantic and number processing, default mode network, awareness, and social cognition (445).

Taking into account that the primary input to the thalamus comes from sensory areas, and the confirmed pattern of thalamic functional over-connectivity with primary and associative sensory cortical areas, it is tempting to interpret this finding through theories of sensory gating disruptions in schizophrenia and psychotic disorders. However, one of the regions, previously

used to explain thalamic over-connectivity with sensory cortical regions via reduction in top-down regulatory tone, was conspicuous for its absence – the prefrontal cortex. In our previously published analysis of thalamo-cortical dysconnectivity (403), we postulated that there is a case to be made for changes in functional connectivity including reduced prefrontal-thalamic connectivity, increased connectivity between prefrontal and sensory regions, and finally increased thalamic connectivity with sensory regions, with prefrontal regions playing an inhibitory/regulatory role and in schizophrenia exhibiting inadequate top-down control indirectly through basal ganglia (446). It is important to note that reduced connectivity with prefrontal areas is indeed noticeable in unthresholded Figures 3 and 8, but these effects do not survive statistical thresholding. Given the wider focus on prefrontal functions disruption in schizophrenia (447-449), explanation including dysfunction of top-down prefrontal inhibitory tone seems to be mechanistically sound. Although the absence of significant prefrontal-thalamic connectivity differences between psychosis/SCZ and healthy control groups in the current analysis does not rule out the role of prefrontal regions, it naturally warrants discussion on possible explanations of thalamic over-connectivity in SCZ patients in the absence of prefrontal effects.

We already mentioned models that move away from conceptualizations of the thalamus as a simple relay, or relatively passive 'switchboard' on the path of sensory information flow, and these models are exactly the ones that could explain primary dysfunctions located in the thalamus as driving downstream effects (e.g. observed increased connectivity with sensory cortical areas). Dysfunction of glutamatergic neurotransmission, primarily through NMDA receptor dysfunction on GABA interneurons, has repeatedly been identified as a possible point of origin for defects seen in schizophrenia, and NMDA receptor dysfunction has also been hypothesized to be present in the thalamus and to underlie cortico-thalamo-cortical network deficits. One of the hypothesized ways in which this could take place is by indirectly compromising sensory driver inputs via NMDA receptor-mediated GABA interneuron dysfunction, or through thalamic higher-order nuclei dysfunction caused by direct NMDA receptor-related attenuation of driver feedforward excitatory inputs projecting from cortical areas (450).

Reticular thalamic nucleus, a thin sheet of inhibitory GABAergic interneurons that receives collateral afferents and connects widely with the rest of the thalamus providing a strong inhibitory signal, represents an appealing target for the hypothesized primary thalamic dysfunction leading to deficits in thalamo-cortical communication and large scale cortical communication as well as higher cognitive functions (311). RTN is suggested to be a vital communication hub between cortical areas and the thalamus, and disinhibition in thalamo-cortical circuits has been proposed to significantly affect behavior and cognitive functions

(311). We could, therefore, imagine NMDA receptor dysfunction affecting GABAergic inhibitory tone in both prefrontal cortex and the thalamus separately, resulting in the disruption in widely distributed networks communication, affecting complex cognitive functions and the underlying symptoms of psychosis. Important interactions between the thalamus and prefrontal cortex would most likely make these changes correlated, but the correlation would not necessarily mean causation. Shifting the point of origin towards primary thalamic dysfunction would be in line with conceptualizations of 'cognitive thalamus' (259), and, although it would remove the need for prefrontal effect as the one driving these disruptions, it in no way invalidates the critical role the prefrontal cortex plays in the entire model. Interestingly, in our already published analysis of thalamo-cortical disturbances (403), we found specifically thalamic over-connectivity with sensorimotor cortical areas to correlate with general psychopathology score, while the same was not seen for under-connectivity with prefrontal areas. This in itself, of course, does not allow any clear inference about a possible hierarchy or directionality, the least of all any inference about relative importance of prefrontal effects (as over-connectivity effects might just be closer to behavioral expression). However, at the very least it confirms that over-connectivity with large sensorimotor areas presents a stable finding, valuable in overall conceptualizations of thalamo-cortical dysconnectivity, its nature, and phenomenological/clinical consequences.

One of the findings regarding thalamic connectivity changes in schizophrenia and psychotic disorders, consistent across almost all investigations, like the sensorimotor cortex effect, is rarely mentioned or additionally analyzed – the thalamic over-connectivity with almost all cerebellar areas in schizophrenia patients. The same effect was clearly replicated in the current analysis, in wider psychosis-spectrum population, as well as in schizophrenia patients when they were analyzed separately. The cerebellum has been somewhat neglected in biological models explaining psychotic disorders or their symptoms, but that has been slowly changing with the expanding knowledge of the cerebellar role in non-motor functions. It has been shown that schizophrenia patients exhibit changes in the size of the cerebellum, density and size of Purkinje cells, as well as decreased blood flow in a range of tasks (e.g. tasks evaluating memory, attention, social cognition) (145). Andreasen and Pierson (145) have outlined possible models of cerebellar function extending beyond motor control, and motor and associative learning, that include modulation of cognitive processes ranging from timing to detecting patterns and providing feedback to the cortex following detection of errors (in thought as well as in movement). Realization of the role of the cerebellum in schizophrenia, and development of wider function models, lead to the conceptualization of dysfunction of integration in cortical-subcortical-cerebellar circuits as underlying schizophrenia, with

'cognitive dysmetria' coined to describe phenomenological outcome of the circuit disruption (144, 145, 323).

6.4. Thalamic functional subdivision analyses and group-by-seed interactions

With the aim of performing a more finely grained analyses of thalamic connectivity, functional subdivision of the thalamus already reported by our lab (432) was used in separate seed based analyses. As seen in Figure 2, of the 12 networks only three did not chart onto the thalamus: ventral multimodal (VMM), language (LAN), and orbito-affective (ORA) network. For the remaining nine networks, the corresponding functionally connected areas of the thalamus were entered into connectivity analysis with averaged signal across all voxels from each of the seeds and correlating that averaged value with signal from each other brain voxel. In order to investigate the group-by-seed interaction, a 2x9 interaction for groups of psychosis patients and healthy controls across all nine functional networks thalamic seeds was calculated. As seen from interaction effect reported in Figures 13 and 14, numerous cortical and subcortical regions emerge as significant in the interaction, and the regions surviving the analysis largely follow those reported in the previously discussed main effects. Reported finding confirms that there are significant differences between the two groups as the factor of seeds used for connectivity analyses, and the separate look into individual seed connectivity analyses clarifies which of the seeds drive the effects. As already reported, for the three of functional thalamic seeds no group differences survived the thresholding (frontoparietal cognitive control, cingulo-opercular, and posterior multimodal), and the cortical surface representation of the remaining six thalamic seeds connectivity group difference is reported in Figure 15. As can be seen, although there are clear differences in the number and size of cortical regions surviving the thresholding for group-difference connectivity maps for each of the six thalamic seeds, the overall pattern of affected regions seems not to deviate from the one seen in the whole-thalamus seed-based analyses. Some seeds had just a few effects that survived for regions we would naturally link to the underlying networks, like the auditory seed. Some seeds like one of the visual seeds, although seemingly specialized, surprisingly showed increased connectivity with large swathes of wider primary sensorimotor cortical areas. Interestingly, one of the seeds (dorsal attention network) seemed to strongly capture all of the previously reported whole-thalamus group-difference effects, but also, importantly, medial (anterior cingulate) and lateral prefrontal areas in the right hemisphere (under-connectivity effect). The pattern of over- and under-connectivity for dorsal attention thalamic nucleus is shown in Figure 15, and the regions outlined in Tables 11 and 12.

Dorsal attention network is, along with fronto-parietal and cingulo-opercular networks, a part of task-positive systems that are active during performance of specific tasks, as opposed to task-negative default mode network that contains brain regions active during the resting state. Dorsal attention network includes DLPFC, inferior precentral sulcus, frontal eye fields, superior parietal lobule, superior occipital gyrus, and motion complex of middle temporal gyrus (451, 452). As can be seen in Figure 2, dorsal attention thalamic subnucleus (light green) positions itself roughly in the posterior lateral region adjacent to the pulvinar, but clear anatomical divisions should not be inferred. Spreng et al. (452) found that fronto-parietal control network serves as a flexible modulator positioning itself between anti-correlated default mode and dorsal attention networks, and coupling with one or the other based on the task. While fronto-parietal thalamic seed effects did not survive the thresholding, interestingly, seed-based analysis map for default mode network follows the same overall general pattern of over-connectivity with sensorimotor cortex, seen with dorsal attention network seed and the whole thalamus effect.

The approach used to achieve parcellation of the thalamus was based on assignment of functional networks to the thalamus reported from our lab by Ji et al. (432). This approach has resulted in identification of new functional networks: ventral and posterior multimodal networks, and orbito-affective network. Identification of novel networks has been enabled by multiband imaging technique and analyses improvements, as the three novel networks have been identified in areas that previously suffered from dropout of the signal caused by magnetic field inhomogeneity near sinuses (432). New identified networks, however, did not prove to be significant for the current thalamic subnuclei connectivity analyses, as ventral multimodal network and orbito-affective network do not actually chart onto the thalamus, and were therefore not a part of nine thalamic seeds we used, and posterior multimodal network did not show any group-difference effects that survived permutation analyses and thresholding.

Since it is well known that thalamic subnuclei create specific separated networks with different cortical regions, the approach of using functional cortical networks to assign 'functional thalamic subnuclei' has been validated through investigation of assignments of lateral and medial geniculate nuclei. As expected, using this method of assigning functional networks, later geniculate nucleus is assigned to the primary visual network (VIS1), and medial geniculate nucleus to the auditory network (AUD) (432). Regardless of this validation of this model of functional networks being assigned to functional thalamic subnuclei, it is important to keep in mind that we are dealing with functional and not anatomical thalamic nuclei, and that there can be a blurring overlap between anatomically defined subnuclei. Two areas anatomically separate and with different projection areas, if they are indirectly connected as parts of widely distributed complex networks, can show congruent fMRI signal oscillations, and

consequently be assigned to the same network and be identified as functionally connected. To reiterate what has already previously been outlined, functional connectivity does not automatically imply anatomical connectivity.

In an attempt to simplify the analyses, associative and sensorimotor thalamic seeds were lumped together, and the 2x2 group-by-seed interaction was again calculated for both wider psychosis sample, and separately for schizophrenia patients. Table 13 (psychosis sample) and Table 14 (schizophrenia sample) report regions that were identified in 2x2 interaction, and that showed the difference between groups as a factor of seed. From the interaction effect, it is clear that no significant pattern differences emerged between groups as a factor of seed. Certain differences are seen when individually inspecting between-group differences for each of the seeds (associative and sensorimotor), not in terms of different patterns but in the sense of associative seed still being robustly linked to larger spatial effects and additional connectivity effects identified. Robustness of the reported pattern of over- and under-connectivity across different thalamic subdivisions, with minor differences in the size of the effect but not in the overall pattern differences, warrants a discussion, especially given that it has been previously stated how thalamic subnuclei show different anatomical connections and form separate circuits with almost no intra-thalamic communication between subnuclei.

We previously reported (403) that the thalamic dysconnectivity effect, which includes strong over-connectivity with bilateral sensorimotor regions, is primarily driven by area of the thalamus converging on MD nucleus, although MD is known to be primarily strongly reciprocally linked to prefrontal cortex. We also reported (406) that connectivity patterns for thalamic subnuclei with known different anatomical projections forming separate circuits (MD – prefrontal vs. lateral geniculate nucleus – occipital cortex) show striking overall over- and under-connectivity similarities, with just several regional specific findings (lateral geniculate nucleus increased connectivity with primary visual regions and anterior cingulate). Additionally, although BD patients show somewhat different dysconnectivity pattern, prominently including absence of cerebellar effect, BD patients with psychosis history exhibit more severe and SCZ-like alterations (406).

Similar patterns seen for some of the nine thalamic functional subnuclei might seem to suggest there has to be an technique-related overlap in seeds, given that BOLD fMRI signal's resolution is not at the level of anatomical boundaries. Several points, however, speak against that conclusion. As outlined, three thalamic seeds showed no group difference connectivity effects, and the resolution issue with blurring of boundaries would affect those seeds like the others. Additionally, for the auditory seed that showed similar but reduced over-connectivity pattern with sensory areas, the effect was specifically restricted to superior temporal gyrus important for processing of auditory information, arguing for the ability of achieving spatial

specificity. Current results, along with our previously reported correlated thalamic over- and under-connectivity results (403), and especially our previous finding of similar connectivity patterns in subnuclei with anatomically segregated networks (406), suggest the existence of connected widely distributed network level disturbances in schizophrenia and psychosis spectrum, captured by functional connectivity analyses that do not imply direct anatomical connections.

Previously mentioned hypothesis of dysfunction of GABAeric modulatory/inhibitory signal originating from reticular nucleus (possibly due to NMDA receptor dysfunction) could also be seen as a possible factor in emergence of correlated connectivity changes patterns shared across thalamic subnuclei. As already mentioned, reticular nuclei receive collaterals from different input signals and in turn connect to multiple thalamic subnuclei, modulating their activity and possibly imposing synchronization. In order to assess the hypothesis of a possible role of reticular nucleus in creating the observed effects adequately, investigations including multiple research modalities would need to be undertaken, combined with computational modeling and pharmacological interventions that mimic specific receptor disturbances (396).

6.5.   Clustering results

Since thalamic connectivity analyses were performed by 'imposing' functional thalamic subnuclei, previously defined through connectivity with segregated cortical networks, dysconnectivity data-driven clustering using between-group signal differences was undertaken for a qualitative comparison. Clustering algorithm that was used lumps together voxels based on similarity of their dysconnectivity pattern. Clustering was done for both wider psychosis spectrum sample, and for the schizophrenia group. Taking into account that nine thalamic functional seeds were used, 9-cluster solution was reported. Figure 25, panel a, reports the 9-cluster solution for psychosis spectrum, and when compared to results for schizophrenia sample (reported in Figure 28), it is clear that both yield robust division, and spatially similarly distributed nine clusters emerge. It is also clear, however, that nine clusters formed based on thalamic 'intrinsic' dysconnectivity group differences do not match the nine functional thalamic seeds, additionally proving that different divisions we use in segregating the thalamus do not usually follow as equally segregated dysconnectivity patterns.

In line with our previously reported findings (403), 2-cluster solution yielded a large cluster centered on MD nucleus but also large areas of lateral thalamic regions, and the smaller one in the posterior and anterior thalamic regions. Also, calculated dissimilarity index showed voxels exhibiting greatest between group differences to be centered on mediodorsal and

ventral lateral thalamic regions, for both psychosis spectrum and for schizophrenia assessed separately.

6.6. Relationship with symptoms

Correlating symptoms with a biological finding represents a point of specific and possibly ultimate interest for any clinician, but in analyses like this, for a number of reasons it also offers the least opportunity for robust and clear inferences and conclusions. One of the problems for this is the way we measure psychopathology. Although psychopathology scales we use for different disorders generally fulfill their role in the context of phenomenological taxonomy approach, they fall short of helping us fill the gap between biology and clinical phenomena. RDoC initiative aims specifically at bridging that gap through integration of information spanning from genes, molecules and circuits to behavior, and, recognizing inadequacy of current tools, introduces specific systems, constructs and subconstructs that might chart onto the underlying circuits/networks disruptions better than symptoms (203). Therefore, instead of a specific symptom and a symptom cluster, within this framework, for example, we would be talking about positive valence system, subsumed constructs of reward responsiveness, and subconstruct of reward satiation.

Although PANSS is one of the most widely used scales to assess positive and negative symptoms in psychotic disorders, even the perfunctory glance at its structure might point to problems in using it for correlation with possible underlying biology. Although the name itself focuses on positive and negative syndromes, most of the items are originally subsumed under General Psychopathology subscale, meaning that most of the composite PANSS score might be driven by psychopathology that we do not even specifically designate. That issue can partially be overcome by using alternative PANSS loading algorithms that result in 5-factor psychopathology systems, practically reorganizing items in the PANSS General Psychopathology to yield syndromes like Disorganization, Emotional Distress, and Excitation. Another issue cannot, however, be managed by alternative item loadings, and that is the diversity of items in the positive and negative subscale. Composite score of the positive subscale can tell us little about specific elements of the positive syndrome, and we could theoretically imagine patients showing the same score with substantially different item-based psychopathology structure. For example, a patient with no hallucinations (score 1) and an active stable set of numerous delusions that permeate all aspects of their life and interfere with functioning (score 7), will have the same composite score (score 8) as a patient with frequently occurring hallucinations that affect their behavior to a minor extent (score 4) and one or two vague delusions that do not affect their behavior or social relations (score 3). Since positive

syndrome subscale consists of five items that can be scored from one to seven, the number of different combinations that can yield the same composite score is significant. Separate items (e.g. hallucinations and conceptual disorganization), although part of the same syndrome, can be expected to show different underlying biological processes.

Taking all of these PANSS characteristics into consideration, as well as the fact that no *a priori* assumptions about specific psychopathology phenomena and their link to thalamic pathology were made, investigation of link between the thalamic dysconnectivity and symptoms was restricted to just a few questions. Another reason for restrictions in the situation where no specific *a priori assumptions* are made is the fact that PANSS item-level analyses would necessarily lead to spurious correlations that would be difficult to interpret, regardless of Type I error protections used.

In our previously reported thalamo-cortical dysconnectivity findings (403), thalamic over-connectivity with sensorimotor cortex, but not under-connectivity with prefrontal regions and the cerebellum, was found to correlate with total PANSS score as a measure of the overall symptom severity. In a slightly more detailed evaluation, no correlation with dysconnectivity effects was seen for positive or negative symptoms, but general psychopathology subscale significantly correlated with over-connectivity effects, leading to the conclusion that thalamic disturbances might be more related to non-specific illness severity (403). In the current analysis, for psychosis spectrum population, only general psychopathology subscale showed a significant association with the thalamic under-connectivity effect ($F(1,434)=5.12$, $p=0.024$, $R^2=0.00886$). Restricting analysis to just schizophrenia patients, as reported in Table 17, there was a significant association to both composite PANSS score and for general psychopathology, for both thalamic over-connectivity and under-connectivity. Interestingly, although both over-connectivity and under-connectivity were related to total PANSS score and general psychopathology, in line with our previous findings identifying association with over-connected regions, the effect was clearly stronger for thalamic over-connectivity.

As already reiterated, the more finely grained evaluation using GLM model was done through applying Van der Gaag loading to PANSS items, resulting in 5-factor psychopathology structure. Analyses of those five symptom clusters failed to find any correlations between thalamic over- and under-connectivity and Positive or Emotional Distress subscales. On the other hand, there was a significant effect for Negative symptoms subscale and over-connected regions ($F(1,165)=11.85$, $p<.001$, $R^2=0.06137$), and Negative subscale and under-connected regions ($F(1,165)=5.33$, $p=0.022$, $R^2=0.02543$). Similarly, a significant effect was found for Excitation subscale and over-connected regions ($F(1,165)=10.55$, $p=0.001$, $R^2=0.05442$), and Excitation subscale and under-connected regions ($F(1,165)= 7.21$, $p=0.008$, $R^2=0.03607$). There was no significant scaling between under-connected regions and Disorganization

subscale, but there was a statistically significant effect for under-connected regions (F(1,165=9.34, p=0.002, R^2=0.04785).

As a rule, more pronounced effect, whether it was over- or under-connectivity, predicted increased severity of the symptoms.

Several points from these findings warrant discussion. Although lower values of R-squared for all analyses seem to point to a relatively poor fit to regression models, given the attempt at predicting human behavior, for which lower values are expected, the nature of behavioral data, and the expected 'separation' between biological measures and behavioral scores, these results can still be taken to represent a meaningful information on how changes in biological predictor value affect changes in the psychopathology response value. In line with our previous findings (403), over-connectivity effect seems to consistently be more associated with the general symptom severity. Previously identified General Psychopathology effect associated with thalamo-cortical dysconnectivity (403) now seems to be successfully parsed into Excitation and Disorganization clusters that keep the correlation with the dysconnectivity pattern. Additionally, the sample size that significantly increased since the previous analyses, also helped identify a possible association with negative symptoms. Taken together, these results seem to suggest that thalamo-cortical dysconnectivity shows no meaningful relationship with positive symptoms, but that it could be associated with symptoms considered more to be SCZ 'signature symptoms', negative symptoms, and disorganization cluster that can be associated with cognitive disturbances. Even Excitation subscale, given the items used to determine its score, could be taken to imply a loss of coherence in specific cognitive functions. In addition, these results seem to confirm the interconnection between over- and under-connectivity, which corroborates the previously reported findings. Importance of the correlation between thalamic over- and under-connectivity effects, in the context of their relationship with symptoms, can be important in assessing therapeutic interventions. Knowing that the thalamus connects with segregated networks, amelioration of one effect through pharmacological or non-pharmacological interventions (e.g. over-connectivity), will not necessarily correct the opposing disturbances, possibly leading to residual symptoms and functional impairment.

One significant problem in analyzing psychopathology relationship with thalamo-cortical connectivity changes, and the one that could also explain the absence of most of the effects in the wider psychosis spectrum sample, is the fact that we were analyzing a relatively stable population with low psychopathology scores across almost all symptom clusters. By far least affected population was the population of bipolar patients with a history of psychotic symptoms, and analyses including them could result in an attenuation of effect. That assertion cannot be made, however, without a formal comparison of the different groups. Additionally,

with the inclusion of SCAD and BDp populations, we saw certain additional regions, or increase in the size of regions identified, that appear in the connectivity analyses (whether they follow the same pattern of regions seen in SCZ or are novel like posterior cingulate). Since mean Fz for linear regression analyses is calculated by averaging the signal across all over- or under-connected regions, additional regions might lead to the 'blurring' and reduce the ability to detect association of specific brain regions with the symptoms. If we follow that line of thinking, although we have the same general connectivity pattern, a restricted list of regions surviving the SCZ-only analyses might be in better position to capture the meaningful connections, as they are free from the 'noise' induced by additional identified regions. It is among those regions that we might look for candidate regions that would help analyze symptom biology in a more mechanistic way. This explanation can also help us understand the incongruence with results reported by Ferri et al. (411) showing a positive correlation between increased connectivity with middle temporal gyrus and hallucinations and delusions. It is possible that isolating just one over- or under-connected region might show specifically significant relationship with positive symptoms or other psychopathology phenomena, and this approach seems to be a valuable approach in the future testing of specifically focused hypotheses.

A follow-up exploratory analysis in psychosis spectrum population with five specific PANSS items was done using dorsal attention seed. That specific seed was chosen since it was the only one for which prefrontal effects survived the stringent analysis algorithm and thresholding. Due to lack of *a priori* formed hypothesis about links of specific regions with specific items, averaging across all over-connected and then all under-connected regions was utilized, notwithstanding the previously described risk for the 'signal blurring'. Psychosis spectrum population was analyzed to increase the power of the analysis. Of all the items examined, for only one the linear regression model showed a statistical significance when entered into the model with under-connectivity effect – disorientation ($F_{(1,434)}$= 4.87, p=0.028, R^2=0.008809). Even with all the limitations of making inferences from these results already mentioned, the nature of dorsal attention network and the fact that corresponding thalamic seed showed link to disorientation score suggest a trend that warrants further more focused investigation. Furthermore, it serves as the proof of a concept for using thalamic subnuclei connectivity to expand knowledge on biological underpinning of specific phenomena.

Any future studies examining the role of specific thalamic subnuclei and their connectivity changes in the context of symptoms will need to combine different research modalities (e.g. task- and resting state-based fMRI models combined with DTI and computational modelling) in a longitudinal approach that will help to better control for possible confounders.

6.7. Limitations

Several limitations of the study have already been mentioned throughout the previous section but it is necessary to emphasize them again. Arguably, the biggest impediment for making clear inferences based on current analyses is their cross-sectional nature that reduces the ability to control for specific factors possibly exerting a confounding effect. Although duration of illness, age, sex, and antipsychotic medication expressed in CPZ equivalents were entered into the PALM model, and did not alter the reported effects, the only way to adequately address their possible impact would be through a longitudinal study design. Longitudinal design would also allow a more detailed investigation of the correlation of symptoms with thalamocortial changes, observing simultaneously changes in both of them over time (possible as a factor of medication and other variables), putting us also in a positon of making inferences on whether the observed changes represent a trait or a state factor.

Lumping of all antipsychotic medications together might also present a weak spot of most of the current studies utilizing such approach, as there is expected to be a difference in the ways drugs with significantly different receptor profiles affect neural networks dependent on a number of neurotransmitter systems perturbed by medications. A detailed classification of medications used and comparison to not-medicated population will help clarify some of the effects.

The patient population identified for this study included mostly non-acute patients, which can be seen from relatively low psychopathology scores (especially in BDp population), limiting the power for making strong inferences regarding biology underlying the symptoms. If we assume the existence of a specific state-related biological 'signature' for symptoms, we are most likely to capture those patterns during an acute state. We are otherwise more likely to identify trait-related phenomena, although such phenomena might also identify the population with proneness to specific symptom profile. A longitudinal study following individuals across different illness stages would allow for more robust conclusions regarding the nature of the disturbances to be made.

Research attempting to analyze complex network disturbances and their link to clinical phenomena is always severely limited in case it does not use multiple and complementary research modalities. As an example, a detailed investigation into thalamo-cortical disturbances and their relationship with symptoms would benefit from additions to the resting-state paradigm, including utilizing tasks targeting specific functions, DTI, MRS, and computational modelling. It is only with multiple research modalities offering complementary information about

the researched phenomenon, that complex models of disturbances in correlated and widely distributed networks can be made.

Although we used state-of-the-art fMRI algorithms and protocols, parcellation of the thalamus still presents a difficult task, with current fMRI resolution not matching the anatomy, which could create the possibility of overlap between different regions with inclusion of different tissue types within a voxel. Previous studies, however, argue against a significant effect of major registration issues for subcortical nuclei, as we already reported (403). Additionally, there is a certain circularity in achieving parcellation of the thalamus by using functional connectivity with previously identified cortical networks, just to in turn assess the functional connectivity of those same subnuclei. If there is a change in connectivity with specific networks in certain disorders, we might expect then that functionally defined subnuclei might differ between healthy population and those showing changes due to that specific disorder. We offered a possible future solution for those problems in the form of data-driven clustering that would enable us to identify areas of significant connectivity differences within the thalamus without imposing any *a priori* defined models.

7. Conclusions

- In schizophrenia, changes of the thalamo-cortical functional connectivity, measured by fMRI, show robust over-connectivity effects centered primarily on sensory and motor regions, and associative cortical regions important for information integration, as well as under-connectivity with multiple cerebellar regions. Thalamo-cortical disturbances seem to represent correlated disruptions in widely distributed networks, with severely restricted connectivity variations in psychotic patients.

- Analyzing schizophrenia as just the far end of the larger psychosis spectrum (that includes schizoaffective disorder and psychotic bipolar disorder patients) does not result in overall 'attenuation' of previously seen thalamic connectivity effects, suggesting that robust thalamo-cortical connectivity changes exist across psychotic disorders, and might underlie processes shared across psychosis spectrum, standing in line with genetic, family, structural, clinical, and phenomenological evidence. However, it cannot be excluded that thalamic dysconnectivity, suggesting wider system disruptions associated with psychosis, might also potentially differently affect specific phenomena seen in individuals disorders that make up the spectrum.

- Although previously linked more specifically with affective disorders, the insular cortex emerged robustly as one of the regions with altered thalamic connectivity across the psychosis spectrum, as it was also clearly seen in schizophrenia patients when analyzed separately.

- Parcellation of the thalamus using thalamic connectivity with separate functional cortical networks results in nine thalamic 'functional subnuclei' (not matching anatomical division) that show different connectivity changes in psychosis spectrum patients. For three of those functional subnuclei, frontoparietal cognitive control, cingulo-opercular, and posterior multimodal, no regions show between group differences (psychosis vs. healthy controls), while main effect seems to be driven by visual, default mode network, and dorsal attention functional seeds.

- Although previously reported thalamic under-connectivity with prefrontal cortical areas did not survive the stringent permutation analyses and thresholding,

unthresholded connectivity images suggest prefrontal under-connectivity trend, and furthermore, prefrontal areas thalamic under-connectivity was seen for the dorsal attention functional subnucleus seed-based fMRI analysis in psychosis spectrum patients. Reported results suggest that dorsal attention functional thalamic subnucleus might be driving prefrontal connectivity effects, and also call into question previous conceptualizations of the role of prefrontal disturbances in driving other described effects.

- Grouping nine functional thalamic subnuclei into associative and sensorimotor groups resulted in overall similar main connectivity patterns, replicated robustly across seeds and analyses, but also resulted in little added value, and ultimately in the loss of information that was gained from more finely grained analysis using multiple functional subnuclei (e.g. specific prefrontal connectivity effect seen for dorsal attention functional subnucleus). Associative seed analyses did show more pronounced effects when compared to sensorimotor seed or the whole thalamus, confirming again that majority of the effects seem to be driven by areas of thalamus functionally connected to associative areas.

- Data-driven thalamic clustering based on the between-group connectivity differences results in clusters that do not match *a priori* defined functional subnuclei. Two-cluster clustering solution identifies a large cluster centered on the mediodorsal nucleus and large areas of lateral thalamic regions, and the smaller one in the posterior and the anterior thalamic regions. Areas roughly corresponding to the mediodorsal nucleus and ventral lateral thalamic regions show most pronounced between-group connectivity differences.

- Identified thalamo-cortical connectivity changes seem not to be related to positive symptoms of psychosis, but in schizophrenia sample (characterized by more pronounced negative and cognitive symptoms) are associated with negative symptoms, and scores for the Excitation and Disorganization aspects of the PANSS' general psychopathology. The more pronounced over- /under-connectivity effects predict more severe symptoms.

- The thalamo-cortical connectivity changes might underlie more non-specific trait features and overall severity of the disorder, in line with previous robust relationship with general psychopathology scores, but given the relationship with negative, excitation, and disorganizations symptoms in our large schizophrenia sample, could also prove to confer a risk for a specific and more schizophrenia-

like clinical presentation. Due to reported relationships with symptoms, links between symptoms (e.g. negative and cognitive symptoms) and specific brain regions warrant evaluation by using regions that were identified in the analyses of the schizophrenia sample.

- Connectivity changes of the dorsal attention thalamic functional subnucleus (under-connectivity that includes prefrontal areas) correlate specifically with disorientation, suggesting a possible trend and the utility of using item-based approach (avoiding composite psychopathology scores) and separate thalamic subnuclei as opposed to whole-thalamus approaches, in attempts to elucidate biological underpinnings of specific psychopathology phenomena.

8. Sažetak

Naslov: Utvrđivanje obilježja talamo-kortikalnih promjena i njihovog odnosa sa simptomima u shizofreniji

Hipoteza doktorskog rada bila je da će se kod pacijenata kojima je dijagnosticirana shizofrenija, uz uporabu funkcijske magnetske rezonance u stanju mirovanja, pokazati stabilni i specifični obrasci promjene funkcijske povezanosti talamusa, koji će imati različitu vezu sa specifilnim simptoma psihotičnih poremećaja.

Ciljevi istraživanja su bili detaljnije utvrđivanje obilježja promjene talamo-kortikalne funkcijske povezanosti (jača ili slabija funkcijska povezanost) u kliničkoj skupini uspoređenoj sa zdravim kontrolnim ispitanicima, koristeći najsuvremenije protokole funkcijske magnetske rezonance i Projekta ljudskog konektoma (engl. Human Connectome Project), kao i specifičnije određivanje razlika unutar samog talamusa i određivanje njihovog relativnog doprinosa opisanim promjenama u funkcijskim vezama. Konačno, cilj je bio utvrditi vezu između utvrđenih promjena u funkcijskoj povezanosti i specifičnih simptoma poremećaja.

Ispitanici za istraživanje prikupljeni su multicentrično, u sklopu postojeće incijative, konzorcij Bipolarna-shizofrenija mreža indermedijarnih fenotipa (engl. Bipolar-Schizophrenia Network on Intermediate Phenotypes – B-SNIP), koja je nastala s ciljem istraživanja intermedijarnih fenotipa kroz sve psihotične poremećaje. Procedure istraživanja i analiza podataka provedeni su u sklopu odobrenog projekta na Sveučilištu Yale *Identificiranje obilježja kliničkih i farmakoloških neuroslikovnih bioloških biljega* (engl. Characterizing Clinical and Pharmacological Neuroimaging Biomarkers). Nakon identificiranja ispitanika koji su prošli strogu kontrolu kvalitete podataka funkcijske magnetske rezonance, istraživanje je uključivalo 436 ispitanika s psihotičnim poremećajem (167 pacijenata s dijagnosticiranom shizofrenijom, 119 sa shizoafektivnim poremećajem i 150 sa bipolarnim poremećajem raspoloženja s poviješću psihoze) i 219 demografski usklađenih zdravih kontrolnih ispitanika. Analize temeljene na ispitivanju povezanosti cijelog talamusa provedene su kako bi se utvrdile opće promjene u funkcijskim vezama talamusa, praćene zatim podjelom talamusa uporabom *a priori* definiciranim funkcijskim talamičkim jezgrama, te grupiranjem temeljenom na funkcijskim neuroslikovnim podacima kako bi se definirali detalji poremećaja povezanosti talamusa s moždanom korom u shizofreniji i psihotičnim poremećajima.

Kako u shizofreniji tako i u širem spektru psihoza utvrđen je jasan obrazac pojačanih funkcijskih veza sa senzoričkim i motoričkim područjima kore, kao i s asocijatvinim područjima zaduženim za integraciju ulaznih podataka s nižih razina, te slabije funkcijske povezanosti s područjima malog mozga. Prethodno objavljeno sniženje u funkcijskoj povezanosti s prefrontalnim područjima bilo je vidljivo samo u mapi funkcijskih veza za funkcijsku talamičku

jezgru dorzalne pozornosti. Devet funkcijskih talamičkih jezgri imalo je donekle različite promjene talamičke funkcijske povezanosti, u rasponu od toga da je rezultat potpuno nedostajao za neke funkcijske jezgre, do postojanja proširenih promjene pojačane ili oslabljene talamičke povezanosti, no u načelu te su promjene općenito pratile obrasce promjene povezanosti koji su uočeni i za cijeli talamus. Grupiranje područja talamusa je pokazalo da postupci grupiranja temeljeni na podacima, oslobođeni okvira *a priori* definiranih talamičkih jezgri, imaju za rezultat rješenja koja se razlikuju od prethodno postojećih funkcijskih jezgri ili anatomskih podjela, s područjima oko mediodorzalne jezgre i ventralnih lateralnih područja kao nositeljima razlika u talamičkim vezama između kliničke populacije i kontrola.

U shizofreniji su promjene u talamo-kortikalnim funkcijskim vezama pokazale vezu s negativnim simptomima, kao i s rezultatom skala uzbuđenja i dezoganiziranosti, navodeći na zaključak da izraženija promjena (pojačanje ili slabljenje funkcijskih veza) predviđa izraženiji specifični symptom. Sniženje funkcijske povezanosti funkcijske talamičke jezgre dorzalne pozornosti (uključujući sniženu povezanost s prefrontalnim regijama moždane kore) također je koreliralo s dezorijentacijom.

Zaključno, obrasci izgledno povezanih promjene talamičkih funkcijskih veza (pojačne i oslabljene funkcijske povezanosti) snažno su prisutni u shizofreniji ali i u spektru psihoza. Iako je sličan obrazac prisutan u različitim talamičkim regijama, njegov se opseg razlikuje među talamičkim funkcijskim jezgrama, navodeći na zaključak kako su rezultati primarno vođeni upravo specifičnim asocijativnim funkcijskim talamičkim jezgrama. Konačno, iako bi talamo-kortikalne promjene u funkcijskoj povezanosti mogle biti više vezane uz nespecifične značajke kao što su težina poremćaja ili indikatori osobina poremećaja, čini se kako su ipak negativni simptomi, dezorganiziranost i uzbuđenje izravnije povezani s tim promjenama nego li su to pozitivni simptomi ili disregulacija emocija.

9. Abstract

Hypothesis of the doctoral thesis was that, using resting-state functional magnetic resonance imaging (fMRI), patients diagnosed with schizophrenia would exhibit stable and specific patterns of thalamic connectivity changes that will show different relationship with specific symptoms of psychotic disorders.

The aims of the study were to characterize in a more detailed way changes in thalamo-cortical connectivity (over- and under-connectivity) in a clinical sample compared to healthy controls, by using state-of-the-art resting-state functional resonance and Human Connectome Project protocols, as well as to more specifically determine within-thalamus differences and their relative contribution to described connectivity changes. Finally, the aim was to determine relationship between identified connectivity changes and specific symptoms of the disorder.

Subjects for the study were pooled from multiple centers, as part of an existing initiative, Bipolar-Schizophrenia Network on Intermediate Phenotypes (B-SNIP) consortium, created with a goal of investigating intermediate phenotypes across psychotic disorders. Study procedures and data analyses were done under the approved Yale University project *Characterizing Clinical and Pharmacological Neuroimaging Biomarkers.* Following identification of subjects that passed stringent quality controls for fMRI data, and matching with the clinical and healthy control populations, study included 436 psychosis probands (167 schizophrenia patients, 119 schizoaffective disorder patients, and 150 patients diagnosed with bipolar disorder with history of psychosis) and 219 matched healthy controls. Whole-thalamus seed-based analyses were used to determine thalamic connectivity changes, followed by parcellation of thalamus using *a priori* defined functional subnuclei, and data-driven clustering, to define details of the thalamo-cortical dysconnectivity in schizophrenia and psychotic disorders.

Both in schizophrenia, and in the wider psychosis spectrum, there was a robust pattern of thalamic over-connectivity with sensory and motor regions, as well as with associative areas tasked with integration of lower-level inputs, and under-connectivity with cerebellar regions. Interestingly, previously reported under-connectivity with prefrontal regions was evident only in dorsal attention functional thalamic subnucleus connectivity map. Nine functional thalamic subnuclei showed relatively different thalamic connectivity changes, ranging from altogether missing effects to wide-spread over- /under-connectivity, but overall followed same general dysconnectivity pattern described for the whole thalamus. Clustering analyses revealed that the data-driven clustering, released from constraints of *a priori* defined thalamic subnuclei, resulted in solutions that significantly differed from existing functional subnuclei or anatomical divisions, with areas centered on mediodorsal nucleus and ventral lateral areas driving the dysconnectivity effect.

In schizophrenia, thalamo-cortical connectivity changes showed relationship with negative symptoms, as well as with excitation and disorganization subscale scores, suggesting that a more pronounced over- or under-connectivity effect predicted more pronounced specific symptoms. Under-connectivity effect of the dorsal attention functional subnucleus (including reduced connectivity with prefrontal cortical regions) also correlated with disorientation.

In conclusion, thalamo-cortical dysconnectivity patterns of seemingly correlated over- and under-connectivity effects seems to be robustly present in schizophrenia, but also across the psychosis spectrum. Although the same general pattern exists across different thalamic regions, its extent differs among different thalamic functional subnuclei suggesting that the effect is driven by specific associative functional subnuclei. Finally, although thalamo-cortical connectivity changes might be linked to a more non-specific disease severity or trait indicators, negative symptoms, disorganization, and excitation seem to be connected more directly to those changes than positive symptoms or emotional dysregulation.

10. References

1.   Dollfus S, Lyne J. Negative symptoms: History of the concept and their position in diagnosis of schizophrenia. Schizophr Res. 2017;186:3-7.

2.   Tsoi DTY, Hunter MD, Woodruff PWR. History, aetiology, and symptomatology of schizophrenia. Psychiatry. 2008;7(10):404-9.

3.   Klosterkotter J, Schultze-Lutter F, Ruhrmann S. Kraepelin and psychotic prodromal conditions. Eur Arch Psychiatry Clin Neurosci. 2008;258 Suppl 2:74-84.

4.   Craddock N, Owen MJ. The beginning of the end for the Kraepelinian dichotomy. Br J Psychiatry. 2005;186:364-6.

5.   Bleuler E. Dementia praecox, or the group of schizophrenias. New York: International Universities Press; 1950.

6.   Ayer A, Yalincetin B, Aydinli E, Sevilmis S, Ulas H, Binbay T, et al. Formal thought disorder in first-episode psychosis. Compr Psychiatry. 2016;70:209-15.

7.   Galderisi S, Farden A, Kaiser S. Dissecting negative symptoms of schizophrenia: History, assessment, pathophysiological mechanisms and treatment. Schizophr Res. 2017;186:1-2.

8.   Hafner H, Riecher-Rossler A, Hambrecht M, Maurer K, Meissner S, Schmidtke A, et al. IRAOS: an instrument for the assessment of onset and early course of schizophrenia. Schizophr Res. 1992;6(3):209-23.

9.   Brewer WJ, Wood SJ, Phillips LJ, Francey SM, Pantelis C, Yung AR, et al. Generalized and specific cognitive performance in clinical high-risk cohorts: a review highlighting potential vulnerability markers for psychosis. Schizophr bull. 2006;32(3):538-55.

10.   Nuechterlein KH, Dawson ME. Information processing and attentional functioning in the developmental course of schizophrenia disorders. Schizophr Bull. 1984;10(2):160-203.

11.   Heinrichs RW, Zakzanis KK. Neurocognitive deficit in schizophrenia: a quantitative review of the evidence. Neuropsychology. 1998;12(3):426-45.

12.   Keefe RS, Fox KH, Harvey PD, Cucchiaro J, Siu C, Loebel A. Characteristics of the MATRICS Consensus Cognitive Battery in a 29-site antipsychotic schizophrenia clinical trial. Schizophr Res. 2011;125(2-3):161-8.

13.   Nuechterlein KH, Barch DM, Gold JM, Goldberg TE, Green MF, Heaton RK. Identification of separable cognitive factors in schizophrenia. Schizophr Res. 2004;72(1):29-39.

14.   Palmer BW, Heaton RK, Paulsen JS, Kuck J, Braff D, Harris MJ, et al. Is it possible to be schizophrenic yet neuropsychologically normal? Neuropsychology. 1997;11(3):437-46.

15.   Keefe RS, Eesley CE, Poe MP. Defining a cognitive function decrement in schizophrenia. Biol Psychiatry. 2005;57(6):688-91.

16.   Harvey PD, Koren D, Reichenberg A, Bowie CR. Negative symptoms and cognitive deficits: what is the nature of their relationship? Schizophr. Bull. 2006;32(2):250-8.

17.   Addington J, Addington D, Maticka-Tyndale E. Cognitive functioning and positive and negative symptoms in schizophrenia. Schizophr Res. 1991;5(2):123-34.

18.   Dickerson FB, Ringel NB, Boronow JJ. Neuropsychological deficits in chronic schizophrenics. Relationship with symptoms and behavior. J Nerv Ment Dis. 1991;179(12):744-9.

19.   Michel NM, Goldberg JO, Heinrichs RW, Miles AA, Ammari N, McDermid Vaz S. WAIS-IV profile of cognition in schizophrenia. Assessment. 2013;20(4):462-73.

20.   Keefe RS, Goldberg TE, Harvey PD, Gold JM, Poe MP, Coughenour L. The Brief Assessment of Cognition in Schizophrenia: reliability, sensitivity, and comparison with a standard neurocognitive battery. Schizophr Res. 2004;68(2-3):283-97.

21.   Kopelowicz A, Ventura J, Liberman RP, Mintz J. Consistency of Brief Psychiatric Rating Scale factor structure across a broad spectrum of schizophrenia patients. Psychopathology. 2008;41(2):77-84.

22.   Andreasen NC. The Scale for the Assessment of Negative Symptoms (SANS): Conceptual and theoretical foundations. Br J Psychiatry. 1989;155(S7):49-52.

23.   Andreasen NC. Methods for assessing positive and negative symptoms. Mod Probl Pharmacopsychiatry. 1990;24:73-88.

24.   Kay SR, Fiszbein A, Opler LA. The positive and negative syndrome scale (PANSS) for schizophrenia. Schizophr Bull. 1987;13(2):261-76.

25.   Kay SR, Opler LA, Lindenmayer JP. The Positive and Negative Syndrome Scale (PANSS): rationale and standardisation. Br J Psychiatry Suppl. 1989(7):59-67.

26.   van der Gaag M, Hoffman T, Remijsen M, Hijman R, de Haan L, van Meijel B, et al. The five-factor model of the Positive and Negative Syndrome Scale II: A ten-fold cross-validation of a revised model. Schizophr Res. 2006;85(1):280-7.

27.   Wallwork RS, Fortgang R, Hashimoto R, Weinberger DR, Dickinson D. Searching for a consensus five-factor model of the Positive and Negative Syndrome Scale for schizophrenia. Schizophr Res. 2012;137(1):246-50.

28.   Lindenmayer JP, Bernstein-Hyman R, Grochowski S. Five-factor model of schizophrenia. Initial validation. J Nerv Ment Dis. 1994;182(11):631-8.

29.   Ruggeri M, Koeter M, Schene A, Bonetto C, Vazquez-Barquero JL, Becker T, et al. Factor solution of the BPRS-expanded version in schizophrenic outpatients living in five European countries. Schizophr Res. 2005;75(1):107-17.

30.   McGrath JA, Nestadt G, Liang KY, Lasseter VK, Wolyniec PS, Fallin MD, et al. Five latent factors underlying schizophrenia: analysis and relationship to illnesses in relatives. Schizophr Bull. 2004;30(4):855-73.

31.   Tibber MS, Kirkbride JB, Joyce EM, Mutsatsa S, Harrison I, Barnes TRE, et al. The component structure of the scales for the assessment of positive and negative symptoms in first-episode psychosis and its dependence on variations in analytic methods. Psychiatry Res. 2018;270:869-79.

32.   Silverstein ML, Harrow M. Schneiderian first-rank symptoms in schizophrenia. Arch Gen Psychiatry. 1981;38(3):288-93.

33.   Andreasen NC. The American concept of schizophrenia. Schizophr Bull. 1989;15(4):519-31.

34.   Nordgaard J, Arnfred SM, Handest P, Parnas J. The diagnostic status of first-rank symptoms. Schizophr Bull. 2008;34(1):137-54.

35.   Tandon R, Gaebel W, Barch DM, Bustillo J, Gur RE, Heckers S, et al. Definition and description of schizophrenia in the DSM-5. Schizophr Res. 2013;150(1):3-10.

36.   Diagnostic and statistical manual of mental disorders: DSM-5™, 5th ed. Arlington, VA, US: American Psychiatric Publishing, Inc.; 2013.

37.   Carpenter WT, Tandon R. Psychotic disorders in DSM-5: Summary of changes. Asian J Psychiatr. 2013;6(3):266-8.

38.   Welham J, Saha S, Chant D, McGrath J. Schizophrenia: A Concise Overview of Incidence, Prevalence, and Mortality. Epidemiol Rev. 2008;30(1):67-76.

39.   Saha S, Chant D, Welham J, McGrath J. A systematic review of the prevalence of schizophrenia. PLoS Med. 2005;2(5):e141.

40.   Charlson FJ, Ferrari AJ, Santomauro DF, Diminic S, Stockings E, Scott JG, et al. Global Epidemiology and Burden of Schizophrenia: Findings From the Global Burden of Disease Study 2016. Schizophr Bull. 2018;44(6):1195-203.

41.   Messias EL, Chen C-Y, Eaton WW. Epidemiology of schizophrenia: review of findings and myths. Psychiatr Clin North Am. 2007;30(3):323-38.

42.   Sadock BJ, Sadock VA, Ruiz P. Kaplan & Sadock's synopsis of psychiatry : behavioral sciences/clinical psychiatry. Eleventh ed: Philadelphia : Wolters Kluwer; 2015.

43.   Bitter I, Czobor P, Borsi A, Feher L, Nagy BZ, Bacskai M, et al. Mortality and the relationship of somatic comorbidities to mortality in schizophrenia. A nationwide matched-cohort study. Eur Psychiatry. 2017;45:97-103.

44.   Olfson M, Gerhard T, Huang C, Crystal S, Stroup TS. Premature mortality among adults with schizophrenia in the United States. JAMA Psychiatry. 2015;72(12):1172-81.

45.   Robinson DG. Early mortality among people with schizophrenia. Am J Psychiatry. 2016;173(6):554-5.

46.   Hjorthoj C, Sturup AE, McGrath JJ, Nordentoft M. Years of potential life lost and life expectancy in schizophrenia: a systematic review and meta-analysis. Lancet Psychiatry. 2017;4(4):295-301.

47.   Global, regional, and national incidence, prevalence, and years lived with disability for 301 acute and chronic diseases and injuries in 188 countries, 1990-2013: a systematic analysis for the Global Burden of Disease Study 2013. Lancet. 2015;386(9995):743-800.

48.   Chong HY, Teoh SL, Wu DB, Kotirum S, Chiou CF, Chaiyakunapruk N. Global economic burden of schizophrenia: a systematic review. Neuropsychiatr Dis Treat. 2016;12:357-73.

49.   Conus P, Cotton SM, Francey SM, O'Donoghue B, Schimmelmann BG, McGorry PD, et al. Predictors of favourable outcome in young people with a first episode psychosis without antipsychotic medication. Schizophr Res. 2017;185:130-6.

50.   Jääskeläinen E, Juola P, Hirvonen N, McGrath JJ, Saha S, Isohanni M, et al. A systematic review and meta-analysis of recovery in schizophrenia. Schizophr Bull. 2013;39(6):1296-306.

51.   Wunderink L, Sytema S, Nienhuis FJ, Wiersma D. Clinical recovery in first-episode psychosis. Schizophr Bull. 2009;35(2):362-9.

52.   White C, Stirling J, Hopkins R, Morris J, Montague L, Tantam D, et al. Predictors of 10-year outcome of first-episode psychosis. Psychol Med. 2009;39(9):1447-56.

53.   Leung A, Chue P. Sex differences in schizophrenia, a review of the literature. Acta Psychiatr Scand Suppl. 2000;401:3-38.

54.   Chang WC, Ho RWH, Tang JYM, Wong CSM, Hui CLM, Chan SKW, et al. Early-Stage Negative Symptom Trajectories and Relationships With 13-Year Outcomes in First-Episode Nonaffective Psychosis. Schizophr Bull. 2019;45(3):610-619.

55.   Alvarez-Jimenez M, Gleeson JF, Henry LP, Harrigan SM, Harris MG, Killackey E, et al. Road to full recovery: longitudinal relationship between symptomatic remission and psychosocial recovery in first-episode psychosis over 7.5 years. Psychol Med. 2012;42(3):595-606.

56.   Upthegrove R, Marwaha S, Birchwood M. Depression and Schizophrenia: Cause, Consequence, or Trans-diagnostic Issue? Schizophr Bull. 2017;43(2):240-4.

57.   Rosenheck R, Leslie D, Keefe R, McEvoy J, Swartz M, Perkins D, et al. Barriers to employment for people with schizophrenia. Am J Psychiatry. 2006;163(3):411-7.

58.   Ho BC, Nopoulos P, Flaum M, Arndt S, Andreasen NC. Two-year outcome in first-episode schizophrenia: predictive value of symptoms for quality of life. Am J Psychiatry. 1998;155(9):1196-201.

59.   Green MF. What are the functional consequences of neurocognitive deficits in schizophrenia? Am J Psychiatry. 1996;153(3):321-30.

60.   Evans JD, Heaton RK, Paulsen JS, Palmer BW, Patterson T, Jeste DV. The relationship of neuropsychological abilities to specific domains of functional capacity in older schizophrenia patients. Biol Psychiatry. 2003;53(5):422-30.

61.   McGurk SR, Meltzer HY. The role of cognition in vocational functioning in schizophrenia. Schizophr Res. 2000;45(3):175-84.

62.   Evans JD, Bond GR, Meyer PS, Kim HW, Lysaker PH, Gibson PJ, et al. Cognitive and clinical predictors of success in vocational rehabilitation in schizophrenia. Schizophr Res. 2004;70(2-3):331-42.

63.   Jeste SD, Patterson TL, Palmer BW, Dolder CR, Goldman S, Jeste DV. Cognitive predictors of medication adherence among middle-aged and older outpatients with schizophrenia. Schizophr Res. 2003;63(1-2):49-58.

64.   Jarboe KS, Schwartz SK. The relationship between medication noncompliance and cognitive function in patients with schizophrenia. J Am Psychiatr Nurses Assoc. 1999;5(2):S2-S8.

65.   Green MF, Kern RS, Braff DL, Mintz J. Neurocognitive deficits and functional outcome in schizophrenia: are we measuring the "right stuff"? Schizophr Bull Special Issue: Psychosocial treatment for schizophrenia. 2000;26(1):119-36.

66.   Leeson VC, Barnes TR, Hutton SB, Ron MA, Joyce EM. IQ as a predictor of functional outcome in schizophrenia: a longitudinal, four-year study of first-episode psychosis. Schizophr Res. 2009;107(1):55-60.

67.   Waltz JA, Gold JM. Motivational Deficits in Schizophrenia and the Representation of Expected Value. Curr Top Behav Neurosci. 2016;27:375-410.

68.   Gejman PV, Sanders AR, Duan J. The role of genetics in the etiology of schizophrenia. Psychiatr Clin North Am. 2010;33(1):35-66.

69.   Hilker R, Helenius D, Fagerlund B, Skytthe A, Christensen K, Werge TM, et al. Heritability of Schizophrenia and Schizophrenia Spectrum Based on the Nationwide Danish Twin Register. Biol psychiatry. 2018;83(6):492-8.

70.   Sullivan PF, Kendler KS, Neale MC. Schizophrenia as a complex trait: evidence from a meta-analysis of twin studies. Arch Gen Psychiatry. 2003;60(12):1187-92.

71.   Tienari PJ, Wynne LC. Adoption Studies of Schizophrenia. Ann Med. 1994;26(4):233-7.

72.   Wahlberg KE, Wynne LC, Oja H, Keskitalo P, Pykalainen L, Lahti I, et al. Gene-environment interaction in vulnerability to schizophrenia: findings from the Finnish Adoptive Family Study of Schizophrenia. Am J Psychiatry. 1997;154(3):355-62.

73.   Tienari P, Sorri A, Lahti I, Naarala M, Wahlberg KE, Rönkkö T, et al. The Finnish adoptive family study of schizophrenia. Yale J Biol Med. 1985;58(3):227-37.

74.   Davies G, Welham J, Chant D, Torrey EF, McGrath J. A systematic review and meta-analysis of Northern Hemisphere season of birth studies in schizophrenia. Schizophr Bull. 2003;29(3):587-93.

75.   Carrion-Baralt JR, Smith CJ, Rossy-Fullana E, Lewis-Fernandez R, Davis KL, Silverman JM. Seasonality effects on schizophrenic births in multiplex families in a tropical island. Psychiatry Res. 2006;142(1):93-7.

76.   Cannon M, Jones PB, Murray RM. Obstetric complications and schizophrenia: historical and meta-analytic review. Am J Psychiatry. 2002;159(7):1080-92.

77.   Geddes JR, Lawrie SM. Obstetric complications and schizophrenia: a meta-analysis. Br J Psychiatry. 1995;167(6):786-93.

78.   Geddes JR, Verdoux H, Takei N, Lawrie SM, Bovet P, Eagles JM, et al. Schizophrenia and complications of pregnancy and labor: an individual patient data meta-analysis. Schizophr Bull. 1999;25(3):413-23.

79.   Zammit S, Allebeck P, Andreasson S, Lundberg I, Lewis G. Self reported cannabis use as a risk factor for schizophrenia in Swedish conscripts of 1969: historical cohort study. BMJ (Clinical research ed). 2002;325(7374):1199.

80.   Arseneault L, Cannon M, Poulton R, Murray R, Caspi A, Moffitt TE. Cannabis use in adolescence and risk for adult psychosis: longitudinal prospective study. BMJ (Clinical research ed). 2002;325(7374):1212.

81.   Henquet C, Murray R, Linszen D, van Os J. The environment and schizophrenia: the role of cannabis use. Schizophr Bull. 2005;31(3):608-12.

82.   Wilkinson ST, Radhakrishnan R, D'Souza DC. Impact of cannabis use on the development of psychotic disorders. Curr Addict Rep. 2014;1(2):115-28.

83.   Mayo D, Corey S, Kelly LH, Yohannes S, Youngquist AL, Stuart BK, et al. The role of trauma and stressful life events among Individuals at Clinical High Risk for psychosis: A Review. Front Psychiatry. 2017;8:55.

84.   Gibson LE, Alloy LB, Ellman LM. Trauma and the psychosis spectrum: A review of symptom specificity and explanatory mechanisms. Clin Psychol Rev. 2016;49:92-105.

85.   Owen MJ, Craddock N, Jablensky A. The genetic deconstruction of psychosis. Schizophr Bull. 2007;33(4):905-11.

86.   Badner JA, Gershon ES. Meta-analysis of whole-genome linkage scans of bipolar disorder and schizophrenia. Mol Psychiatry. 2002;7(4):405-11.

87.   Berrettini W. Evidence for shared susceptibility in bipolar disorder and schizophrenia. Am J Medl Genet C Semin Med Gen. 2003;123c(1):59-64.

88.   Craddock N, O'Donovan MC, Owen MJ. The genetics of schizophrenia and bipolar disorder: dissecting psychosis. J Med Genet. 2005;42(3):193-204.

89.   Hamshere ML, Bennett P, Williams N, Segurado R, Cardno A, Norton N, et al. Genomewide linkage scan in schizoaffective disorder: significant evidence for linkage at 1q42 close to DISC1, and suggestive evidence at 22q11 and 19p13. Arch Gen Psychiatry. 2005;62(10):1081-8.

90.   Craddock N, Owen MJ, O'Donovan MC. The catechol-O-methyl transferase (COMT) gene as a candidate for psychiatric phenotypes: evidence and lessons. Mol Psychiatry. 2006;11(5):446-58.

91.   Stefansson H, Sigurdsson E, Steinthorsdottir V, Bjornsdottir S, Sigmundsson T, Ghosh S, et al. Neuregulin 1 and susceptibility to schizophrenia. Am J Hum Genet. 2002;71(4):877-92.

92.   Petryshen TL, Middleton FA, Kirby A, Aldinger KA, Purcell S, Tahl AR, et al. Support for involvement of neuregulin 1 in schizophrenia pathophysiology. Mol Psychiatry. 2005;10(4):366-74, 328.

93.   Straub RE, Jiang Y, MacLean CJ, Ma Y, Webb BT, Myakishev MV, et al. Genetic variation in the 6p22.3 gene DTNBP1, the human ortholog of the mouse dysbindin gene, is associated with schizophrenia. Am J Hum Genet. 2002;71(2):337-48.

94.   Williams NM, O'Donovan MC, Owen MJ. Is the dysbindin gene (DTNBP1) a susceptibility gene for schizophrenia? Schizophr Bull. 2005;31(4):800-5.

95.   Kukreti R, Tripathi S, Bhatnagar P, Gupta S, Chauhan C, Kubendran S, et al. Association of DRD2 gene variant with schizophrenia. Neurosci Lett. 2006;392(1-2):68-71.

96.   He H, Wu H, Yang L, Gao F, Fan Y, Feng J, et al. Associations between dopamine D2 receptor gene polymorphisms and schizophrenia risk: a PRISMA compliant meta-analysis. Neuropsychiatr Dis Treat. 2016;12:3129-44.

97.	Rees E, O'Donovan MC, Owen MJ. Genetics of schizophrenia. Curr Opin Behav Sci. 2015;2:8-14.

98.	Schizophrenia Working Group of the Psychiatric Genomics C. Biological insights from 108 schizophrenia-associated genetic loci. Nature. 2014;511(7510):421-7.

99.	Seeman P, Lee T. Antipsychotic drugs: direct correlation between clinical potency and presynaptic action on dopamine neurons. Science. 1975;188(4194):1217-9.

100.	Matthysse S. Antipsychotic drug actions: a clue to the neuropathology of schizophrenia? Fed Proc. 1973;32(2):200-5.

101.	Davis KL, Kahn RS, Ko G, Davidson M. Dopamine in schizophrenia: a review and reconceptualization. Am J Psychiatry. 1991;148(11):1474-86.

102.	Howes OD, Kapur S. The dopamine hypothesis of schizophrenia: version III--the final common pathway. Schizophr Bull. 2009;35(3):549-62.

103.	Howes OD, Nour MM. Dopamine and the aberrant salience hypothesis of schizophrenia. World psychiatry. 2016;15(1):3-4.

104.	Hammond JC, Shan D, Meador-Woodruff JH, McCullumsmith RE. Evidence of Glutamatergic Dysfunction in the Pathophysiology of Schizophrenia. In: Popoli M, Diamond D, Sanacora G, editors. Synaptic Stress and Pathogenesis of Neuropsychiatric Disorders. New York, NY: Springer New York; 2014. pp. 265-94.

105.	Funk AJ, McCullumsmith RE, Haroutunian V, Meador-Woodruff JH. Abnormal activity of the MAPK- and cAMP-associated signaling pathways in frontal cortical areas in postmortem brain in schizophrenia. Neuropsychopharmacology. 2012;37(4):896-905.

106.	Javitt DC. Glutamate and schizophrenia: phencyclidine, N-methyl-D-aspartate receptors, and dopamine-glutamate interactions. Int Rev Neurobiol. 2007;78:69-108.

107.	Krystal JH, Karper LP, Seibyl JP, Freeman GK, Delaney R, Bremner JD, et al. Subanesthetic effects of the noncompetitive NMDA antagonist, ketamine, in humans. Psychotomimetic, perceptual, cognitive, and neuroendocrine responses. Arch Gen Psychiatry. 1994;51(3):199-214.

108.	McGuire P, Howes OD, Stone J, Fusar-Poli P. Functional neuroimaging in schizophrenia: diagnosis and drug discovery. Trends Pharmacol Sci. 2008;29(2):91-8.

109.	Howes O, McCutcheon R, Stone J. Glutamate and dopamine in schizophrenia: an update for the 21st century. J Psychopharmacol. 2015;29(2):97-115.

110.	Cohen SM, Tsien RW, Goff DC, Halassa MM. The impact of NMDA receptor hypofunction on GABAergic neurons in the pathophysiology of schizophrenia. Schizophr Res. 2015;167(1-3):98-107.

111.	Nakazawa K, Zsiros V, Jiang Z, Nakao K, Kolata S, Zhang S, et al. GABAergic interneuron origin of schizophrenia pathophysiology. Neuropharmacology. 2012;62(3):1574-83.

112.	Wang H-X, Gao W-J. Cell type-specific development of NMDA receptors in the interneurons of rat prefrontal cortex. Neuropsychopharmacology. 2009;34(8):2028-40.

113.   Jadi MP, Behrens MM, Sejnowski TJ. Abnormal Gamma Oscillations in N-Methyl-D-Aspartate Receptor Hypofunction Models of Schizophrenia. Biol Psychiatry. 2016;79(9):716-26.

114.   Carlen M, Meletis K, Siegle JH, Cardin JA, Futai K, Vierling-Claassen D, et al. A critical role for NMDA receptors in parvalbumin interneurons for gamma rhythm induction and behavior. Mol Psychiatry. 2012;17(5):537-48.

115.   Coyle JT, Balu DT, Puhl MD, Konopaske GT. History of the Concept of Disconnectivity in Schizophrenia. Harv Rev Psychiatry. 2016;24(2):80-6.

116.   Friston KJ. Theoretical neurobiology and schizophrenia. Br Med Bull. 1996;52(3):644-55.

117.   Stephan KE, Friston KJ, Frith CD. Dysconnection in schizophrenia: from abnormal synaptic plasticity to failures of self-monitoring. Schizophr Bull. 2009;35(3):509-27.

118.   Starc M, Murray JD, Santamauro N, Savic A, Diehl C, Cho YT, et al. Schizophrenia is associated with a pattern of spatial working memory deficits consistent with cortical disinhibition. Schizophr Res. 2017;181:107-16.

119.   Plum F. Prospects for research on schizophrenia. 3. Neurophysiology. Neuropathological findings. Neurosc Res Program Bull. 1972;10(4):384-8.

120.   Haug JO. Pneumoencephalographic evidence of brain atrophy in acute and chronic schizophrenic patients. Acta Psychiatr Scand. 1982;66(5):374-83.

121.   DeLisi LE, Szulc KU, Bertisch HC, Majcher M, Brown K. Understanding structural brain changes in schizophrenia. Dialogues Clin Neurosci. 2006;8(1):71-8.

122.   Karlsgodt KH, Sun D, Cannon TD. Structural and Functional Brain Abnormalities in Schizophrenia. Curr Dir Psychol Sci. 2010;19(4):226-31.

123.   Weinberger DR. Implications of normal brain development for the pathogenesis of schizophrenia. Arch Gen Psychiatry. 1987;44(7):660-9.

124.   Lieberman J, Chakos M, Wu H, Alvir J, Hoffman E, Robinson D, et al. Longitudinal study of brain morphology in first episode schizophrenia. Biol Psychiatry. 2001;49(6):487-99.

125.   Kasai K, Shenton ME, Salisbury DF, Hirayasu Y, Lee CU, Ciszewski AA, et al. Progressive decrease of left superior temporal gyrus gray matter volume in patients with first-episode schizophrenia. Am J Psychiatry. 2003;160(1):156-64.

126.   Wood SJ, Velakoulis D, Smith DJ, Bond D, Stuart GW, McGorry PD, et al. A longitudinal study of hippocampal volume in first episode psychosis and chronic schizophrenia. Schizophr Res. 2001;52(1-2):37-46.

127.   Rich AM, Cho YT, Tang Y, Savic A, Krystal JH, Wang F, et al. Amygdala volume is reduced in early course schizophrenia. Psychiatry res Neuroimaging. 2016;250:50-60.

128.   Ho BC, Andreasen NC, Nopoulos P, Arndt S, Magnotta V, Flaum M. Progressive structural brain abnormalities and their relationship to clinical outcome: a longitudinal magnetic resonance imaging study early in schizophrenia. Arch Gen Psychiatry. 2003;60(6):585-94.

129. Andreasen NC, Rezai K, Alliger R, Swayze VW, 2nd, Flaum M, Kirchner P, et al. Hypofrontality in neuroleptic-naive patients and in patients with chronic schizophrenia. Assessment with xenon 133 single-photon emission computed tomography and the Tower of London. Arch Gen Psychiatry. 1992;49(12):943-58.

130. Gur RE, Cowell P, Turetsky BI, Gallacher F, Cannon T, Bilker W, et al. A follow-up magnetic resonance imaging study of schizophrenia. Relationship of neuroanatomical changes to clinical and neurobehavioral measures. Arch Gen Psychiatry. 1998;55(2):145-52.

131. Sun D, Phillips L, Velakoulis D, Yung A, McGorry PD, Wood SJ, et al. Progressive brain structural changes mapped as psychosis develops in 'at risk' individuals. Schizophr Res. 2009;108(1-3):85-92.

132. Sun D, Stuart GW, Jenkinson M, Wood SJ, McGorry PD, Velakoulis D, et al. Brain surface contraction mapped in first-episode schizophrenia: a longitudinal magnetic resonance imaging study. Mol Psychiatry. 2009;14(10):976-86.

133. Palaniyappan L, Marques TR, Taylor H, Handley R, Mondelli V, Bonaccorso S, et al. Cortical folding defects as markers of poor treatment response in first-episode psychosis. JAMA Psychiatry. 2013;70(10):1031-40.

134. Glantz LA, Lewis DA. Decreased dendritic spine density on prefrontal cortical pyramidal neurons in schizophrenia. Arch Gen Psychiatry. 2000;57(1):65-73.

135. Konopaske GT, Lange N, Coyle JT, Benes FM. Prefrontal cortical dendritic spine pathology in schizophrenia and bipolar disorder. JAMA Psychiatry. 2014;71(12):1323-31.

136. Sweet RA, Henteleff RA, Zhang W, Sampson AR, Lewis DA. Reduced dendritic spine density in auditory cortex of subjects with schizophrenia. Neuropsychopharmacology. 2009;34(2):374-89.

137. Alba-Ferrara LM, de Erausquin GA. What does anisotropy measure? Insights from increased and decreased anisotropy in selective fiber tracts in schizophrenia. Front Integr Neurosci. 2013;7:9.

138. Shizukuishi T, Abe O, Aoki S. Diffusion tensor imaging analysis for psychiatric disorders. Magn Reson Med Sci. 2013;12(3):153-9.

139. Hatton SN, Lagopoulos J, Hermens DF, Hickie IB, Scott E, Bennett MR. White matter tractography in early psychosis: clinical and neurocognitive associations. J Psychiatry Neurosci. 2014;39(6):417-27.

140. von Hohenberg CC, Pasternak O, Kubicki M, Ballinger T, Vu M-A, Swisher T, et al. White matter microstructure in individuals at clinical high risk of psychosis: a whole-brain diffusion tensor imaging study. Schizophr Bull. 2014;40(4):895-903.

141. Vijayakumar N, Bartholomeusz C, Whitford T, Hermens DF, Nelson B, Rice S, et al. White matter integrity in individuals at ultra-high risk for psychosis: a systematic review and discussion of the role of polyunsaturated fatty acids. BMC psychiatry. 2016;16(1):287-.

142. Kyriakopoulos M, Vyas NS, Barker GJ, Chitnis XA, Frangou S. A diffusion tensor imaging study of white matter in early-onset schizophrenia. Biol Psychiatry. 2008;63(5):519-23.

143. Karlsgodt KH, van Erp TG, Poldrack RA, Bearden CE, Nuechterlein KH, Cannon TD. Diffusion tensor imaging of the superior longitudinal fasciculus and working memory in recent-onset schizophrenia. Biol Psychiatry. 2008;63(5):512-8.

144. Andreasen NC, Paradiso S, O'Leary DS. "Cognitive dysmetria" as an integrative theory of schizophrenia: a dysfunction in cortical-subcortical-cerebellar circuitry? Schizophr Bull. 1998;24(2):203-18.

145. Andreasen NC, Pierson R. The role of the cerebellum in schizophrenia. Biol Psychiatry. 2008;64(2):81-8.

146. Koutsouleris N, Meisenzahl EM, Davatzikos C, Bottlender R, Frodl T, Scheuerecker J, et al. Use of neuroanatomical pattern classification to identify subjects in at-risk mental states of psychosis and predict disease transition. Arch Gen Psychiatry. 2009;66(7):700-12.

147. Siris SG, Addington D, Azorin JM, Falloon IR, Gerlach J, Hirsch SR. Depression in schizophrenia: recognition and management in the USA. Schizophr Res. 2001;47(2-3):185-97.

148. Peralta V, Cuesta MJ, Zandio M. Cycloid psychosis: an examination of the validity of the concept. Curr Psychiatry Rep. 2007;9(3):184-92.

149. Keck PE, Jr., McElroy SL, Havens JR, Altshuler LL, Nolen WA, Frye MA, et al. Psychosis in bipolar disorder: phenomenology and impact on morbidity and course of illness. Compr Psychiatry. 2003;44(4):263-9.

150. Peralta V, Cuesta MJ. Diagnostic significance of Schneider's first-rank symptoms in schizophrenia. Comparative study between schizophrenic and non-schizophrenic psychotic disorders. Br J Psychiatry. 1999;174:243-8.

151. Ruggero CJ, Carlson GA, Kotov R, Bromet EJ. Ten-year diagnostic consistency of bipolar disorder in a first-admission sample. Bipolar Disord. 2010;12(1):21-31.

152. van Os J, Kapur S. Schizophrenia. Lancet. 2009;374(9690):635-45.

153. Owen MJ. New approaches to psychiatric diagnostic classification. Neuron. 2014;84(3):564-71.

154. Allardyce J, Gaebel W, Zielasek J, van Os J. Deconstructing Psychosis conference February 2006: the validity of schizophrenia and alternative approaches to the classification of psychosis. Schizophr Bull. 2007;33(4):863-7.

155. Maric N, Myin-Germeys I, Delespaul P, de Graaf R, Vollebergh W, Van Os J. Is our concept of schizophrenia influenced by Berkson's bias? Soc Psychiatry Psychiatr Epidemiol. 2004;39(8):600-5.

156. Guloksuz S, van Os J. The slow death of the concept of schizophrenia and the painful birth of the psychosis spectrum. Psychol Med. 2018;48(2):229-44.

157. Allardyce J, Suppes T, Van Os J. Dimensions and the psychosis phenotype. Int J Methods Psychiatr Res. 2007;16 Suppl 1:S34-40.

158. McGlashan TH. A selective review of recent North American long-term followup studies of schizophrenia. Schizophr Bull. 1988;14(4):515-42.

159.   Kasanin J. The acute schizoaffective psychoses. 1933. Am J Psychiatry. 1994;151(6 Suppl):144-54.

160.   Maier W, Lichtermann D, Franke P, Heun R, Falkai P, Rietschel M. The dichotomy of schizophrenia and affective disorders in extended pedigrees. Schizophr Res. 2002;57(2-3):259-66.

161.   Vallès V, Van Os J, Guillamat R, Gutiérrez B, Campillo M, Gento P, et al. Increased morbid risk for schizophrenia in families of in-patients with bipolar illness. Schizophr Res. 2000;42(2):83-90.

162.   Heckers S. Is schizoaffective disorder a useful diagnosis? Curr Psychiatry Rep. 2009;11(4):332-7.

163.   Malhi GS, Green M, Fagiolini A, Peselow ED, Kumari V. Schizoaffective disorder: diagnostic issues and future recommendations. Bipolar Disord. 2008;10(1 Pt 2):215-30.

164.   Cardno AG, Owen MJ. Genetic relationships between schizophrenia, bipolar disorder, and schizoaffective disorder. Schizophr Bull. 2014;40(3):504-15.

165.   Laursen TM, Agerbo E, Pedersen CB. Bipolar disorder, schizoaffective disorder, and schizophrenia overlap: a new comorbidity index. J Clin Psychiatry. 2009;70(10):1432-8.

166.   Keshavan MS, Morris DW, Sweeney JA, Pearlson GD, Thaker G, Seidman LJ, et al. A dimensional approach to the psychosis spectrum between bipolar disorder and schizophrenia: the Schizo-Bipolar Scale. Schizophr Res. 2011;133(1-3):250-4.

167.   Peralta V, Cuesta MJ. Exploring the borders of the schizoaffective spectrum: a categorical and dimensional approach. J Affect Disord. 2008;108(1-2):71-86.

168.   Frangou S. A systems neuroscience perspective of schizophrenia and bipolar disorder. Schizophr Bull. 2014;40(3):523-31.

169.   Schretlen DJ, Cascella NG, Meyer SM, Kingery LR, Testa SM, Munro CA, et al. Neuropsychological functioning in bipolar disorder and schizophrenia. Biol Psychiatry. 2007;62(2):179-86.

170.   Derry S, Moore RA. Atypical antipsychotics in bipolar disorder: systematic review of randomised trials. BMC Psychiatry. 2007;7(1):40.

171.   Gao K, Gajwani P, Elhaj O, Calabrese JR. Typical and atypical antipsychotics in bipolar depression. J Clin Psychiatry. 2005;66(11):1376-85.

172.   Cascade EF, Kalali AH, Buckley PF. Current Management of Schizophrenia: Antipsychotic Monotherapy versus Combination Therapy. Psychiatry (Edgmont). 2008;5(5):28-30.

173.   Yong KH, Sim K, Chan YH, Tan CH, Kua EH, Tor P-C, et al. Adjunctive mood stabilizer treatment for hospitalized schizophrenia patients: Asia psychotropic prescription study (2001–2008). Int J Neuropsychopharmacol. 2011;14(9):1157-64.

174.   Goes FS, Zandi PP, Miao K, McMahon FJ, Steele J, Willour VL, et al. Mood-incongruent psychotic features in bipolar disorder: familial aggregation and suggestive linkage to 2p11-q14 and 13q21-33. Am J Psychiatry. 2007;164(2):236-47.

175.   Vorstman JA, Breetvelt EJ, Thode KI, Chow EW, Bassett AS. Expression of autism spectrum and schizophrenia in patients with a 22q11.2 deletion. Schizophr Res. 2013;143(1):55-9.

176.   Schleifer C, Lin A, Kushan L, Ji JL, Yang G, Bearden CE, et al. Dissociable Disruptions in Thalamic and Hippocampal Resting-State Functional Connectivity in Youth with 22q11.2 Deletions. J Neurosci. 2019;39(7):1301-19.

177.   Green EK, Rees E, Walters JT, Smith KG, Forty L, Grozeva D, et al. Copy number variation in bipolar disorder. Mol Psychiatry. 2016;21(1):89-93.

178.   Raybould R, Green EK, MacGregor S, Gordon-Smith K, Heron J, Hyde S, et al. Bipolar disorder and polymorphisms in the dysbindin gene (DTNBP1). Biol Psychiatry. 2005;57(7):696-701.

179.   McDonald C, Bullmore ET, Sham PC, Chitnis X, Wickham H, Bramon E, et al. Association of genetic risks for schizophrenia and bipolar disorder with specific and generic brain structural endophenotypes. Arch Gen Psychiatry. 2004;61(10):974-84.

180.   Pearlson GD. Etiologic, phenomenologic, and endophenotypic overlap of schizophrenia and bipolar disorder. Annu Rev Clin Psychol. 2015;11:251-81.

181.   Lenzenweger MF. Schizotypy and schizotypic psychopathology: Mapping an alternative expression of schizophrenia liability. In: Lenzenweger MF, Dworkin RF, editors. Origins and developement of schizophrenia: Advances in experimental psychopathology. Washington, DC: American Psychological Association; 1998. pp. 93-122.

182.   Meehl PE. Schizotaxia, schizotypy, schizophrenia. Am Psychol. 1962;17(12):827-38.

183.   Meehl PE. Schizotaxia Revisited. Arch Gen Psychiatry. 1989;46(10):935–944.

184.   Esterberg ML, Compton MT. The psychosis continuum and categorical versus dimensional diagnostic approaches. Curr Psychiatry Rep. 2009;11(3):179-84.

185.   van Os J, Hanssen M, Bijl RV, Ravelli A. Strauss (1969) revisited: a psychosis continuum in the general population? Schizophr Res. 2000;45(1-2):11-20.

186.   Kendler KS, Gallagher TJ, Abelson JM, Kessler RC. Lifetime prevalence, demographic risk factors, and diagnostic validity of nonaffective psychosis as assessed in a US community sample. The National Comorbidity Survey. Arch Gen Psychiatry. 1996;53(11):1022-31.

187.   Ohayon MM. Prevalence of hallucinations and their pathological associations in the general population. Psychiatry Res. 2000;97(2-3):153-64.

188.   Kråkvik B, Larøi F, Kalhovde AM, Hugdahl K, Kompus K, Salvesen Ø, et al. Prevalence of auditory verbal hallucinations in a general population: A group comparison study. Scand J Psychol. 2015;56(5):508-15.

189.   Wigman JT, van Winkel R, Jacobs N, Wichers M, Derom C, Thiery E, et al. A twin study of genetic and environmental determinants of abnormal persistence of psychotic experiences in young adulthood. Am J Med Genet B Neuropsychiatr Genet. 2011;156b(5):546-52.

190.   Dominguez MD, Saka MC, Lieb R, Wittchen HU, van Os J. Early expression of negative/disorganized symptoms predicting psychotic experiences and subsequent clinical psychosis: a 10-year study. Am J Psychiatry. 2010;167(9):1075-82.

191.   Barnett JH, McDougall F, Xu MK, Croudace TJ, Richards M, Jones PB. Childhood cognitive function and adult psychopathology: associations with psychotic and non-psychotic symptoms in the general population. Br J Psychiatry. 2012;201(2):124-30.

192.   Kelleher I, Clarke MC, Rawdon C, Murphy J, Cannon M. Neurocognition in the extended psychosis phenotype: performance of a community sample of adolescents with psychotic symptoms on the MATRICS neurocognitive battery. Schizophr Bull. 2013;39(5):1018-26.

193.   Weiser M, Reichenberg A, Kravitz E, Lubin G, Shmushkevich M, Glahn DC, et al. Subtle cognitive dysfunction in nonaffected siblings of individuals affected by nonpsychotic disorders. Biol Psychiatry. 2008;63(6):602-8.

194.   Tamminga CA, Medoff DR. The biology of schizophrenia. Dialogues Clin Neurosci. 2000;2(4):339-48.

195.   van Os J, Reininghaus U. Psychosis as a transdiagnostic and extended phenotype in the general population. World Psychiatry. 2016;15(2):118-24.

196.   Perala J, Suvisaari J, Saarni SI, Kuoppasalmi K, Isometsa E, Pirkola S, et al. Lifetime prevalence of psychotic and bipolar I disorders in a general population. Arch Gen Psychiatry. 2007;64(1):19-28.

197.   Van Os J. Are psychiatric diagnoses of psychosis scientific and useful? The case of schizophrenia. J Ment Health. 2010;19(4):305-17.

198.   Jablensky A. Subtyping schizophrenia: implications for genetic research. Mol Psychiatry. 2006;11(9):815-36.

199.   Tamminga CA, Ivleva EI, Keshavan MS, Pearlson GD, Clementz BA, Witte B, et al. Clinical phenotypes of psychosis in the Bipolar-Schizophrenia Network on Intermediate Phenotypes (B-SNIP). Am J Psychiatry. 2013;170(11):1263-74.

200.   Murray RM, Sham P, Van Os J, Zanelli J, Cannon M, McDonald C. A developmental model for similarities and dissimilarities between schizophrenia and bipolar disorder. Schizophr Res. 2004;71(2-3):405-16.

201.   Cuthbert BN, Insel TR. Toward new approaches to psychotic disorders: the NIMH Research Domain Criteria project. Schizophr Bull. 2010;36(6):1061-2.

202.   Craddock N, Owen MJ. The Kraepelinian dichotomy - going, going... but still not gone. Br J Psychiatry. 2010;196(2):92-5.

203.   Cuthbert BN, Insel TR. Toward the future of psychiatric diagnosis: the seven pillars of RDoC. BMC medicine. 2013;11:126.

204.   Xu W, Sudhof TC. A neural circuit for memory specificity and generalization. Science. 2013;339(6125):1290-5.

205.   Constantinople CM, Bruno RM. Deep cortical layers are activated directly by thalamus. Science. 2013;340(6140):1591-4.

206.   Bruno RM, Sakmann B. Cortex is driven by weak but synchronously active thalamo-cortical synapses. Science. 2006;312(5780):1622-7.

207.   Poulet JFA, Fernandez LMJ, Crochet S, Petersen CCH. Thalamic control of cortical states. Nat Neurosci. 2012;15:370.

208.   Saalmann YB, Pinsk MA, Wang L, Li X, Kastner S. The pulvinar regulates information transmission between cortical areas based on attention demands. Science. 2012;337(6095):753-6.

209.   Nagalski A, Puelles L, Dabrowski M, Wegierski T, Kuznicki J, Wisniewska MB. Molecular anatomy of the thalamic complex and the underlying transcription factors. Brain Struct Funct. 2016;221(5):2493-510.

210.   Herrero MT, Barcia C, Navarro JM. Functional anatomy of thalamus and basal ganglia. Child's nervous system. 2002;18(8):386-404.

211.   Percheron G, Francois C, Talbi B, Yelnik J, Fenelon G. The primate motor thalamus. Brain Res Brain Res Rev. 1996;22(2):93-181.

212.   Guillery RW. Anatomical evidence concerning the role of the thalamus in corticocortical communication: a brief review. J Anat. 1995;187 (Pt 3):583-92.

213.   Vertes RP. Interactions among the medial prefrontal cortex, hippocampus and midline thalamus in emotional and cognitive processing in the rat. Neuroscience. 2006;142(1):1-20.

214.   Oh SW, Harris JA, Ng L, Winslow B, Cain N, Mihalas S, et al. A mesoscale connectome of the mouse brain. Nature. 2014;508:207.

215.   Evangelio M, García-Amado M, Clascá F. Thalamo-cortical Projection Neuron and Interneuron Numbers in the Visual Thalamic Nuclei of the Adult C57BL/6 Mouse. Front Neuroanat. 2018;12:27-.

216.   Bhattacharya BS, Bond TP, O'Hare L, Turner D, Durrant SJ. Causal Role of Thalamic Interneurons in Brain State Transitions: A Study Using a Neural Mass Model Implementing Synaptic Kinetics. Front Comput Neurosci. 2016;10(115).

217.   Cavdar S, Bay HH, Yildiz SD, Akakin D, Sirvanci S, Onat F. Comparison of numbers of interneurons in three thalamic nuclei of normal and epileptic rats. Neurosci Bull. 2014;30(3):451-60.

218.   Rodriguez JJ, Noristani HN, Hoover WB, Linley SB, Vertes RP. Serotonergic projections and serotonin receptor expression in the reticular nucleus of the thalamus in the rat. Synapse. 2011;65(9):919-28.

219.   Lorincz ML, Kekesi KA, Juhasz G, Crunelli V, Hughes SW. Temporal framing of thalamic relay-mode firing by phasic inhibition during the alpha rhythm. Neuron. 2009;63(5):683-96.

220.   Barbas H, Garcia-Cabezas MA, Zikopoulos B. Frontal-thalamic circuits associated with language. Brain Lang. 2013;126(1):49-61.

221.   Pergola G, Selvaggi P, Trizio S, Bertolino A, Blasi G. The role of the thalamus in schizophrenia from a neuroimaging perspective. Neurosci Biobehav Rev. 2015;54:57-75.

222.   Fama R, Sullivan EV. Thalamic structures and associated cognitive functions: Relations with age and aging. Neurosci Biobehav Rev. 2015;54:29-37.

223.   Mai JK, Majtanik M. Toward a Common Terminology for the Thalamus. Front Neuroanat. 2019;12:114.

224.   Dixon G, Harper CG. Quantitative analysis of glutamic acid decarboxylase-immunoreactive neurons in the anterior thalamus of the human brain. Brain Res. 2001;923(1-2):39-44.

225.   Child ND, Benarroch EE. Anterior nucleus of the thalamus. Neurology. 2013;81(21):1869.

226.   Harding A, Halliday G, Caine D, Kril J. Degeneration of anterior thalamic nuclei differentiates alcoholics with amnesia. Brain. 2000;123 (Pt 1):141-54.

227.   Aggleton JP, O'Mara SM, Vann SD, Wright NF, Tsanov M, Erichsen JT. Hippocampal-anterior thalamic pathways for memory: uncovering a network of direct and indirect actions. Eur J Neurosci. 2010;31(12):2292-307.

228.   Heckers S, Geula C, Mesulam MM. Cholinergic innervation of the human thalamus: dual origin and differential nuclear distribution. J Comp Neurol. 1992;325(1):68-82.

229.   Vann SD. Gudden's ventral tegmental nucleus is vital for memory: re-evaluating diencephalic inputs for amnesia. Brain. 2009;132(Pt 9):2372-84.

230.   Ogawa K, Toita T, Kakinohana Y, Tominaga D, Miyagi K, Yoshii Y, et al. A patient with improvement in short-term memory disturbance brought about by radiation therapy for germinoma involving Papez circuit. Radiat Med. 1999;17(4):317-22.

231.   Mai JK, Forutan F. Chapter 19 - Thalamus. In: Mai JK, Paxinos G, editors. The Human Nervous System (Third Edition). San Diego: Academic Press; 2012. pp. 618-77.

232.   Pepin EP, Auray-Pepin L. Selective dorsolateral frontal lobe dysfunction associated with diencephalic amnesia. Neurology. 1993;43(4):733-41.

233.   Churchill L, Kalivas PW. The involvement of the mediodorsal nucleus of the thalamus and the midbrain extrapyramidal area in locomotion elicited from the ventral pallidum. Behav Brain Res. 1999;104(1-2):63-71.

234.   Ray JP, Russchen FT, Fuller TA, Price JL. Sources of presumptive glutamatergic/aspartatergic afferents to the mediodorsal nucleus of the thalamus in the rat. J Comp Neurol. 1992;320(4):435-56.

235.   Forutan F, Mai JK, Ashwell KW, Lensing-Hohn S, Nohr D, Voss T, et al. Organisation and maturation of the human thalamus as revealed by CD15. J Comp Neurol. 2001;437(4):476-95.

236.   Ongur D, Price JL. The organization of networks within the orbital and medial prefrontal cortex of rats, monkeys and humans. Cereb Cortex. 2000;10(3):206-19.

237.   Klein JC, Rushworth MFS, Behrens TEJ, Mackay CE, de Crespigny AJ, D'Arceuil H, et al. Topography of connections between human prefrontal cortex and mediodorsal thalamus studied with diffusion tractography. Neuroimage. 2010;51(2):555-64.

238.	Aggleton JP. Multiple anatomical systems embedded within the primate medial temporal lobe: implications for hippocampal function. Neurosci Biobehav Rev. 2012;36(7):1579-96.

239.	Mitchell AS, Chakraborty S. What does the mediodorsal thalamus do? Front Syst Neurosci. 2013;7:37.

240.	Yaniv D, Desmedt A, Jaffard R, Richter-Levin G. The amygdala and appraisal processes: stimulus and response complexity as an organizing factor. Brain Res Brain Res Rev. 2004;44(2-3):179-86.

241.	Vogt BA, Sikes RW. Chapter 16 - The medial pain system, cingulate cortex, and parallel processing of nociceptive information. In: Mayer EA, Saper CB, editors. Progress in Brain Research. 122: Elsevier; 2000. pp. 223-35.

242.	Engelborghs S, Marien P, Pickut BA, Verstraeten S, De Deyn PP. Loss of psychic self-activation after paramedian bithalamic infarction. Stroke. 2000;31(7):1762-5.

243.	Tham WW, Stevenson RJ, Miller LA. The functional role of the medio dorsal thalamic nucleus in olfaction. Brain Res Rev. 2009;62(1):109-26.

244.	van Donkelaar P, Stein JF, Passingham RE, Miall RC. Temporary inactivation in the primate motor thalamus during visually triggered and internally generated limb movements. J Neurophysiol. 2000;83(5):2780-90.

245.	Canavan AG, Nixon PD, Passingham RE. Motor learning in monkeys (Macaca fascicularis) with lesions in motor thalamus. Exp Brain Res. 1989;77(1):113-26.

246.	Padberg J, Krubitzer L. Thalamo-cortical connections of anterior and posterior parietal cortical areas in New World titi monkeys. J Comp Neurol. 2006;497(3):416-35.

247.	Grieve KL, Acuña C, Cudeiro J. The primate pulvinar nuclei: vision and action. Trends Neurosci. 2000;23(1):35-9.

248.	Gutierrez C, Cola MG, Seltzer B, Cusick C. Neurochemical and connectional organization of the dorsal pulvinar complex in monkeys. J Comp Neurol. 2000;419(1):61-86.

249.	Sherman SM, Guillery RW. The role of the thalamus in the flow of information to the cortex. Philos Trans R Soc Lond B Biol Sci. 2002;357(1428):1695-708.

250.	Ren S, Wang Y, Yue F, Cheng X, Dang R, Qiao Q, et al. The paraventricular thalamus is a critical thalamic area for wakefulness. Science. 2018;362(6413):429.

251.	Van der Werf YD, Witter MP, Groenewegen HJ. The intralaminar and midline nuclei of the thalamus. Anatomical and functional evidence for participation in processes of arousal and awareness. Brain Res Brain Res Rev. 2002;39(2-3):107-40.

252.	Saalmann YB. Intralaminar and medial thalamic influence on cortical synchrony, information transmission and cognition. Front Syst Neursci. 2014;8(83).

253.	Lam Y-W, Sherman SM. Functional Organization of the Thalamic Input to the Thalamic Reticular Nucleus. J Neurosci. 2011;31(18):6791.

254.	Crabtree JW. Functional Diversity of Thalamic Reticular Subnetworks. Front Syst Neurosci. 2018;12(41).

255. Behrens TEJ, Johansen-Berg H, Woolrich MW, Smith SM, Wheeler-Kingshott CAM, Boulby PA, et al. Non-invasive mapping of connections between human thalamus and cortex using diffusion imaging. Nat Neurosci. 2003;6(7):750-7.

256. Zhang D, Snyder AZ, Shimony JS, Fox MD, Raichle ME. Noninvasive functional and structural connectivity mapping of the human thalamo-cortical system. Cereb Cortex. 2010;20(5):1187-94.

257. Sherman SM, Guillery RW. Distinct functions for direct and transthalamic corticocortical connections. J Neurophysiol. 2011;106(3):1068-77.

258. Sherman SM. Functioning of Circuits Connecting Thalamus and Cortex. Compr Physiol. 2017;7(2):713-39.

259. Wolff M, Vann SD. The Cognitive Thalamus as a Gateway to Mental Representations. J Neurosci. 2019;39(1):3.

260. Hunt PR, Aggleton JP. Neurotoxic lesions of the dorsomedial thalamus impair the acquisition but not the performance of delayed matching to place by rats: a deficit in shifting response rules. J Neurosci. 1998;18(23):10045-52.

261. Bolkan SS, Stujenske JM, Parnaudeau S, Spellman TJ, Rauffenbart C, Abbas AI, et al. Thalamic projections sustain prefrontal activity during working memory maintenance. Nat Neurosci. 2017;20(7):987-96.

262. Marton TF, Seifikar H, Luongo FJ, Lee AT, Sohal VS. Roles of Prefrontal Cortex and Mediodorsal Thalamus in Task Engagement and Behavioral Flexibility. J Neurosci. 2018;38(10):2569-78.

263. Vann SD. Dismantling the Papez circuit for memory in rats. eLife. 2013;2:e00736.

264. Mitchell AS, Dalrymple-Alford JC, Christie MA. Spatial working memory and the brainstem cholinergic innervation to the anterior thalamus. J Neurosci. 2002;22(5):1922-8.

265. Galvan A, Smith Y. The primate thalamostriatal systems: Anatomical organization, functional roles and possible involvement in Parkinson's disease. Basal ganglia. 2011;1(4):179-89.

266. Kato S, Fukabori R, Nishizawa K, Okada K, Yoshioka N, Sugawara M, et al. Action selection and flexible switching controlled by the intralaminar thalamic neurons. Cell rep. 2018;22(9):2370-82.

267. Schepers IM, Beck AK, Brauer S, Schwabe K, Abdallat M, Sandmann P, et al. Human centromedian-parafascicular complex signals sensory cues for goal-oriented behavior selection. Neuroimage. 2017;152:390-9.

268. Ullsperger M, Danielmeier C, Jocham G. Neurophysiology of performance monitoring and adaptive behavior. Physiol Rev. 2014;94(1):35-79.

269. Leung BK, Balleine BW. Ventral pallidal projections to mediodorsal thalamus and ventral tegmental area play distinct roles in outcome-specific Pavlovian-instrumental transfer. J Neurosci. 2015;35(12):4953-64.

270. Klostermann F, Krugel LK, Ehlen F. Functional roles of the thalamus for language capacities. Front Syst Neurosci. 2013;7:32.

271.   Haber SN, Calzavara R. The cortico-basal ganglia integrative network: the role of the thalamus. Brain Res Bull. 2009;78(2-3):69-74.

272.   Barch DM, Ceaser A. Cognition in schizophrenia: core psychological and neural mechanisms. Trends Cogn Sci. 2012;16(1):27-34.

273.   Anticevic A. Understanding the role of thalamic circuits in schizophrenia neuropathology. Schizophr Res. 2017;180:1-3.

274.   Andreasen NC. The role of the thalamus in schizophrenia. Can J Psychiatry. 1997;42(1):27-33.

275.   Carrera E, Bogousslavsky J. The thalamus and behavior: effects of anatomically distinct strokes. Neurology. 2006;66(12):1817-23.

276.   Schmahmann JD. Vascular syndromes of the thalamus. Stroke. 2003;34(9):2264-78.

277.   Crail-Melendez D, Atriano-Mendieta C, Carrillo-Meza R, Ramirez-Bermudez J. Schizophrenia-like psychosis associated with right lacunar thalamic infarct. Neurocase. 2013;19(1):22-6.

278.   Manford M, Andermann F. Complex visual hallucinations. Clinical and neurobiological insights. Brain. 1998;121 (Pt 10):1819-40.

279.   Cronenwett WJ, Csernansky J. Thalamic pathology in schizophrenia. Curr Top Behav Neurosci. 2010;4:509-28.

280.   Benke T. Peduncular hallucinosis: a syndrome of impaired reality monitoring. J Neurol. 2006;253(12):1561-71.

281.   Young KA, Manaye KF, Liang C, Hicks PB, German DC. Reduced number of mediodorsal and anterior thalamic neurons in schizophrenia. Biol Psychiatry. 2000;47(11):944-53.

282.   Konick LC, Friedman L. Meta-analysis of thalamic size in schizophrenia. Biol Psychiatry. 2001;49(1):28-38.

283.   Shepherd AM, Laurens KR, Matheson SL, Carr VJ, Green MJ. Systematic meta-review and quality assessment of the structural brain alterations in schizophrenia. Neurosci Biobehav Rev. 2012;36(4):1342-56.

284.   Haijma SV, Van Haren N, Cahn W, Koolschijn PC, Hulshoff Pol HE, Kahn RS. Brain volumes in schizophrenia: a meta-analysis in over 18 000 subjects. Schizophr Bull. 2013;39(5):1129-38.

285.   Fornito A, Yucel M, Patti J, Wood SJ, Pantelis C. Mapping grey matter reductions in schizophrenia: an anatomical likelihood estimation analysis of voxel-based morphometry studies. Schizophr Res. 2009;108(1-3):104-13.

286.   Wagner G, Koch K, Schachtzabel C, Schultz CC, Gaser C, Reichenbach JR, et al. Structural basis of the fronto-thalamic dysconnectivity in schizophrenia: A combined DCM-VBM study. NeuroImage Clin. 2013;3:95-105.

287.   Steen RG, Mull C, McClure R, Hamer RM, Lieberman JA. Brain volume in first-episode schizophrenia: systematic review and meta-analysis of magnetic resonance imaging studies. Br J Psychiatry. 2006;188:510-8.

288.   Adriano F, Spoletini I, Caltagirone C, Spalletta G. Updated meta-analyses reveal thalamus volume reduction in patients with first-episode and chronic schizophrenia. Schizophr Res. 2010;123(1):1-14.

289.   Csernansky JG, Schindler MK, Splinter NR, Wang L, Gado M, Selemon LD, et al. Abnormalities of thalamic volume and shape in schizophrenia. Am J Psychiatry. 2004;161(5):896-902.

290.   Lawrie SM, Whalley HC, Abukmeil SS, Kestelman JN, Donnelly L, Miller P, et al. Brain structure, genetic liability, and psychotic symptoms in subjects at high risk of developing schizophrenia. Biol Psychiatry. 2001;49(10):811-23.

291.   Lawrie SM, McIntosh AM, Hall J, Owens DG, Johnstone EC. Brain structure and function changes during the development of schizophrenia: the evidence from studies of subjects at increased genetic risk. Schizophr Bull. 2008;34(2):330-40.

292.   Cullen TJ, Walker MA, Parkinson N, Craven R, Crow TJ, Esiri MM, et al. A postmortem study of the mediodorsal nucleus of the thalamus in schizophrenia. Schizophr Res. 2003;60(2-3):157-66.

293.   Pakkenberg B. Pronounced reduction of total neuron number in mediodorsal thalamic nucleus and nucleus accumbens in schizophrenics. Arch Gen Psychiatry. 1990;47(11):1023-8.

294.   Pakkenberg B. The volume of the mediodorsal thalamic nucleus in treated and untreated schizophrenics. Schizophr Res. 1992;7(2):95-100.

295.   Selemon LD, Goldman-Rakic PS. The reduced neuropil hypothesis: a circuit based model of schizophrenia. Biol Psychiatry. 1999;45(1):17-25.

296.   Benes FM. Neurobiological investigations in cingulate cortex of schizophrenic brain. Schizophr Bull. 1993;19(3):537-49.

297.   Shimizu M, Fujiwara H, Hirao K, Namiki C, Fukuyama H, Hayashi T, et al. Structural abnormalities of the adhesio interthalamica and mediodorsal nuclei of the thalamus in schizophrenia. Schizophr Res. 2008;101(1-3):331-8.

298.   Byne W, Buchsbaum MS, Kemether E, Hazlett E, Shinware A, Mitropoulou V, et al. Magnetic resonance imaging of the thalamic mediodorsal nucleus and pulvinar in schizophrenia and schizotypal personality disorder. Arch Gen Psychiatry. 2001;58(2):133-40.

299.   Gilbert AR, Rosenberg DR, Harenski K, Spencer S, Sweeney JA, Keshavan MS. Thalamic volumes in patients with first-episode schizophrenia. Am J Psychiatry. 2001;158(4):618-24.

300.   Byne W, Hazlett EA, Buchsbaum MS, Kemether E. The thalamus and schizophrenia: current status of research. Acta Neuropathol. 2009;117(4):347-68.

301.   Bora E, Fornito A, Radua J, Walterfang M, Seal M, Wood SJ, et al. Neuroanatomical abnormalities in schizophrenia: a multimodal voxelwise meta-analysis and meta-regression analysis. Schizophr Res. 2011;127(1-3):46-57.

302.   Byne W, Buchsbaum MS, Mattiace LA, Hazlett EA, Kemether E, Elhakem SL, et al. Postmortem assessment of thalamic nuclear volumes in subjects with schizophrenia. Am J Psychiatry. 2002;159(1):59-65.

303. Dorph-Petersen KA, Lewis DA. Postmortem structural studies of the thalamus in schizophrenia. Schizophr Res. 2017;180:28-35.

304. Salgado-Pineda P, Junque C, Vendrell P, Baeza I, Bargallo N, Falcon C, et al. Decreased cerebral activation during CPT performance: structural and functional deficits in schizophrenic patients. Neuroimage. 2004;21(3):840-7.

305. Cobia DJ, Smith MJ, Salinas I, Ng C, Gado M, Csernansky JG, et al. Progressive deterioration of thalamic nuclei relates to cortical network decline in schizophrenia. Schizophr Res. 2017;180:21-7.

306. Ferrarelli F, Tononi G. Reduced sleep spindle activity point to a TRN-MD thalamus-PFC circuit dysfunction in schizophrenia. Schizophr Res. 2017;180:36-43.

307. Clinton SM, Meador-Woodruff JH. Thalamic dysfunction in schizophrenia: neurochemical, neuropathological, and in vivo imaging abnormalities. Schizophr Res. 2004;69(2):237-53.

308. Frohlich J, Van Horn JD. Reviewing the ketamine model for schizophrenia. J Psychopharmacol. 2014;28(4):287-302.

309. Sharp FR, Tomitaka M, Bernaudin M, Tomitaka S. Psychosis: pathological activation of limbic thalamo-cortical circuits by psychomimetics and schizophrenia? Trends Neurosci. 2001;24(6):330-4.

310. Watis L, Chen SH, Chua HC, Chong SA, Sim K. Glutamatergic abnormalities of the thalamus in schizophrenia: a systematic review. J Neural Transm (Vienna). 2008;115(3):493-511.

311. Pratt J, Dawson N, Morris BJ, Grent-'t-Jong T, Roux F, Uhlhaas PJ. Thalamo-cortical communication, glutamatergic neurotransmission and neural oscillations: A unique window into the origins of ScZ? Schizophr Res. 2017;180:4-12.

312. Yasuno F, Suhara T, Okubo Y, Sudo Y, Inoue M, Ichimiya T, et al. Low dopamine d(2) receptor binding in subregions of the thalamus in schizophrenia. Am J Psychiatry. 2004;161(6):1016-22.

313. Dandash O, Pantelis C, Fornito A. Dopamine, fronto-striato-thalamic circuits and risk for psychosis. Schizophr Res. 2017;180:48-57.

314. Zhang Y, Su TP, Liu B, Zhou Y, Chou KH, Lo CY, et al. Disrupted thalamo-cortical connectivity in schizophrenia: a morphometric correlation analysis. Schizophr Res. 2014;153(1-3):129-35.

315. Hulshoff Pol HE, Schnack HG, Mandl RC, Cahn W, Collins DL, Evans AC, et al. Focal white matter density changes in schizophrenia: reduced inter-hemispheric connectivity. Neuroimage. 2004;21(1):27-35.

316. Wagner G, De la Cruz F, Schachtzabel C, Gullmar D, Schultz CC, Schlosser RG, et al. Structural and functional dysconnectivity of the fronto-thalamic system in schizophrenia: a DCM-DTI study. Cortex. 2015;66:35-45.

317. Clark KA, Nuechterlein KH, Asarnow RF, Hamilton LS, Phillips OR, Hageman NS, et al. Mean diffusivity and fractional anisotropy as indicators of disease and genetic liability to schizophrenia. J Psychiatr Res. 2011;45(7):980-8.

318.   Marenco S, Stein JL, Savostyanova AA, Sambataro F, Tan HY, Goldman AL, et al. Investigation of anatomical thalamo-cortical connectivity and FMRI activation in schizophrenia. Neuropsychopharmacology. 2012;37(2):499-507.

319.   Kubota M, Miyata J, Sasamoto A, Sugihara G, Yoshida H, Kawada R, et al. Thalamo-cortical disconnection in the orbitofrontal region associated with cortical thinning in schizophrenia. JAMA Psychiatry. 2013;70(1):12-21.

320.   Wagner G, Koch K, Schachtzabel C, Schultz CC, Gaser C, Reichenbach JR, et al. Structural basis of the fronto-thalamic dysconnectivity in schizophrenia: A combined DCM-VBM study. NeuroImage Clin. 2013;3:95-105.

321.   Ellison-Wright I, Bullmore E. Meta-analysis of diffusion tensor imaging studies in schizophrenia. Schizophr Res. 2009;108(1-3):3-10.

322.   Mitelman SA, Byne W, Kemether EM, Hazlett EA, Buchsbaum MS. Correlations between volumes of the pulvinar, centromedian, and mediodorsal nuclei and cortical Brodmann's areas in schizophrenia. Neurosci Lett. 2006;392(1-2):16-21.

323.   Barch DM. Cerebellar-thalamic connectivity in schizophrenia. Schizophr Bull. 2014;40(6):1200-3.

324.   Han HJ, Jung WH, Jang JH, Hwang JY, Kim SN, Byun MS, et al. Reduced volume in the anterior internal capsule but its maintained correlation with the frontal gray matter in subjects at ultra-high risk for psychosis. Psychiatry Res. 2012;204(2-3):82-90.

325.   Cho KI, Shenton ME, Kubicki M, Jung WH, Lee TY, Yun JY, et al. Altered Thalamo-Cortical White Matter Connectivity: Probabilistic Tractography Study in Clinical-High Risk for Psychosis and First-Episode Psychosis. Schizophr Bull. 2016;42(3):723-31.

326.   Huang P, Xi Y, Lu Z-L, Chen Y, Li X, Li W, et al. Decreased bilateral thalamic gray matter volume in first-episode schizophrenia with prominent hallucinatory symptoms: A volumetric MRI study. Scientific Reports. 2015;5:14505.

327.   Hazlett EA, Buchsbaum MS, Kemether E, Bloom R, Platholi J, Brickman AM, et al. Abnormal glucose metabolism in the mediodorsal nucleus of the thalamus in schizophrenia. Am J Psychiatry. 2004;161(2):305-14.

328.   Coscia DM, Narr KL, Robinson DG, Hamilton LS, Sevy S, Burdick KE, et al. Volumetric and shape analysis of the thalamus in first-episode schizophrenia. Hum Brain Mapp. 2009;30(4):1236-45.

329.   Masdeu JC. Neuroimaging in psychiatric disorders. Neurotherapeutics. 2011;8(1):93-102.

330.   Phillips ML. Neuroimaging in psychiatry: bringing neuroscience into clinical practice. Br J Psychiatry. 2012;201(1):1-3.

331.   Raichle ME. Cognitive neuroscience. Bold insights. Nature. 2001;412(6843):128-30.

332.   Grover VP, Tognarelli JM, Crossey MM, Cox IJ, Taylor-Robinson SD, McPhail MJ. Magnetic Resonance Imaging: Principles and Techniques: Lessons for Clinicians. J Clin Exp Hepatol. 2015;5(3):246-55.

333.   Huettel S, W Song A, McCarthy G. Functional Magnetic Resonance Imaging, Second Edition. Sunderland, Massachusetts, U.S.A. : Sinauer Associates, Inc., Publishers; 2008.

334.   Soher BJ, Dale BM, Merkle EM. A review of MR physics: 3T versus 1.5T. Magn Reson Imaging Clin N Am. 2007;15(3):277-90.

335.   Ogawa S, Lee TS, Nayak AS, Glynn P. Oxygenation-sensitive contrast in magnetic resonance image of rodent brain at high magnetic fields. Magn Reson Med. 1990;26:68-78.

336.   Ogawa S, Tank DW, Menon R, Ellermann JM, Kim SG, Merkle H, et al. Intrinsic signal changes accompanying sensory stimulation: functional brain mapping with magnetic resonance imaging. Proc Natl Acad Sci U S A. 1992;89(13):5951-5.

337.   Huettel S, W Song A, McCarthy G. BOLD fMRI: Origins and Properties. Functional Magnetic Resonance Imaging, Second Edition. Sunderland, Massachusetts, U.S.A. : Sinauer Associates, Inc., Publishers; 2008. pp. 194-242.

338.   Fox PT, Raichle ME. Focal physiological uncoupling of cerebral blood flow and oxidative metabolism during somatosensory stimulation in human subjects. Proc Natl Acad Sci U S A. 1986;83:1140-4.

339.   Aguirre GK, Zarahn E, D'Esposito M. The variability of human, BOLD hemodynamic responses. Neuroimage. 1998;8(4):360-9.

340.   Ances BM. Coupling of changes in cerebral blood flow with neural activity: what must initially dip must come back up. J Cereb Blood Flow Metab. 2004;24(1):1-6.

341.   Hirano Y, Stefanovic B, Silva AC. Spatiotemporal evolution of the functional magnetic resonance imaging response to ultrashort stimuli. J Neurosci. 2011;31(4):1440-7.

342.   Yesilyurt B, Ugurbil K, Uludag K. Dynamics and nonlinearities of the BOLD response at very short stimulus durations. Magn Reson Imaging. 2008;26(7):853-62.

343.   Buxton RB, Uludag K, Dubowitz DJ, Liu TT. Modeling the hemodynamic response to brain activation. Neuroimage. 2004;23 Suppl 1:S220-33.

344.   West KL, Zuppichini MD, Turner MP, Sivakolundu DK, Zhao Y, Abdelkarim D, et al. BOLD hemodynamic response function changes significantly with healthy aging. NeuroImage. 2019;188:198-207.

345.   Handwerker DA, Ollinger JM, D'Esposito M. Variation of BOLD hemodynamic responses across subjects and brain regions and their effects on statistical analyses. Neuroimage. 2004;21(4):1639-51.

346.   Lindquist MA, Meng Loh J, Atlas LY, Wager TD. Modeling the hemodynamic response function in fMRI: efficiency, bias and mis-modeling. NeuroImage. 2009;45(1 Suppl):S187-S98.

347.   Logothetis NK, Pauls J, Augath M, Tinath T, Oeltermann A. Neurophysiological investigation of the basis of the fMRI signal. Nature. 2001;412:150-7.

348.   Ogawa S, Lee TM, Stepnoski R, Chen W, Zhu XH, Ugurbil K. An approach to probe some neural systems interaction by functional MRI at neural time scale down to milliseconds. Proc Natl Acad Sci U S A. 2000;97(20):11026-31.

349.   Lin F-H, Witzel T, Raij T, Ahveninen J, Tsai KW-K, Chu Y-H, et al. fMRI hemodynamics accurately reflects neuronal timing in the human brain measured by MEG. NeuroImage. 2013;78:372-84.

350.   Richter W, Ugurbil K, Georgopoulos A, Kim SG. Time-resolved fMRI of mental rotation. Neuroreport. 1997;8(17):3697-702.

351.   Huettel S, W Song A, McCarthy G. Basic Principles of MR Image Formation. Functional Magnetic Resonance Imaging, Second Edition. Sunderland, Massachusetts, U.S.A. : Sinauer Associates, Inc., Publishers; 2008. pp. 57-120.

352.   Poustchi-Amin M, Mirowitz SA, Brown JJ, McKinstry RC, Li T. Principles and applications of echo-planar imaging: a review for the general radiologist. Radiographics. 2001;21(3):767-79.

353.   Huettel S, W Song A, McCarthy G. MRI Contrast Mechanisms and Pulse Sequences. Functional Magnetic Resonance Imaging, Second Edition. Sunderland, Massachusetts, U.S.A. : Sinauer Associates, Inc., Publishers; 2008. pp. 121-57.

354.   Casey BJ, Davidson M, Rosen B. Functional magnetic resonance imaging: basic principles of and application to developmental science. Dev Sci. 2002;5(3):301-9.

355.   Cheng K, Waggoner RA, Tanaka K. Human ocular dominance columns as revealed by high-field functional magnetic resonance imaging. Neuron. 2001;32(2):359-74.

356.   Gore JC. Principles and practice of functional MRI of the human brain. J Clin Invest. 2003;112(1):4-9.

357.   Birn RM, Saad ZS, Bandettini PA. Spatial heterogeneity of the nonlinear dynamics in the FMRI BOLD response. Neuroimage. 2001;14(4):817-26.

358.   Dale AM, Buckner RL. Selective averaging of rapidly presented individual trials using fMRI. Hum Brain Mapp. 1997;5:329-40.

359.   Menon RS, Kim SG. Spatial and temporal limits in cognitive neuroimaging with fMRI. Trends Cogn Sci. 1999;3(6):207-16.

360.   Huettel S, W Song A, McCarthy G. Signal, Noise, and Preprocessing of fMRI Data. Functional Magnetic Resonance Imaging, Second Edition. Sunderland, Massachusetts, U.S.A. : Sinauer Associates, Inc., Publishers; 2008. pp. 243-91.

361.   Peters AM, Brookes MJ, Hoogenraad FG, Gowland PA, Francis ST, Morris PG, et al. T2* measurements in human brain at 1.5, 3 and 7 T. Magn Reson Imaging. 2007;25(6):748-53.

362.   Triantafyllou C, Hoge RD, Wald LL. Effect of spatial smoothing on physiological noise in high-resolution fMRI. Neuroimage. 2006;32(2):551-7.

363.   Churchill NW, Oder A, Abdi H, Tam F, Lee W, Thomas C, et al. Optimizing preprocessing and analysis pipelines for single-subject fMRI. I. Standard temporal motion and physiological noise correction methods. Hum Brain Mapp. 2012;33(3):609-27.

364.   Huettel S, W Song A, McCarthy G. Experimental Design. Functional Magnetic Resonance Imaging, Second Edition. Sunderland, Massachusetts, U.S.A. : Sinauer Associates, Inc., Publishers; 2008. pp. 293-329.

365.   Biswal B, Yetkin FZ, Haughton VM, Hyde JS. Functional connectivity in the motor cortex of resting human brain using echo-planar MRI. Mag Reson Med. 1995;34(4):537-41.

366.   Raichle ME, MacLeod AM, Snyder AZ, Powers WJ, Gusnard DA, Shulman GL. A default mode of brain function. Proc Natl Acad Sci USA. 2001;98(2):676.

367.   Honey CJ, Kötter R, Breakspear M, Sporns O. Network structure of cerebral cortex shapes functional connectivity on multiple time scales. Proc Natl Acad Sci USA. 2007;104(24):10240-5.

368.   Johnston JM, Vaishnavi SN, Smyth MD, Zhang D, He BJ, Zempel JM, et al. Loss of resting interhemispheric functional connectivity after complete section of the corpus callosum. J Neurosci. 2008;28(25):6453-8.

369.   Cordes D, Haughton VM, Arfanakis K, Carew JD, Turski PA, Moritz CH, et al. Frequencies contributing to functional connectivity in the cerebral cortex in "resting-state" data. Am J Neuroradiol. 2001;22(7):1326-33.

370.   Weissenbacher A, Kasess C, Gerstl F, Lanzenberger R, Moser E, Windischberger C. Correlations and anticorrelations in resting-state functional connectivity MRI: a quantitative comparison of preprocessing strategies. Neuroimage. 2009;47(4):1408-16.

371.   van den Heuvel MP, Hulshoff Pol HE. Exploring the brain network: A review on resting-state fMRI functional connectivity. Eur Neuropsychopharmacol. 2010;20(8):519-34.

372.   Shen HH. Core Concept: Resting-state connectivity. Proc Natl Acad Sci USA. 2015;112(46):14115.

373.   Buckner RL, Vincent JL. Unrest at rest: default activity and spontaneous network correlations. Neuroimage. 2007;37(4):1091-6.

374.   Lv H, Wang Z, Tong E, Williams LM, Zaharchuk G, Zeineh M, et al. Resting-State Functional MRI: Everything That Nonexperts Have Always Wanted to Know. Am J Neuroradiol. 2018.

375.   Smitha KA, Akhil Raja K, Arun KM, Rajesh PG, Thomas B, Kapilamoorthy TR, et al. Resting state fMRI: A review on methods in resting state connectivity analysis and resting state networks. Neuroradiol J. 2017;30(4):305-17.

376.   Huettel S, W Song A, McCarthy G. Statistical Analysis: Basic Analyses. Functional Magnetic Resonance Imaging, Second Edition. Sunderland, Massachusetts, U.S.A. : Sinauer Associates, Inc., Publishers; 2008. pp. 331-75.

377.   Wang L, Shen H, Tang F, Zang Y, Hu D. Combined structural and resting-state functional MRI analysis of sexual dimorphism in the young adult human brain: an MVPA approach. Neuroimage. 2012;61(4):931-40.

378.   Koster-Hale J, Saxe R, Dungan J, Young LL. Decoding moral judgments from neural representations of intentions. Proc Natl Acad Sci U S A. 2013;110(14):5648-53.

379.   Weil RS, Rees G. Decoding the neural correlates of consciousness. Curr Opin Neurol. 2010;23(6):649-55.

380.   Madsen KH, Krohne LG, Cai XL, Wang Y, Chan RCK. Perspectives on Machine Learning for Classification of Schizotypy Using fMRI Data. Schizophr Bull. 2018;44(suppl_2):S480-s90.

381.   Ingvar DH, Franzen G. Abnormalities of cerebral blood flow distribution in patients with chronic schizophrenia. Acta Psychiatr Scand. 1974;50(4):425-62.

382.   Holcomb HH, Cascella NG, Thaker GK, Medoff DR, Dannals RF, Tamminga CA. Functional sites of neuroleptic drug action in the human brain: PET/FDG studies with and without haloperidol. Am J Psychiatry. 1996;153(1):41-9.

383.   MacDonald AW, 3rd, Cohen JD, Stenger VA, Carter CS. Dissociating the role of the dorsolateral prefrontal and anterior cingulate cortex in cognitive control. Science. 2000;288(5472):1835-8.

384.   Medoff DR, Holcomb HH, Lahti AC, Tamminga CA. Probing the human hippocampus using rCBF: contrasts in schizophrenia. Hippocampus. 2001;11(5):543-50.

385.   Anticevic A, Hu X, Xiao Y, Hu J, Li F, Bi F, et al. Early-course unmedicated schizophrenia patients exhibit elevated prefrontal connectivity associated with longitudinal change. J Neurosci. 2015;35(1):267-86.

386.   Gur RE, Gur RC. Functional magnetic resonance imaging in schizophrenia. Dialogues Clin Neurosci. 2010;12(3):333-43.

387.   Barch DM, Csernansky JG. Abnormal parietal cortex activation during working memory in schizophrenia: verbal phonological coding disturbances versus domain-general executive dysfunction. Am J Psychiatry. 2007;164(7):1090-8.

388.   Minzenberg MJ, Laird AR, Thelen S, Carter CS, Glahn DC. Meta-analysis of 41 functional neuroimaging studies of executive function in schizophrenia. Arch Gen Psychiatry. 2009;66(8):811-22.

389.   Karlsgodt KH, Sanz J, van Erp TG, Bearden CE, Nuechterlein KH, Cannon TD. Re-evaluating dorsolateral prefrontal cortex activation during working memory in schizophrenia. Schizophr Res. 2009;108(1-3):143-50.

390.   Braus DF, Weber-Fahr W, Tost H, Ruf M, Henn FA. Sensory information processing in neuroleptic-naive first-episode schizophrenic patients: a functional magnetic resonance imaging study. Arch Gen Psychiatry. 2002;59(8):696-701.

391.   MacDonald AW, 3rd, Thermenos HW, Barch DM, Seidman LJ. Imaging genetic liability to schizophrenia: systematic review of FMRI studies of patients' nonpsychotic relatives. Schizophr Bull. 2009;35(6):1142-62.

392.   Habel U, Klein M, Shah NJ, Toni I, Zilles K, Falkai P, et al. Genetic load on amygdala hypofunction during sadness in nonaffected brothers of schizophrenia patients. Am J Psychiatry. 2004;161(10):1806-13.

393.   Ruiz S, Birbaumer N, Sitaram R. Abnormal Neural Connectivity in Schizophrenia and fMRI-Brain-Computer Interface as a Potential Therapeutic Approach. Front Psychiatry. 2013;4:17-.

394.   Buckner RL. The brain's default network: origins and implications for the study of psychosis. Dialogues Clin Neurosci. 2013;15(3):351-8.

395.   Whitfield-Gabrieli S, Thermenos HW, Milanovic S, Tsuang MT, Faraone SV, McCarley RW, et al. Hyperactivity and hyperconnectivity of the default network in schizophrenia and in first-degree relatives of persons with schizophrenia. Proc Natl Acad Sci USA. 2009;106(4):1279-84.

396.   Anticevic A, Cole MW, Repovs G, Savic A, Driesen NR, Yang G, et al. Connectivity, pharmacology, and computation: toward a mechanistic understanding of neural system dysfunction in schizophrenia. Front Psychiatry. 2013;4:169.

397.   Anticevic A, Corlett PR, Cole MW, Savic A, Gancsos M, Tang Y, et al. N-methyl-D-aspartate receptor antagonist effects on prefrontal cortical connectivity better model early than chronic schizophrenia. Biol Psychiatry. 2015;77(6):569-80.

398.   Birnbaum R, Weinberger DR. Functional neuroimaging and schizophrenia: a view towards effective connectivity modeling and polygenic risk. Dialogues Clin Neurosci. 2013;15(3):279-89.

399.   Murray JD, Anticevic A. Toward understanding thalamo-cortical dysfunction in schizophrenia through computational models of neural circuit dynamics. Schizophr Res. 2017;180:70-7.

400.   Welsh RC, Chen AC, Taylor SF. Low-frequency BOLD fluctuations demonstrate altered thalamo-cortical connectivity in schizophrenia. Schizophr Bull. 2010;36(4):713-22.

401.   Woodward ND, Karbasforoushan H, Heckers S. Thalamo-cortical dysconnectivity in schizophrenia. Am J Psychiatry. 2012;169(10):1092-9.

402.   Wang HL, Rau CL, Li YM, Chen YP, Yu R. Disrupted thalamic resting-state functional networks in schizophrenia. Front Behav Neurosci. 2015;9:45.

403.   Anticevic A, Cole MW, Repovs G, Murray JD, Brumbaugh MS, Winkler AM, et al. Characterizing thalamo-cortical disturbances in schizophrenia and bipolar illness. Cereb Cortex. 2014;24(12):3116-30.

404.   Skatun KC, Kaufmann T, Brandt CL, Doan NT, Alnaes D, Tonnesen S, et al. Thalamo-cortical functional connectivity in schizophrenia and bipolar disorder. Brain Imaging Behav. 2018;12(3):640-52.

405.   Gong Q, Puthusseryppady V, Dai J, He M, Xu X, Shi Y, et al. Dysconnectivity of the medio-dorsal thalamic nucleus in drug-naïve first episode schizophrenia: diagnosis-specific or trans-diagnostic effect? Transl Psychiatry. 2019;9(1):9.

406.   Anticevic A, Yang G, Savic A, Murray JD, Cole MW, Repovs G, et al. Mediodorsal and visual thalamic connectivity differ in schizophrenia and bipolar disorder with and without psychosis history. Schizophr Bull. 2014;40(6):1227-43.

407.   Woodward ND, Heckers S. Mapping Thalamo-cortical Functional Connectivity in Chronic and Early Stages of Psychotic Disorders. Biol Psychiatry. 2016;79(12):1016-25.

408.   Anticevic A, Haut K, Murray JD, Repovs G, Yang GJ, Diehl C, et al. Association of Thalamic Dysconnectivity and Conversion to Psychosis in Youth and Young Adults at Elevated Clinical Risk. JAMA Psychiatry. 2015;72(9):882-91.

409.   Cao H, Chén OY, Chung Y, Forsyth JK, McEwen SC, Gee DG, et al. Cerebello-thalamo-cortical hyperconnectivity as a state-independent functional neural signature for psychosis prediction and characterization. Nat Commun. 2018;9(1):3836.

410.   Buchy L, Cannon TD, Anticevic A, Lyngberg K, Cadenhead KS, Cornblatt BA, et al. Evaluating the impact of cannabis use on thalamic connectivity in youth at clinical high risk of psychosis. BMC Psychiatry. 2015;15:276.

411. Ferri J, Ford JM, Roach BJ, Turner JA, van Erp TG, Voyvodic J, et al. Resting-state thalamic dysconnectivity in schizophrenia and relationships with symptoms. Psychol Med. 2018;48(15):2492-9.

412. Pergola G, Selvaggi P, Trizio S, Bertolino A, Blasi G. The role of the thalamus in schizophrenia from a neuroimaging perspective. Neurosci Biobehav Rev. 2015;54:57-75.

413. Kumari V, Gray JA, Honey GD, Soni W, Bullmore ET, Williams SC, et al. Procedural learning in schizophrenia: a functional magnetic resonance imaging investigation. Schizophr Res. 2002;57(1):97-107.

414. Schlösser RGM, Koch K, Wagner G, Nenadic I, Roebel M, Schachtzabel C, et al. Inefficient executive cognitive control in schizophrenia is preceded by altered functional activation during information encoding: an fMRI study. Neuropsychologia. 2008;46(1):336-47.

415. Ragland JD, Gur RC, Valdez J, Loughead J, Elliott M, Kohler C, et al. Levels-of-processing effect on frontotemporal function in schizophrenia during word encoding and recognition. Am J Psychiatry. 2005;162:1840-8.

416. Huang AS, Rogers BP, Woodward ND. Disrupted modulation of thalamus activation and thalamo-cortical connectivity during dual task performance in schizophrenia. Schizophr Res. 2019;210:270-277.

417. Hill SK, Reilly JL, Keefe RSE, Gold JM, Bishop JR, Gershon ES, et al. Neuropsychological impairments in schizophrenia and psychotic bipolar disorder: findings from the Bipolar-Schizophrenia Network on Intermediate Phenotypes (B-SNIP) study. Am J Psychiatry. 2013;170(11):1275-84.

418. First MB, Spitzer RL, Gibbon M, Williams JBW. Structured Clnical Interview for DSM-IV Axis I Disorders - Patient Edition (SCID-I/P, Version 2.0). New York: New York State Psychiatric Institute; 1995.

419. Tamminga CA, Pearlson G, Keshavan M, Sweeney J, Clementz B, Thaker G. Bipolar and schizophrenia network for intermediate phenotypes: outcomes across the psychosis continuum. Schizophr Bull. 2014;40 Suppl 2(Suppl 2):S131-S7.

420. Andreasen NC, Pressler M, Nopoulos P, Miller D, Ho B-C. Antipsychotic dose equivalents and dose-years: a standardized method for comparing exposure to different drugs. Biol Psychiatry. 2010;67(3):255-62.

421. Keefe RS, Harvey PD, Goldberg TE, Gold JM, Walker TM, Kennel C, et al. Norms and standardization of the Brief Assessment of Cognition in Schizophrenia (BACS). Schizophr Res. 2008;102(1-3):108-15.

422. Wang Z, Meda SA, Keshavan MS, Tamminga CA, Sweeney JA, Clementz BA, et al. Large-Scale Fusion of Gray Matter and Resting-State Functional MRI Reveals Common and Distinct Biological Markers across the Psychosis Spectrum in the B-SNIP Cohort. Front Psychiatry. 2015;6(174).

423. Glasser MF, Sotiropoulos SN, Wilson JA, Coalson TS, Fischl B, Andersson JL, et al. The minimal preprocessing pipelines for the Human Connectome Project. Neuroimage. 2013;80:105-24.

424. Marcus DS, Harwell J, Olsen T, Hodge M, Glasser MF, Prior F, et al. Informatics and data mining tools and strategies for the human connectome project. Front Neuroinform. 2011;5:4.

425.   Jenkinson M, Bannister P, Brady M, Smith S. Improved optimization for the robust and accurate linear registration and motion correction of brain images. Neuroimage. 2002;17(2):825-41.

426.   Reuter M, Schmansky NJ, Rosas HD, Fischl B. Within-subject template estimation for unbiased longitudinal image analysis. Neuroimage. 2012;61(4):1402-18.

427.   Fischl B. FreeSurfer. Neuroimage. 2012;62(2):774-81.

428.   Power JD, Plitt M, Laumann TO, Martin A. Sources and implications of whole-brain fMRI signals in humans. Neuroimage. 2017;146:609-25.

429.   Power JD, Barnes KA, Snyder AZ, Schlaggar BL, Petersen SE. Spurious but systematic correlations in functional connectivity MRI networks arise from subject motion. Neuroimage. 2012;59(3):2142-54.

430.   Winkler AM, Ridgway GR, Webster MA, Smith SM, Nichols TE. Permutation inference for the general linear model. Neuroimage. 2014;92:381-97.

431.   Smith SM, Nichols TE. Threshold-free cluster enhancement: addressing problems of smoothing, threshold dependence and localisation in cluster inference. Neuroimage. 2009;44(1):83-98.

432.   Ji JL, Spronk M, Kulkarni K, Repovs G, Anticevic A, Cole MW. Mapping the human brain's cortical-subcortical functional network organization. Neuroimage. 2019;185:35-57.

433.   Glasser MF, Coalson TS, Robinson EC, Hacker CD, Harwell J, Yacoub E, et al. A multi-modal parcellation of human cerebral cortex. Nature. 2016;536(7615):171-8.

434.   Klein A, Andersson J, Ardekani BA, Ashburner J, Avants B, Chiang M-C, et al. Evaluation of 14 nonlinear deformation algorithms applied to human brain MRI registration. Neuroimage. 2009;46(3):786-802.

435.   Cohen AL, Fair DA, Dosenbach NUF, Miezin FM, Dierker D, Van Essen DC, et al. Defining functional areas in individual human brains using resting functional connectivity MRI. Neuroimage. 2008;41(1):45-57.

436.   Ohi K, Sumiyoshi C, Fujino H, Yasuda Y, Yamamori H, Fujimoto M, et al. A Brief Assessment of Intelligence Decline in Schizophrenia As Represented by the Difference between Current and Premorbid Intellectual Quotient. Front Psychiatry. 2017;8(293).

437.   Revheim N, Corcoran CM, Dias E, Hellmann E, Martinez A, Butler PD, et al. Reading deficits in schizophrenia and individuals at high clinical risk: relationship to sensory function, course of illness, and psychosocial outcome. Am J Psychiatry. 2014;171(9):949-59.

438.   Henigsberg N, Savic A, Rados M, Sarac H, Rados M, Ozretic D, et al. Choline and N-acetyl aspartate levels in the dorsolateral prefrontal cortex at the beginning of the recovery phase as markers of increased risk for depressive episode recurrence under different duration of maintenance therapy and after it: a retrospective cohort study. Croat Med J. 2018;59(5):244-52.

439.   Li J, Kong R, Liegeois R, Orban C, Tan Y, Sun N, et al. Global signal regression strengthens association between resting-state functional connectivity and behavior. Neuroimage. 2019;196:126-41.

440.   Murphy K, Fox MD. Towards a consensus regarding global signal regression for resting state functional connectivity MRI. NeuroImage. 2017;154:169-73.

441.   Hubbard EM, Ramachandran VS. Neurocognitive Mechanisms of Synesthesia. Neuron. 2005;48(3):509-20.

442.   Devlin JT, Jamison HL, Gonnerman LM, Matthews PM. The role of the posterior fusiform gyrus in reading. J Cog Neurosci. 2006;18(6):911-22.

443.   Iidaka T. Role of the fusiform gyrus and superior temporal sulcus in face perception and recognition: An empirical review. Jpn Psychol Res. 2014;56(1):33-45.

444.   Uddin LQ, Nomi JS, Hébert-Seropian B, Ghaziri J, Boucher O. Structure and Function of the Human Insula. J Clin Neurophysiol. 2017;34(4):300-6.

445.   Seghier ML. The angular gyrus: multiple functions and multiple subdivisions. Neuroscientist. 2013;19(1):43-61.

446.   Haber S, McFarland NR. The place of the thalamus in frontal cortical-basal ganglia circuits. Neuroscientist. 2001;7(4):315-24.

447.   Rao N, Northoff G, Tagore A, Rusjan P, Kenk M, Wilson A, et al. Impaired Prefrontal Cortical Dopamine Release in Schizophrenia During a Cognitive Task: A [11C]FLB 457 Positron Emission Tomography Study. Schizophr Bull. 2018;45(3):670-9.

448.   Knable MB, Weinberger DR. Dopamine, the prefrontal cortex and schizophrenia. J Psychopharmacol. 1997;11(2):123-31.

449.   Salgado-Pineda P, Caclin A, Baeza I, Junque C, Bernardo M, Blin O, et al. Schizophrenia and frontal cortex: where does it fail? Schizophr Res. 2007;91(1-3):73-81.

450.   Vukadinovic Z. NMDA receptor hypofunction and the thalamus in schizophrenia. Physiol Behav. 2014;131:156-9.

451.   Fox MD, Snyder AZ, Vincent JL, Corbetta M, Van Essen DC, Raichle ME. The human brain is intrinsically organized into dynamic, anticorrelated functional networks. Proc Natl Acad Sci USA. 2005;102(27):9673-8.

452.   Spreng RN, Sepulcre J, Turner GR, Stevens WD, Schacter DL. Intrinsic architecture underlying the relations among the default, dorsal attention, and frontoparietal control networks of the human brain. J Cogn Neurosci. 2013;25(1):74-86.

11. Curriculum vitae

Aleksandar Savić was born in Zenica (Bosnia and Herzegovina) on July 15 1981. After graduating from St. Paul Catholic School Center, in 2000 he enrolled in University of Zagreb School of Medicine. He graduated in 2006 with grade point average of 4.97, and was a recipient of the Dean's Award, and the Award of Academic Drago Perović.

After completing internship at the Croatian Institute for Transfusion Medicine, in 2007 he started his residency training in psychiatry in University Psychiatric Hospital Vrapče. After finishing his residency training in 2012, as a recipient of Fulbright Scholarship he spent a year as a visiting researcher at the Yale University's Department of Psychiatry.

Aleksandar Savić additionally specialized in forensic psychiatry, and works at the Department of Diagnostics and Intensive Care, First Episode Psychosis Unit.

He is the author and co-author of over 20 papers, and a number chapters in textbooks and manuals.